UNIVERSITY OF CALIFORNIA, SAN DIEGO

Analysis of Sperm Motility and Physiology using Optical Tweezers

A dissertation submitted in partial satisfaction of the requirements for the degree

Doctor of Philosophy

in

Electrical Engineering (Photonics)

by

Jaclyn Marie Nascimento

Committee in charge:

Professor Michael W. Berns, Chair
Professor Sadik C. Esener, Co-Chair
Professor Michael J. Heller
Professor Yu-Hwa Lo
Professor Victor D. Vacquier

2008

The dissertation of Jaclyn Marie Nascimento is approved, and it is acceptable in quality and form for publication on microfilm:

_____

_____

_____

_____
Co-Chair

_____
Chair

University of California, San Diego

2008

For my loving husband, Aaron, my parents, John and

Diane, my sister, Janna, and my brother, John.

Table of Contents

List of Tables

List of Figures

Abbreviations and Symbols

Abbreviations

BSA: Bovine Serum Albumin

BWW: Biggers, Whittens, and Whittingham

CASA: Computer Assisted Sperm Analysis

DOG: 2-deoxy-D-glucose

HTF: Human Tubal Fluid

NA: numerical aperture

PC: Principal Component

PCA: Principal Component Analysis

Pesc: escape laser power, mW

SLM: spatial light modulator

SOP: Speed of Progression

SSS: Serum Substitute Supplement

VCL: curvilinear velocity, μm/second

VSL: straight-line velocity, μm/second

Symbols

c – speed of light in media with given index of refraction

F – swimming force

F_S – swimming force of a sperm

F_T – force generated by the optical trap

μm – micron

mW – milliWatts

n – index of refraction

P – laser power

pN – picoNewton

Q – geometrically determined trapping efficiency parameter

Acknowledgements

The material presented in Chapter 3 is, in part, a reprint of the material as it appears in "Analysis of sperm motility using optical tweezers," by J. M. Nascimento, E. L. Botvinick, L. Z. Shi, B. Durrant, and M. W. Berns, *J. Biomed. Opt.* **11**(4), 044001 (2006) and in "Computer-based tracking of single sperm," by L. Z. Shi, J. M. Nascimento, M. W. Berns, and E. L. Botvinick, *J. Biomed. Opt.* **11**(5), 054009 (2006). The dissertation author was the first author of the former paper and second author of the latter.

The material presented in Chapter 4 is, in part, a reprint of the material as it appears in "Analysis of sperm motility using optical tweezers," by J. M. Nascimento, E. L. Botvinick, L. Z. Shi, B. Durrant, and M. W. Berns, *J. Biomed. Opt.* **11**(4), 044001 (2006). The dissertation author was the first author of the paper.

The material presented in Chapter 5 is, in part, a reprint of the material as it appears in "Real-time automated tracking and trapping system (RATTS)," by L. Z. Shi, J. M. Nascimento, C. Chandsawangbhuwana, M. W. Berns, and E. L. Botvinick *Microscopy Research and Technology* **69**(11), 894-902 (2007). The dissertation author was the second author of the paper but contributed equal amount of effort as the first author.

The material presented in Chapter 7 is a reprint of the material as it appears in "The use of optical tweezers to study sperm competition and motility in primates," by J. M. Nascimento, L. Z. Shi, S. Meyers, P. Gagneux, N. M. Loskutoff, E. L. Botvinick, and M. W. Berns, *J. R. Soc. Interface* doi:10.1098/rsif.2007.1118 (Online), 2007. The dissertation author was the first author of the paper.

The material presented in Chapter 8 is, in part, a reprint of the material as it appears in "The use of laser tweezers to analyze sperm motility and mitochondrial membrane potential," by J. M. Nascimento, L. Z. Shi, C. Chandsawangbhuwana, J. Tam, B. Durrant, E. Botvinick, M.W. Berns, *J. Biomed. Opt.* In-press (October 2007) and in "Anaerobic Respiration (Glycolysis) is a Main Source of Energy (ATP) for Sperm Motility," by J. M. Nascimento, L. Z. Shi, J. Tam, C. Chandsawangbhuwana, B. Durrant, E. Botvinick, M.W. Berns, In submission (October 2007). The dissertation author was the first author of the two papers.

The material presented in Chapter 9 is, in part, a reprint of the material as it appears in "Analysis of Human and Chimpanzee Sperm Swimming Speed in Laser Trapping Experiments," by J. S. Tam, J. M. Nascimento, L. Z. Shi, and M. W. Berns, *Frontiers in Optics*, Connie J. Chang-Hasnain and Gregory J. Quarles, chairs, September 2007, San Jose, CA. The dissertation author was the second author of this paper and mentor of the first author.

Vita

2003 B.S., Electrical and Computer Engineering
University of California, San Diego, La Jolla, CA

2005 Analytical and Quantitative Light Microscopy Course
Marine Biological Laboratory, Woods Hole, MA

2005 M.S., Electrical and Computer Engineering (Photonics)
University of California, San Diego, La Jolla, CA

2008 Ph.D., Electrical Engineering (Photonics)
University of California, San Diego, La Jolla, CA

Ph.D. Dissertation Title: "Analysis of Sperm Motility and Physiology using Optical Tweezers"

Publications

Peer-Reviewed Publications

1. Nascimento, J.M, Shi, L.Z., Chandsawangbhuwana, C., Tam, J., Durrant, B., Botvinick, E.L., Berns, M.W. "The use of laser tweezers to analyze sperm motility and mitochondrial membrane potential." *J. Biomedical Optics* Acceptance Date: September 11, 2007.
2. Nascimento, J.M, Shi, L.Z., Meyers, S., Gagneux, P., Loskutoff, N., Botvinick, E.L., Berns, M.W. "The use of optical tweezers to study sperm competition and motility in primates." *J. R. Soc. Interface*, 5(20):297-302, 2008.
3. Nascimento, J.M., Botvinick, E.L, Shi, L.Z., Durrant, B., Berns, M.W. 2006. "Analysis of sperm motility using optical tweezers." *J. Biomedical Optics* 11(4):044001, 2006.
4. Shao, B., Nascimento, J.M., Shi, L.Z., Botvinick, E.L. "Automated Motile Cell Capture and Analysis with Optical Traps." in *Methods in Cell Biology*, M.W. Berns and K.O. Greulich, Eds., 82:601-27, 2007.
5. Shao, B., Shi, L.Z., Nascimento, J.M., Botvinick, E.L., Ozkan, M., Berns, M.W., Esener, S. "High-throughput sorting and analysis of human sperm with a ring-shaped laser trap." *Biomedical Microdevices*, 1387-2176 (Print) 1572-8781 (Online), 2007.

6. Shao, B., Nascimento, J.M., Botvinick, E.L., Ozkan, M., Berns, M.W., Esener, S. "Size tunable three-dimensional annular laser trap based on axicons." *Optics Letters* 31(22):3375-3377, 2006.
7. Shi, L.Z., Nascimento, J., Chandsawangbhuwana, C., Berns, M.W., Botvinick, E.L. "Real-time automated tracking and trapping system for sperm." *Microsc Res Tech.* 69:894-902, 2006.
8. Shi, L.Z., Nascimento, J.M., Berns, M.W., Botvinick, E.L. "Computer-Based Tracking of Single Sperm." *Journal of Biomedical Optics* 11(5):054009, 2006.
9. Shao, B., Esener, S., Nascimento, J.M., Botvinick, E., Berns, M.W. "Dynamically adjustable annular laser trapping based on axicons." *Applied Optics* 45(25):6421-6428, 2006.

Manuscripts in Press or Preparation

1. Nascimento, J.M, Shi, L.Z., Tam, J., Chandsawangbhuwana, C., Durrant, B., Botvinick, E.L., Berns, M.W. "Anaerobic Respiration (Glycolysis) is a Main Source of Energy for Sperm Motility." In submission (January 2008).

Peer-Reviewed Conference Proceedings

1. Tam, J., Nascimento, J.M., Shi, L.Z., Berns, M.W. "Analysis of human and chimpanzee sperm swimming speed in laser trapping experiments." OSA Frontiers in Optics, 2007. **Poster Presentation**
2. Shi, L.Z., Nascimento, J.M., Wakida, N., Dvornikov, A., Baker, N., Botvinick, E.L., Berns, M. W. "'RoboLase': A robotic laser scissors and laser tweezers microscope." IEEE, Asilomar Conference on Signals, Systems, and Computers, 2006.
3. Shi, L.Z., Botvinick, E., Nascimento, J.M., Chandsawangbhuwana, C., Berns, M.W. "A Real-time Single Sperm Tracking, Laser Trapping and Ratiometric Fluorescent Imaging System." Proc. of SPIE Vol. 6326:63260V, Optical Trapping and Optical Micromanipulation III: Kishan Dholakia and Gabriel C. Spalding; Eds. 2006. **Poster Presentation**
4. Shao, B., Vinson, J., Botvinick, E., Song, D., Zlatanovic, S., Esener, S., Berns, M. "Dynamically Adjustable Annular Laser Trapping for Sperm Chemotaxis Study." OSA Topical Meetings, Information Photonics, ITuC4, Charlotte, North Carolina, USA, June 6-9, 2005.
5. Shao, B., Vinson, J., Botvinick, E., Esener, S., Berns, M. "Axicon-based annular laser trap for studies on sperm activity." Proc. SPIE Vol. 5930:82-92, Optical Trapping and Optical Micromanipulation II; Kishan Dholakia, Gabriel C. Spalding; Eds. 2005. **Oral Presentation.**
6. Vinson, J., Botvinick, E., Durrant, B., Berns, M. "Correlation of sperms' swimming force to their swimming speed assessed by optical tweezers." Proc. SPIE Vol. 5930:558-567, Optical Trapping and Optical Micromanipulation II; Kishan Dholakia, Gabriel C. Spalding; Eds. 2005. **Poster Presentation.**

7. Vinson, J., Bartsch, D.U. “Scanning laser tomography: Influence of working distance.” Proc. of SPIE Vol. 5368:869-877, Physics of Medical Imaging; Marin J. Yaffe and Michael J. Flynn, Eds. 2004. **Poster Presentation.**

Abstracts and Presentations

1. Nascimento, J.M. “Analysis of Sperm Motility using Optical Tweezers.” Gordon Research Conference: Fertilization and Activation of Development, 2007. **Invited Speaker.**
2. Nascimento, J.M., Shi L.Z., Botvinick E.L., Meyer, S., Gagneux, P., Berns M.W. “Comparison of motility in primate sperm using optical tweezers.” American Society of Cell Biology annual meeting, 2006. **Poster Presentation.**
3. Shi, L.Z., Botvinick, E.L., Vinson, J.M., Berns, M.W. “Real-time single sperm tracking and laser trapping –“track and trap.” American Society of Cell Biology annual meeting, 2005. **Poster Presentation.**

ABSTRACT OF THE DISSERTATION

Analysis of Sperm Motility and Physiology using Optical Tweezers

by

Jaclyn Marie Nascimento

Doctor of Philosophy in Electrical Engineering (Photonics)

University of California, San Diego, 2008

Professor Michael W. Berns, Chair
Professor Sadik C. Esener, Co-Chair

Objective and quantitative assessment of sperm quality is important for human infertility as well as for animal husbandry. Several techniques, including subjectively scoring sperm based on speed of progression and quantitatively measuring sperm motility parameters, are currently used to assess sperm. Optical tweezers provide a non-invasive way to study sperm motility by measuring sperm swimming forces. The minimum amount of laser power needed to hold the sperm in the trap (or the threshold escape power) is directly proportional to the sperm's swimming force ($F = Q * P / c$,

where F is the swimming force, P is the laser power, c is the speed of light in the medium, and Q is the geometrically determined trapping efficiency parameter).

The purpose of this dissertation is to first develop an objective and quantitative method to analyze sperm motility based on sperm swimming force. A custom system is developed to track, trap, and fluorescently image sperm, measuring sperm swimming speed, swimming force and mitochondrial membrane potential in real-time. This system is then used to study sperm. Specifically, the effects of trap duration and laser trapping power on sperm motility are determined, the relationships between sperm swimming force and swimming speed for various mammalian species are defined, both the effects of cryopreservation and sperm competition in primate species on motility are studied, and finally the relationship between sperm motility (swimming force and swimming speed) and energy production is analyzed.

I. Introduction

1.1 Significance

Objective and quantitative assessment of sperm quality is important for human infertility as well as for animal husbandry. For animal husbandry, semen that has been frozen can be used in artificial insemination, maximizing the male breeding potential (Cotter *et al.* 2005; Maxwell *et al.* 2007; Su *et al.* 2007). Additionally, long-term cryopreservation of semen provides a means for gene preservation for endangered species. An objective and universal technique for assessing sperm, therefore, is crucial for ensuring high quality semen samples are being frozen and used for artificial insemination.

In fertility physiology studies both in the clinic and the laboratory, the Speed of Progression (SOP) score is often used as a key parameter in the determination of overall motility score of a semen sample where motility score = (% motile)*(SOP score of sample)^2 (Olson *et al.* 2003). The motility score is used to estimate the probability of a successful fertilization. The SOP score takes on discrete values from 1 – 5. Five qualitatively represents the fastest swimming sperm and 1 represents the sperm that exhibit the least amount of forward progression (Olson *et al.* 2003). Since the SOP score is qualitative, it may be subject to variation between individuals.

Computer Assisted Sperm Analysis (CASA) systems have been developed to track sperm within a field of view and measure motility parameters such as curvilinear velocity, amplitude of lateral head movement, and percent of motile sperm. This provides quantitative information about the overall motility of a sperm population in a

short amount of time (Amann and Katz 2004; Mortimer 1994). CASA, however, has some limitations. CASA software has difficulty tracking sperm that swim with large transverse amplitudes, such as rhesus macaque sperm (Baumber and Meyers 2006). This results in discontinuous swimming trajectories, leading to inaccuracies such as miscounting a single sperm as multiple sperm. In addition, CASA software has difficulty handling collision events (when multiple sperm swimming trajectories collide). For such an event, CASA may miscount one or both of the sperm as multiple sperm and/or swap the sperm trajectories (Shi et al. 2006).

Flow cytometry in combination with fluorescent probes has been used for sperm cell sorting and subsequent analysis. Specifically, it has been used to monitor sperm mitochondrial membrane potential (MMP) (Marchetti *et al.* 2002 and 2004; Gallon *et al.* 2006; Kasai *et al.* 2002). MMP, given by the Nernst equation, is dependent upon the distribution of hydrogen protons across the inner mitochondrial membrane. This electrochemical proton gradient drives the synthesis of ATP that is used for energy. Therefore, the fluorescence intensity of cyanine dyes, such as 3,3'-diethyloxacarbocyanine iodide ($DiOC_2(3)$), which increases as the magnitude of MMP increases, is an indicator of the energetic state of a cell. Studies have demonstrated that high MMP in sperm correlates with increased motility (Marchetti *et al.* 2002). Several fluorescent probes are available, and comparisons between probes have been performed (Marchetti *et al.* 2004; Novo *et al.* 1999). Novo *et al.* (1999) showed that the ratiometric technique for estimation of MMP using $DiOC_2(3)$ was an accurate indicator of bacterial MMP.

Optical forces from a single beam gradient laser trap can be used to confine and manipulate microscopic particles (Ashkin 1991 and 1998). Optical tweezers are non-invasive and have been used to study sperm motility by measuring sperm swimming forces (Konig *et al.* 1996; Araujo *et al.* 1994; Dantas *et al.* 1995; Patrizio *et al.* 2000; Tadir *et al.* 1990 and 1998). These studies determined that the minimum amount of laser power needed to hold the sperm in the trap (or the threshold escape power) is directly proportional to the sperm's swimming force ($F = Q * P / c$, where F is the swimming force, P is the laser power, c is the speed of light in the medium, and Q is the geometrically determined trapping efficiency parameter (Konig *et al.* 1996)). Therefore, this technique, in addition to the other methods mentioned above, is potentially useful in assessing sperm quality by quantifying sperm swimming forces. The purpose of this dissertation is to first develop an objective and quantitative method to analyze sperm motility based on sperm swimming force. Second, this method is used to study sperm quality, to examine the theory of sperm competition in primates, and finally to relate sperm swimming force and swimming speed to energy production.

1.2 Scope

Chapter 2 introduces the theory behind optical trapping. Chapter 3 describes the optical setup used to create the laser tweezers. The effects of optical trapping (trap duration and laser trapping power) on sperm motility are measured. In chapter 4, the modification to the optical setup used to control laser power and measure sperm swimming force is described. The limitations of the SOP scoring method used to

assess sperm quality are discussed. The exact amount of variation among three fertility experts, within the same laboratory, using the SOP scoring method is determined. In addition, a relationship between sperm swimming force and swimming speed is defined after statistical tools are used to classify the sperm.

The custom developed algorithm used to measure sperm swimming speed and swimming force, called Real-time Automated Tracking and Trapping System (RATTS), is described in chapter 5. Cryopreservation of sperm cells and its significance in sperm fertility is discussed in more detail. The effects of cryopreservation on sperm motility are determined. Specifically, swimming speeds and swimming forces of "fresh" and "frozen" sperm samples from different species are measured and statistically compared. In chapter 6, the relationship between sperm swimming force and swimming speed is described for various mammalian species. Regressions for each species are determined and statistically compared. Chapter 7 discusses sperm competition in primate species. Four primates with known mating patterns ranging from multi-partner to monogamous are analyzed. Swimming speed and swimming force distributions as well as the relationships between the two parameters are statistically compared.

In chapter 8, work using fluorescent ratiometric probes to monitor mitochondrial membrane potential (MMP) is reviewed. The modifications to the optical design as well as to the hardware and software used to automatically track, trap, and calculate the fluorescence ratio of sperm in real-time is discussed. The effects of the probe on sperm motility are assessed. The ability to monitor changes in

MMP is quantified for the probe as well as the system. The effects of prolonged exposed to the laser tweezers on swimming speed and MMP are analyzed. The relationships between mitochondrial membrane potential (i.e. oxidative phosphorylation) and sperm swimming force and swimming speed are analyzed in domestic dog, human and gorilla species. The roles of two potential sources of ATP, oxidative phosphorylation which occurs in the mitochondria located in the sperm midpiece and glycolysis which occurs along the principal piece (sperm tail), are studied. The effects of different media, the presence/absence of glucose in the media, oxidative phosphorylation and glycolytic inhibitors on human sperm motility (swimming speed and swimming force) and MMP are quantified.

Finally, in chapter 9, I will discuss some of the project's potential future directions. The custom system's limitations and possible solutions will be discussed. Hardware and software modifications that can optimize the experiments as well as increase throughput will also be discussed.

References

Amann, R. P., Katz, D. F. (2004). Reflections on CASA after 25 years. *J Androl.* **25**(3), 317-325.

Araujo, E. Jr., Tadir, Y., Patrizio, P., Ord, T., Silber, S., Berns, M. W., Asch, R. H. (1994). Relative force of human epididymal sperm. *Fertil. Steril.* **62**(3), 585-590.

Ashkin, A. (1991). The study of cells by optical trapping and manipulation of living cells using infrared laser beams. *ASGSB Bull* **4**(2), 133-146.

Ashkin, A. (1998). Forces of a single-beam gradient laser trap on a dielectric sphere in ray optics regime. *Methods Cell. Biol.* **55**, 1-27.

Baumber, J., Meyers, S. A. (2006). Hyperactivated Motility in Rhesus Macaque (*Macaca mulatta*) Spermatozoa. *J. Androl.* **27**(3), 459-468.

Cotter, P. Z., Goolsby, H. A., Prien, S. D. (2005). Preliminary Evaluation of a Unique Freezing Technology for Bovine Spermatozoa Cryopreservation. *Reprod. Dom. Anim.* **40**, 98-99.

Dantas, Z. N., Araujo, E. Jr., Tadir, Y., Berns, M. W., Schell, M. J., Stone, S. C. (1995). Effect of freezing on the relative escape force of sperm as measured by a laser optical trap. *Fertil. Steril.* **63**(1), 185-188.

Gallon, F., Marchetti, C., Jouy, N., Marchetti, P. (2006). The functionality of mitochondria differentiates human spermatozoa with high and low fertilizing capability. *Fertility and Sterility* **86**(5), 1526-1530.

Kasai, T., Ogawa, K., Mizuno, K., Nagai, S., Uchida, Y., Ohta, S., Fujie, M., Suzuki, K., Hirata, S., Hoshi, K. (2002). Relationship between sperm mitochondrial membrane potential, sperm motility, and fertility potential. *Asian J. Andrology* **4**(2), 97-103.

Konig, K., Svaasand, L., Liu, Y., Sonek, G., Patrizio, P., Tadir, Y., Berns, M. W., Tromberg, B. J. (1996). Determination of motility forces of human spermatozoa using an 800 nm optical trap. *Cell Mol. Biol. (Noisy-le-grand)* **42**(4), 501-509.

Marchetti, C., Obert, G., Deffosez, A., Formstecher, P., Marchetti, P. (2002). Study of mitochondrial membrane potential, reactive oxygen species, DNA fragmentation and cell viability by flow cytometry in human sperm. *Human Reproduction* **17**(5), 1257-1265.

Marchetti, C., Jouy, N., Leroy-Martin, B., Deffosez, A., Formstecher, P., Marchetti, P. (2004). Comparison of four fluorochromes for the detection of the inner mitochondrial membrane potential in human spermatozoa and their correlation with sperm motility. *Human Reproduction* **19**(10), 2267-2276.

Maxwell, W. M. C., Parrilla, I., Caballero, I., Garcia, E., Roca, J., Martinez, E. A., Vazquez, J. M., Rath, D. (2007). Retained Functional integrity of Bull Spermatozoa after Double Freezing and Thawing Using PureSperm® Density Gradient Centrifugation. *Reprod. Dom. Anim.* **42**, 489-494.

Mortimer, D. (1994). *Practical laboratory andrology,* Oxford University Press, New York, NY.

Novo, D., Perlmutter, N. G., Hunt, R. H., Shapiro, H. M. (1999). Accurate flow cytometric membrane potential measurement in bacteria using diethyloxacarbocyanine and a ratiometric technique. *Cytometry* **35**, 55-63.

Olson, M. A., Yan, H., DeSheng, L., Hemin, Z., Durrant, B. (2003). Comparison of Storage Techniques for Giant Panda Sperm. *Zoo Biology* **22,** 335-345.

Patrizio, P., Liu, Y., Sonek, G. J., Berns, M. W., Tadir, Y. (2000). Effect of pentoxifylline on the intrinsic swimming forces of human sperm assessed by optical tweezers. *J. Androl.* **21**(5), 753-756.

Shi, L. Z., Nascimento, J., Berns, M. W., Botvinick, E. (2006). Computer-based tracking of single sperm. *J. Biomed. Opt.* **11**(5), 054009.

Su, L., Li, X., Quan, J., Yang, S., Li, Y., He, X., Tang, X., (2007). A comparison of the protective action of added egg yolks from five avian species to the cryopreservation of bull sperm. *Anim. Reprod. Sci.* doi: 10.1016/j.anireprosci.2007.06.019.

Tadir, Y., Wright, W. H., Vafa, O., Ord, T., Asch, R. H., Berns, M. W. (1989). Micromanipulation of sperm by a laser generated optical trap. *Fertil. Steril.* **52**(5), 870-873.

Tadir, Y., Wright, W. H., Vafa, O., Ord, T., Asch, R. H., Berns, M. W. (1990). Force generated by human sperm correlated to velocity and determined using a laser generated optical trap. *Fertil. Steril.* **53**(5), 944-947.

II. Optical trapping

2.1 Introduction

As stated in chapter 1, the purpose of this dissertation is to develop an objective and quantitative method to analyze sperm motility based on sperm swimming force. Therefore, in this chapter, I will first describe how lasers can be used to generate forces strong enough to stably trap objects in three dimensions. Second, I will show how these forces can be used to measure sperm cells which have their own momentum.

2.2 Theory of optical trapping

A beam of light is composed of photons, each of which carries a momentum that is a function of wavelength. When a photon is incident upon a particle, there is a transfer of momentum through scattering. If the laser light is focused to a small area by a microscope objective, for example, the scattering photons will exert a radiation pressure that will result in an optical force. These forces can be significant if the particle is small. Particle size determines which regime is used to describe how optical forces are used to create a trap.

Particles in the Rayleigh regime (particle size is much smaller than the wavelength of light) act as dipoles. The trapping is thus described as a dipole-electric field interaction, where the dipole feels two forces: scattering force and gradient force (Ashkin 1992). The scattering force pushes the particle in the direction of light propagation. The gradient force pulls the particle towards the high intensity beam

focus. When the gradient force overcomes the scattering force, the particle will be stably trapped.

Geometric optics or ray optics is used when the particles are larger than the wavelength of light. In the ray optics regime, the light beam is decomposed into individual rays. These rays have their own intensity, direction and polarization (Ashkin 1992). The direction will change when the ray reflects and refracts at the particle-medium boundary. The momentum is changed when the light is refracted by the particle. Since momentum must be conserved, an equal and opposite momentum change is imparted to the particle (Neuman and Block 2004). Optical forces are generated as a result of the change in momentum. For particles whose index of refraction is greater than that of surrounding media, for example cells suspended in water, the gradient force is in the direction of maximum light intensity. The scattering force is attributed to any reflections or refractions of the light pointing in an outward propagating direction. Again, when the gradient force overcomes the scattering force, the trap becomes stable. The generated forces are proportional to the intensity of the light (Neuman and Block 2004).

This dissertation focuses on using optical tweezers, generated by an Nd:YVO_4 continuous wave 1064nm wavelength laser (Spectra Physics, Model BL-106C, Mountain View, CA), to trap sperm cells. The sperm are trapped by the head, which are approximately 8-10μm in length. Therefore, the ray optics regime is used to describe the optical forces generated.

Since sperm are motile, they have their own associated momentum. Thus, in order to stably trap a sperm, the laser power must be great enough to overcome the sperm's momentum. The threshold power at which a sperm can escape the trap is directly proportional to the sperm's swimming force ($F = Q * P / c$, where F is the swimming force in pN, P is the laser power in mW, c is the speed of light in the medium, and Q is the geometrically determined trapping efficiency parameter (Konig *et al.* 1996)). Therefore, throughout this dissertation, measurement of escape laser power is considered a direct measurement of sperm swimming force. Figure 2.1 (a) shows how a high numerical aperture (NA) microscope objective is used to generate an optical trap by tightly focusing the laser beam within the cell chamber. Figure 2.1 (b) shows how the laser beam refracts as it passes through the partially transparent sperm head (reflecting rays are not drawn). The trapping force (F_T) must exceed the sperm's swimming force (F_S) in order to stably trap the sperm.

(a)

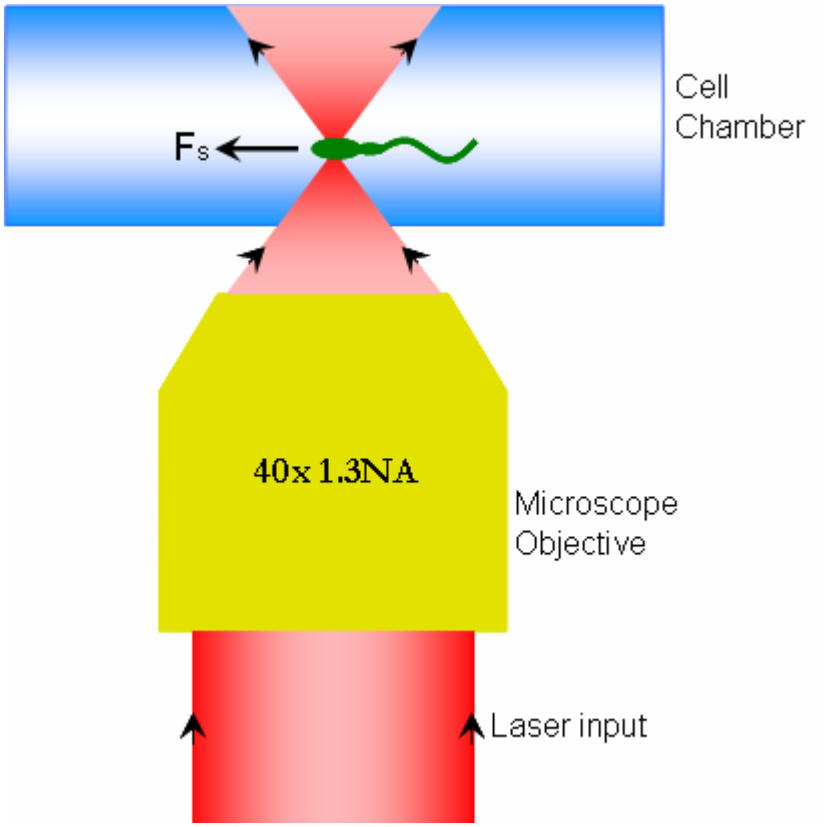

Figure 2.1: (a) Diagram of an optical trap being generated using a microscope objective within a cell chamber. The microscope objective (40x, 1.3NA, in yellow) focuses the laser beam (shown in red) to a diffraction limited spot within the chamber (in blue). A sperm (in green) swims with a force (F_S) and is trapped by the laser. (b) Diagram of how the laser beam refracts as it passes through the partially transparent sperm head (reflecting rays are not drawn). The sperm will be trapped when its swimming force (F_S) is less than the trapping force (F_T).

(b)

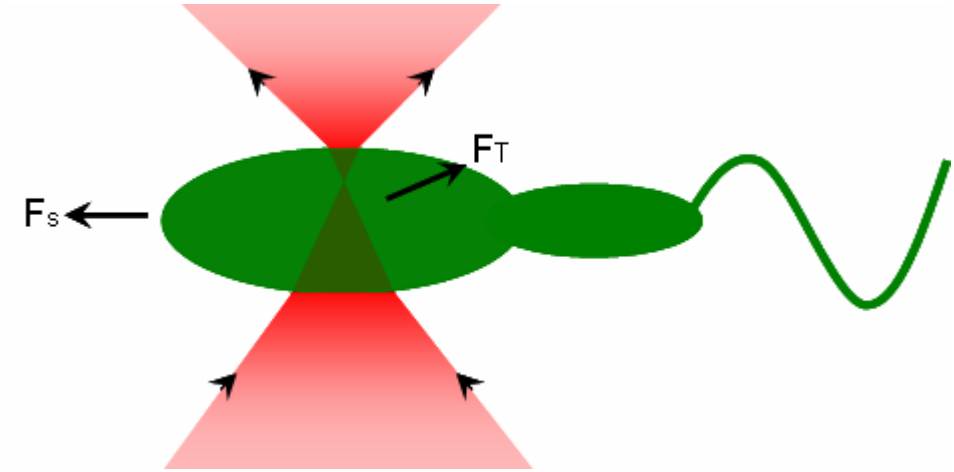

Figure 2.1 (continued): (b) Diagram of how the laser beam refracts as it passes through the partially transparent sperm head.

References

Ashkin, A. (1992). Forces of a single-beam gradient laser trap on a dielectric sphere in the ray optics regime. *Biophys. J.* **61**, 569-582.

Konig, K., Svaasand, L., Liu, Y., Sonek, G., Patrizio, P., Tadir, Y., Berns, M. W., Tromberg, B. J. (1996). Determination of motility forces of human spermatozoa using an 800 nm optical trap. *Cell Mol. Biol. (Noisy-le-grand)* **42**(4), 501-509.

Neuman, K. C., Block, S. M. (2004). Optical trapping. *Rev. Sci. Instrum.* **75**(9), 2787-2809.

III. Effects of optical trapping on sperm motility

3.1 Introduction

Laser tweezers have been used to trap and manipulate sperm cells. This tool is potentially useful in assessing sperm quality by quantifying sperm swimming forces. In order to validate the use of this tool for that application, the negative effects on sperm motility need to be addressed. Previous studies (Tadir *et al.* 1989) showed that for human sperm, trap durations up to 30 seconds using 1 Watt laser power had no significant effect on linear velocity. That study, however, analyzed sperm with velocities ranging from 1 – 60μm/sec. Other species are known to have higher velocities than the maximum value in that study. For example, domestic dog sperm are known to swim with speeds that range as high as 200μm/sec. In addition, that initial study did not address the effects of other laser powers on sperm motility. Therefore, the purpose of this study is to determine the laser trap duration and laser trapping power that have a negligible effect on sperm motility. The optimum duration and optimum laser power that minimally affect sperm swimming speed are to be used for subsequent experiments.

3.2 Materials and Methods

3.2.1 Specimen

Semen samples collected from several dogs were pooled and cryopreserved according to a published protocol (Durrant *et al.* 2000; Harper *et al.* 1998). For each experiment, a sperm sample is thawed in a water bath (37^{o}C) for approximately one to two minutes and its contents are transferred to an Eppendorf centrifuge tube. The

sample is centrifuged at 2000 rpm for ten minutes (centrifuge tip radius is 8.23cm). The supernatant is removed and the remaining sperm pellet is suspended in 1 milliliter (mL) of pre-warmed media (1mg of bovine serum albumin (BSA) per 1mL of Biggers, Whittens, and Whittingham (BWW), osmolarity of 270 – 300 mmol/kg water, pH of 7.2 – 7.4 (Biggers *et al.* 1971)). Final dilutions of 30,000 sperm per mL of media are used in the experiments. The specimen is loaded into a rose chamber and mounted into a microscope stage holder (Liaw and Berns 1981). The sample is kept at room temperature.

3.2.2 Hardware, software and optical design

A single point gradient trap was generated using a Nd:YVO_4 continuous wave 1064nm wavelength laser (Spectra Physics, Model BL-106C, Mountain View, CA) coupled into a Zeiss Axiovert S100 microscope and a 40x, phase III, NA 1.3 oil immersion objective (Zeiss, Thornwood, NY) which is also used for imaging. The optical design is shown in figure 3.1 (top and side views). Laser light is reflected off two dielectric mirrors to orient the beam parallel to the table and along the optical axis of the microscope. The beam is expanded by two lenses (plano-concave lens, f = -25.5mm at λ = 1064nm, and plano-convex lens, f = 76.2mm at λ = 1064 nm) in order to fill the objective's back aperture. A third lens (biconvex lens, f = 200mm) focuses the beam onto the side port of the dual video adaptor to ensure the beam is collimated at the objective's back aperture (Berns *et al.* 2005).

(a)

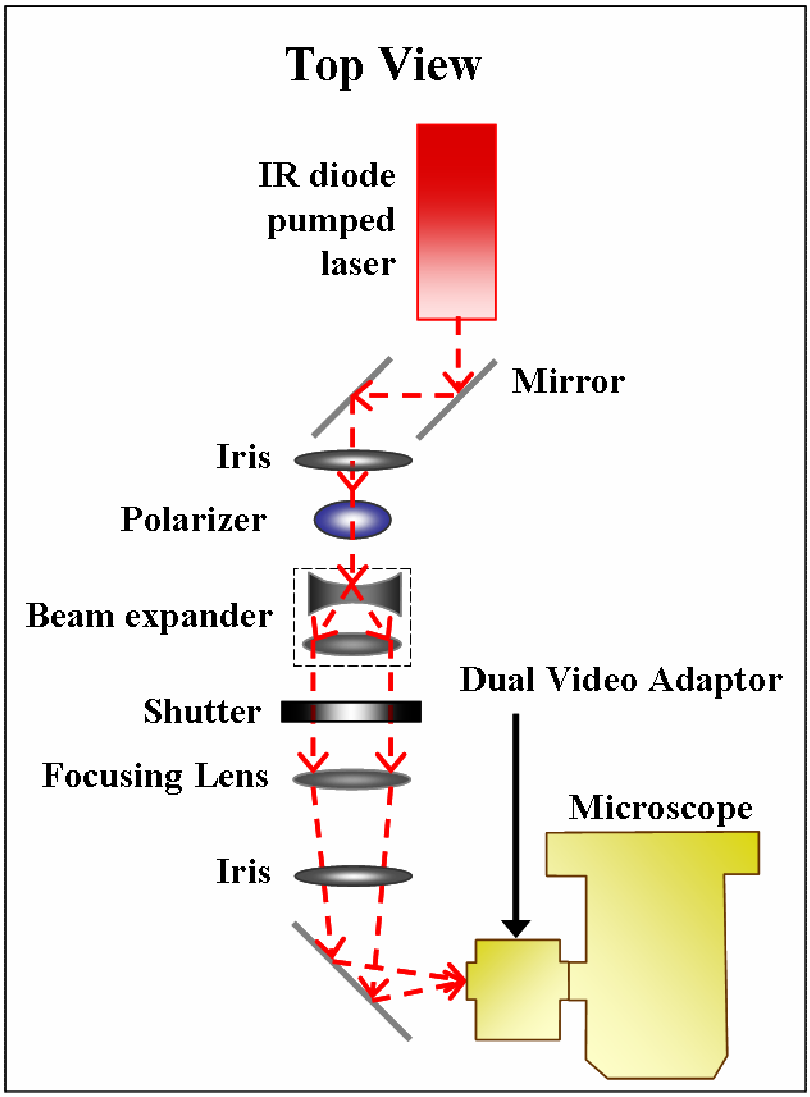

Figure 3.1: Optical schematic (a) Layout of microscope path and optical tweezers from top view. (b) Layout of microscope path and optical tweezers from side view.

(b)

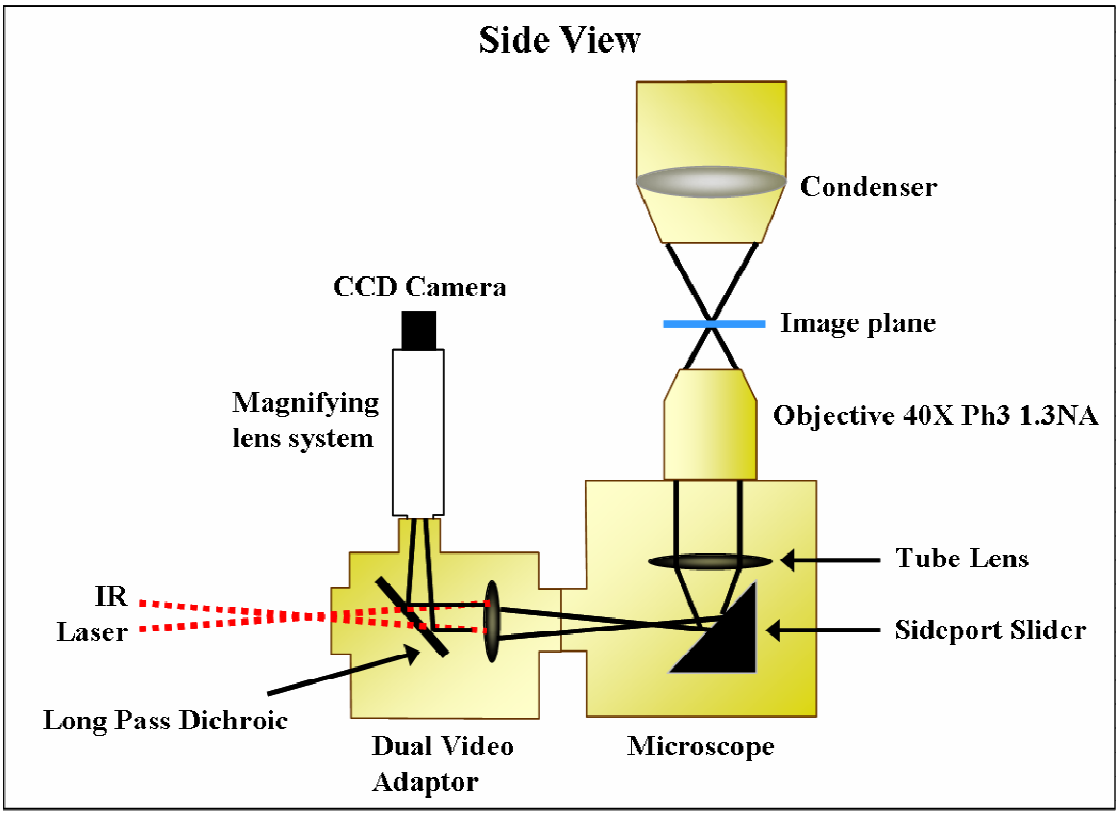

Figure 3.1 (continued): (b) Layout of microscope path and optical tweezers from side view.

The dual video adaptor contains a filter cube with a dichroic that allows laser light entering the side port to be transmitted to the microscope while reflecting visible light to the camera attached to the top port for imaging. A filter (Chroma Technology Corp., Model D535/40M, Rockingham, VT) is placed in the filter cube to block back reflections of IR laser light while allowing visible light to pass. The laser trap remains stationary near the center of the field of view. In order to trap a sperm, the microscope stage is moved to bring the sperm to the laser trap location. The laser trap location is determined prior to each experiment by trapping 10μm-diameter polystyrene beads

suspended in water within a 35 mm diameter glass bottom Petri dish. The trap depth within the sample is kept to approximately 5 um (approximately one sperm head diameter) above the cover glass. This ensures that the trap geometry is not sensitive to spherical aberrations from the surrounding media.

The specimen is imaged at 30 frames per second by a CCD camera (Sony, Model XC – 75, New York City, NY), coupled to a variable zoom lens system (0.33X magnification) to increase the field of view. Analog output (RS-170 format) from the CCD is wired into the video-in port of a digital camcorder to record sperm swimming for off-line analysis. Prior to laser trapping, the microscope stage was momentarily halted (3 to 5 sec) to record video footage of the swimming sperm. Similar footage was acquired after trapping. Video sequences of the swimming sperm from the digital camcorder are converted into bitmap format with Adobe Premier Pro 1.5 (Adobe Systems Incorporated, San Jose, CA). The bitmap images are then loaded into a custom tracking program developed in LabView 7.1 (National Instruments, Austin, TX). Image contrast enhancement and segmentation algorithms are used to identify the sperm head as it transitions in and out of focus. The nearest neighbor method is complemented with a speed-check feature to aid tracking in the presence of additional sperm or other particles. The swimming velocity (curvilinear velocity, VCL, μm/sec) before and after trapping is calculated based on the pixel (x, y) coordinates of the sperm's swimming trajectory:

$$VCL = \frac{\sum_{i=1}^{N}\left(\frac{\sqrt{(x_i - x_{(i-1)})^2 + (y_i - y_{(i-1)})^2}}{\Delta frame} * \frac{micron}{1.39\,pixel} * \frac{30\,frames}{\sec}\right)}{N_{frames}}$$

where *i* is the current frame. This measurement is the same as that made by conventional Computer Assisted Sperm Analysis (CASA) machines. A more detailed description of the tracking algorithm can be found in Shi *et al.* 2006.

3.2.3 Effects of Trap Duration on Sperm Motility

The goal of this experiment is to determine if the duration a sperm is exposed to the laser trap has a significant effect on sperm motility. The effects are tested on sperm from two dog sperm samples pooled together. Laser trapping power is held constant at 420mW in the specimen plane for durations of 15, 10, and 5 seconds. (Laser power is measured using a photodiode just after the oil immersed objective to define the power in the focal plane.) VCL is measured prior to and post trapping for three to five seconds. The ratio of VCL after trapping to VCL before trapping is calculated to measure changes in swimming speed as a result of the laser trap. Since the data were found to be normally distributed using the Lilliefors test (Zar 1984), the Student's T-test (Zar 1984) was used to compare the ratios of sperm held at 15s, 10s, and 5s.

3.2.4 Effects of Laser Trapping Power on Sperm Motility

The goal of this experiment is to determine if the laser trapping power has a significant effect on sperm motility. The laser trap duration is held constant at 5s. The effects are tested on sperm from the same pooled dog sperm sample as in the trapping duration experiment. Sperm are trapped at 420mW, 350mW, 300mW, and 250mW laser power in the specimen plane. The VCL is measured prior to and post trapping as in experiment 1. Since the data were found to be normally distributed

using Lilliefors test (Zar 1984), the Student's T-test (Zar 1984) is used to compare the ratios of sperm held at 420mW, 350mW, 300mW, and 250mW.

3.3 Results

3.3.1 Effects of Trap Duration on Sperm Motility

A total of 179 dog sperm were trapped and analyzed (N values, average VCL pre-trap and range of swimming speed pre-trap are listed in table 3.1). Average velocity ratios of VCL post trapping to VCL pre trapping for various trap durations were determined (table 3.1). Figure 2 plots sperm velocity ratios for the three trapping durations. The ratio of "1" is emphasized in order to distinguish the sperm that swam out of the trap at a higher velocity than before trapping from those that swam out of the trap at a lower velocity. The results of the Student's T-test that compare the means of the sperm velocity ratios are also listed in the figure 3.2. A trap duration of 15s resulted in a greater decrease in VCL than 10s or 5s durations (at 420mW laser power). Average decrease for trap durations of 10s and 5s were negligible and statistically equivalent.

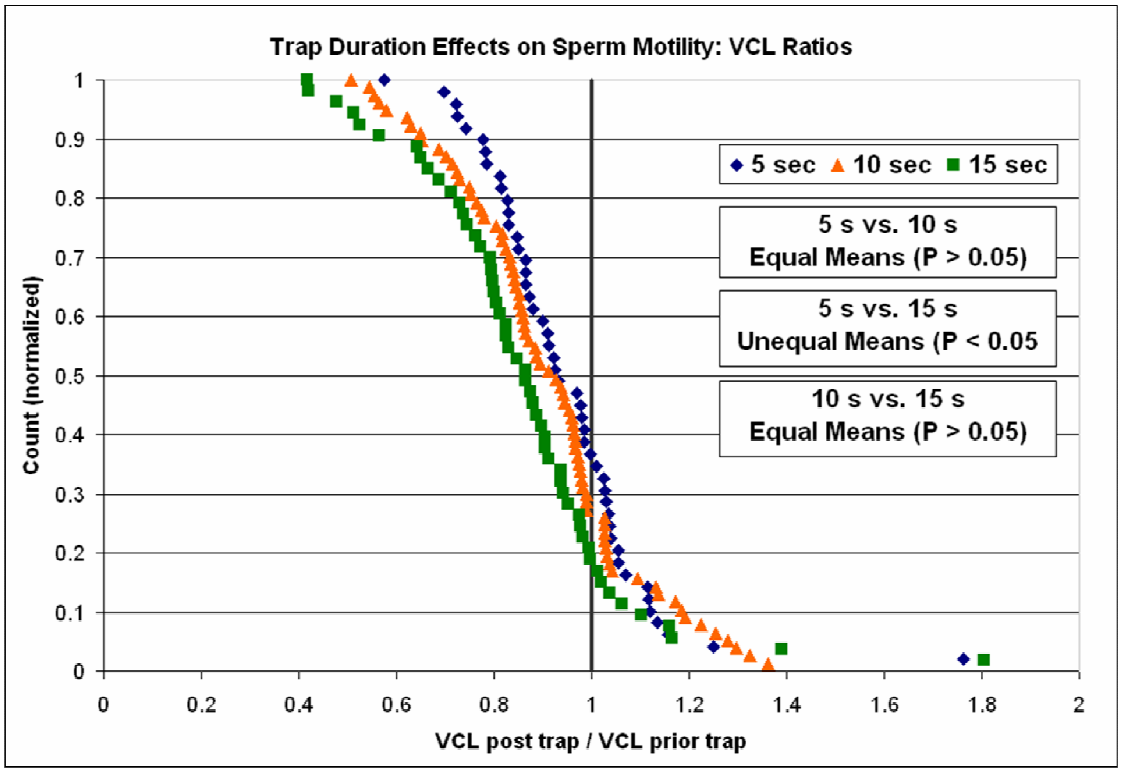

Figure 3.2: Effects of Trap Duration: VCL ratios for the three trap durations tested (15s in green squares, 10s in orange triangles, and 5s in dark blue diamonds) at constant power (420mW). The less time sperm are exposed to the trap, the closer the VCL ratio is to unity (less effect on sperm motility). The results of the Student's T-test (P values) are listed.

3.3.2 Effects of Laser Trapping Power on Sperm Motility

A total of 195 dog sperm were trapped and analyzed (N values, average VCL pre-trap and range of swimming speed pre-trap are listed in table 3.1). Average velocity ratios for various trapping powers are listed in table 3.1. Figure 3.3 plots sperm velocity ratios for all four trapping powers. The data at all four trapping powers were found to be statistically equivalent ($P > 0.05$). The velocity ratio distributions for the sperm trapped at the various powers are tested for a mean value close to unity.

Sperm trapped at 350mW were found to be statistically equal to a maximum value of 0.964 ($P > 0.05$). All other distributions were found to be statistically equal to or greater than 0.987 ($P > 0.05$). Sperm that were observed to stop and start swimming on their own, without using the laser, had a mean velocity ratio of 0.975. Since all but one distribution was found to have a mean VCL ratio value statistically greater than 0.975, the decrease in swimming speed due to laser trapping power is considered negligible.

Table 3.1: Effect of laser trap duration and laser power of sperm motility: N values, average VCL pre-trap and range of VCL values in μm/sec, and average velocity ratios (+/- standard deviation) for various trap durations (constant trapping power, 420mW) and various trapping powers (constant duration, 5s). The 15s trap duration has the greatest average decrease in VCL post trapping.

	N	**Average VCL pre-trap [range] in μm/sec**	**Average VCL Ratio (+/- Standard Deviation)**
5 seconds	49	104 [39.8 - 174]	0.9473 +/- 0.18
10 seconds	77	110 [37.4 - 200]	0.9097 +/- 0.19
15 seconds	53	102 [60.7 - 151]	0.8602 +/- 0.23
420mW	49	104 [39.8 - 174]	0.9473 +/- 0.18
350mW	49	108 [41.7 - 185]	0.9251 +/- 0.14
300mW	51	78.2 [85.5 - 140]	0.9475 +/- 0.14
250mW	46	91.6 [42.0 - 165]	0.9564 +/- 0.13

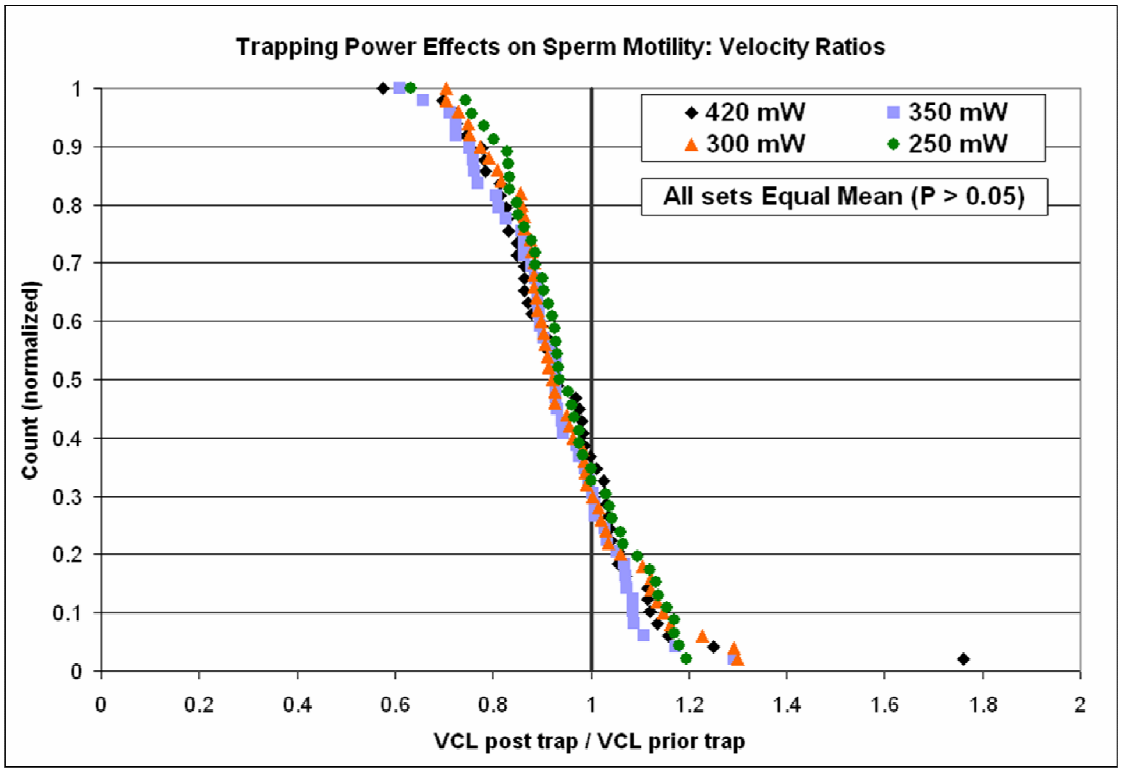

Figure 3.3: Effects of Trapping Power: VCL ratios for the four trapping powers tested (420mW in black diamonds, 350mW in light blue squares, 300mW in orange triangles, and 250mW in green circles). All VCL ratios are close to unity.

3.4 Discussion

A slight decrease in swimming speed post trapping was observed at all tested trapping powers (420mW, 350mW, 300mW and 250mW) for a 5s trap duration. However, since the mean ratio of VCL post trapping to VCL prior to trapping for the majority of distributions is found to be statistically greater than that of sperm that stopped/started swimming without laser interaction, the decrease is considered negligible. A 15 second trap duration at 420mW was found to statistically impede motility. However, at 420mW laser power, 10 second and 5 second trap durations

were equivalent and negligible with respect to sperm motility. Thus, a 10s trap duration at 420mW or less should not significantly affect sperm motility. Accordingly, for subsequent experiments that measure sperm swimming force using a polarizer (see chapter four), power decay occurs in 10 seconds. This softens the pace of laser decay and allows for greater accuracy in escape power measurement.

Similar studies on human sperm found that slower swimming sperm (1 to 60μm/sec) were unaffected by the laser trap for durations up to 30 seconds at a power of 1W in the focal volume using a 1064nm Nd:YAG laser (Tadir *et al.* 1989). While in this study comparatively faster swimming dog sperm (~105μm/sec average, with a maximum swimming speed of 200μm/sec) were affected in as little as 15s trap duration using less laser power (maximum of 420mW). This suggests either species specific laser sensitivity, or faster swimming sperm are more sensitive to the laser trap. Optical trap exposure and power tolerances could be a function of species phenotype; specifically sperm head geometry and biophotonic properties. Future studies should investigate species-dependent differences in the response to laser trapping.

Acknowledgements

The material presented in Chapter 3 is, in part, a reprint of the material as it appears in "Analysis of sperm motility using optical tweezers," by J. M. Nascimento, E. L. Botvinick, L. Z. Shi, B. Durrant, and M. W. Berns, *J. Biomed. Opt.* **11**(4), 044001 (2006) and in "Computer-based tracking of single sperm," by L. Z. Shi, J. M. Nascimento, M. W. Berns, and E. L. Botvinick, *J. Biomed. Opt.* **11**(5), 054009 (2006).

The dissertation author was the first author of the former paper and second author of the latter.

References

Berns, M. W., Botvinick, E., Liaw, L., Sun, C-H, Shah, J. (2005). Micromanipulation of chromosomes and the mitotic spindle using laser microsurgery (laser scissors) and laser-induced optical forces (laser tweezers). in *Cell Biology: A Laboratory Handbook*, Elsevier Press, Burlington.

Biggers, J. D., Whitten, W. D., Whittingham, D. G. (1971). The culture of mouse embryos in vitro. in *Methods of mammalian embryology*, San Francisco: Freeman.

Durrant, B. S., Harper, D., Amodeo, A., Anderson, A. (2000). Effects of freeze rate on cryosurvival of domestic dog epididymal sperm. *J. Andrology*. Suppl. 59, 21.

Harper, S. A., Durrant, B. S., Russ, K. D., Bolamba, D. (1998). Cryopreservation of domestic dog epididymal sperm: A model for the preservation of genetic diversity. *J. Andrology*. Suppl. 50, 19.

Liaw, L. H. and Berns, M. W. (1981). Electron microscope autoradiography on serial sections of preselected single living cells. *J. Ultrastruct* **75**, 187–194.

Shi, L. Z., Nascimento, J., Berns, M. W., Botvinick, E. (2006). Computer-based tracking of single sperm. *J. Biomed. Opt.* **11**(5), 054009.

Tadir, Y., Wright, W. H., Vafa, O., Ord, T., Asch, R. H., Berns, M. W. (1989). Micromanipulation of sperm by a laser generated optical trap. *Fertil. Steril.* **52**(5), 870-873.

Wang, Y., Botvinick, E., Zhao, Y., Berns, M. W., Usami, S., Tsien, R. Y., Chien, S. (2005). Visualizing the mechanical activation of Src. *Nature* **434**(7036), 1040-1045.

Zar, J. H. (1984) *Biostatistical Analysis*, Prentice Hall, Englewood Cliffs.

IV. Correlation of sperm swimming speed, swimming force, and speed of progression score as assessed by optical tweezers

4.1 Introduction

In fertility physiology studies, the Speed of Progression (SOP) score is often used as a key parameter in the determination of overall motility score of a semen sample where motility score = (% motile)*(SOP score of sample)^2 (Olson *et al.* 2003). The motility score is used to estimate the probability of a successful fertilization. The SOP score takes on discrete values from 1 – 5, 5 qualitatively represents the fastest swimming sperm and 1 represents the sperm that exhibit the least amount of forward progression (Olson *et al.* 2003). Also, a sperm may receive a higher SOP score if it is exhibiting hyperactive motility (having large lateral head movement, for example). Since the SOP score is qualitative, it may be subject to variation between individuals. Swimming velocity, trajectory curvature, displacement, and lateral head movement are other parameters used to assess sperm motility.

Optical forces from a single beam gradient laser trap can be used to confine and manipulate microscopic particles (Ashkin 1991 and 1998). These optical traps have been used to study laser-sperm interactions and sperm motility by measuring sperm swimming forces (Konig *et al.* 1996; Araujo *et al.* 1994; Dantas *et al.* 1995; Patrizio *et al.* 2000; Tadir *et al.* 1990 and 1998). These studies determined that the minimum amount of laser power needed to hold the sperm in the trap (or the threshold

escape power) is directly proportional to the sperm's swimming force ($F = Q * P / c$, where F is the swimming force, P is the laser power, c is the speed of light in the medium, and Q is the geometrically determined trapping efficiency parameter (Konig *et al.* 1996)). These studies used the measurement of sperm swimming forces to evaluate sperm viability by characterizing the effects of cryopreservation of sperm (Dantas *et al.* 1995) and comparing the motility of epididymal sperm to ejaculated sperm (Araujo *et al.* 1994). The human sperm studies found that as swimming speed increased, the average escape power also increased (Tadir *et al.* 1990). This correlation was found for a population of relatively slow swimming sperm. SOP scores were not assigned to the sperm in this study; however, sperm of these speeds are typically assigned an SOP score of 2. It is the purpose of the present study more specifically to determine if there is a quantitative relationship between sperm swimming forces, their swimming speeds and the SOP scores (ranging from 2 – 4).

4.2 Materials and Methods

4.2.1 Specimen

Semen samples collected from several dogs were pooled and cryopreserved according to a published protocol (Durrant *et al.* 2000; Harper *et al.* 1998). Semen samples were also collected from two dogs, different than the dogs used in the pooled sperm samples, and cryopreserved individually (dog 1: labeled 04-060, dog 2: labeled 05-037). Dog 2's semen sample was subdivided into two samples in order to test for experimental errors in sperm preparation from one day to the next. For each experiment, a sperm sample is thawed in a water bath (37^{o}C) for approximately one to

two minutes and its contents are transferred to an Eppendorf centrifuge tube. The sample is centrifuged at 2000 rpm for ten minutes (centrifuge tip radius is 8.23cm). The supernatant is removed and the remaining sperm pellet is suspended in 1 milliliter (mL) of pre-warmed media (1mg of bovine serum albumin (BSA) per 1mL of Biggers, Whittens, and Whittingham (BWW), osmolarity of 270 – 300 mmol/kg water, pH of 7.2 – 7.4 (Biggers *et al.* 1971)). Final dilutions of 30,000 sperm per mL of media are used in the experiments. The specimen is loaded into a rose chamber and mounted into a microscope stage holder (Liaw and Berns 1981). The sample is kept at room temperature. To quantify the effects of temperature, control experiments were conducted using an air curtain incubator (NEVTEK, ASI 400 Air Stream Incubator, Burnsville, VA) to achieve 37^{o}C at the specimen.

4.2.2 Hardware, software and optical design

Chapter 3 provides a detailed description (including figures) describing the hardware, software and optical design used for the experiments in this chapter. Briefly, a single point gradient trap was generated using a Nd:YVO4 continuous wave 1064nm wavelength laser (Spectra Physics, Model BL-106C, Mountain View, CA) coupled into a Zeiss Axiovert S100 microscope and a 40x, phase III, NA 1.3 oil immersion objective (Zeiss, Thornwood, NY) which is also used for imaging. An additional optic, a polarizer, is used to control the laser power in the specimen plane for these power decay experiments (see chapter 3, figure 3.1 (a)). Laser power is attenuated by rotating the polarizer, which is mounted in a stepper-motor-controlled rotating mount (Newport Corporation, Model PR50PP, Irvine, CA). The mount is

controlled by a custom program that allows the experimenter to set the power decay rate (rotation rate of polarizer) and record power decay parameters once the sperm escapes the trap.

The specimen is imaged at 30 frames per second by a CCD camera (Sony, Model XC – 75, New York City, NY), coupled to a variable zoom lens system (0.33X magnification) to increase the field of view. Analog output (RS-170 format) from the CCD is wired into the video-in port of a digital camcorder to record sperm swimming for off-line analysis. Prior to laser trapping, the microscope stage was momentarily halted (3 to 5 sec) to record video footage of the swimming sperm. Similar footage was acquired after trapping. Video sequences of the swimming sperm from the digital camcorder are converted into bitmap format with Adobe Premier Pro 1.5 (Adobe Systems Incorporated, San Jose, CA). The bitmap images are then loaded into a custom tracking program developed in LabView 7.1 (National Instruments, Austin, TX). The swimming velocity (curvilinear velocity, VCL, μm/sec) before and after trapping is calculated based on the pixel (x, y) coordinates of the sperm's swimming trajectory.

4.2.3 Relationship between swimming force and swimming speed

The rotation rate of the motorized mount which holds the polarizer is programmed to produce a linear power decay from maximum (100%) to minimum (≈0%) in ten seconds. A maximum trapping power of 366mW in the specimen plane was used in these experiments. Studies were conducted on sperm samples pooled

from four dogs as well as on sperm samples from individual dogs that were not pooled.

A sperm of interest is observed for three to six seconds before and after trapping. Once a sperm is trapped, the user initializes the power decay within one second. The moment the sperm escapes the trap, the user halts the power decay and the escape power is recorded by the computer. Recorded video segments pre and post trapping are analyzed by the custom software to calculate the VCL, straight line velocity (VSL), total distance traveled, and ratio of displacement to total distance traveled. Video of the sperm are independently analyzed by three fertility experts, each blind of the VCL and VSL, who assign each sperm an SOP score (based on the 1 – 5 scale).

The data from the pooled dog sperm sample is organized into a matrix with each row representing a single sperm and each column containing the non-subjective measurements: (1) VCL pre trapping, (2) escape laser power (Pesc), (3) swimming displacement pre trapping, (4) curvilinear distance traveled pre trapping, and (5) ratio of displacement to total distance traveled. Principal components analysis (PCA) of the data matrix was performed in order to seek hidden relationships between the five measurements (StatSoft Inc. 2003). In PCA, the data matrix is linearly mapped into principal component (PC) space after standardizing each column by the estimate of its standard deviation. The data is transformed by:

$$new\_data(n,m) = \sum_{i=1}^{N} \left[\left(std\_data(n,i) - mean(std\_data(:,i)) \right) * w(i.m) \right]$$

where *w(i,m)* are the PC weights for a matrix of *n* rows and *m* columns and *std_data* is the standardized data set. The first two measurements (principal components) of the new data set contain the majority of the variation in the data (the greatest variance, ~50-60%, by any projection of the data set lies on the first axis and the second greatest variance, ~20-30%, on the second axis (StatSoft Inc. 2003)). Plotted against one another, they display a more compact distribution of the data as compared to the original measurements.

A supervised classifier using modified SOP scores for training was implemented to determine the most probable hyperplane(s) for separating classes of sperm in PC space. The SOP scores were modified since the number of separable sperm classes was not found to be necessarily equal to the number of SOP classifications, likely due to the subjectivity of the SOP scoring system. Instead, the number of sperm classes was determined by the number of statistically separable groups within the SOP scoring system, as assessed by the Wilcoxon paired-sample test (Zar 1984). The supervised classifier returns the misclassification error rate, which is the percentage of observations in the data set that are reclassified with respect to the modified SOP scores. Classified data is remapped into the original data space to understand the physical implications of the determined classes. VCL is plotted against Pesc for each class and robust linear fitting is applied to seek a trend within each sperm class.

The trained classifier was tested with naïve data consisting of two individual, as opposed to pooled, dog sperm samples (exclusive from the pooled sperm sample

set). The classifier first maps the naïve data into PC space using PC weights calculated from the pooled dog data set. The data is then classified using the pooled data as a training set. Linear regressions of Pesc vs. VCL are fit to each resulting class of sperm. This procedure is also used to test the effects of sample temperature by analyzing individual dog sperm samples at room temperature (approximately 25^{o}C) and at 37^{o}C.

4.3 Results

Figure 4.1 plots Pesc (mW) against VCL (μm/sec) for the pooled dog sperm data set. A linear relationship between swimming speed and Pesc was found with $R^2 \approx$ 0.9 using a robust linear regression. However, applying this regression is contrary to a qualitative analysis of the data that suggests there may be intrinsic groupings, each with their own Pesc to VCL relationship. For example, potential groupings could be a high escape power group and a low escape power group or a slow group and a fast group with high Pesc outliers. In attempt to identify potential groupings, the data was labeled according to the SOP scores assigned by each of the three qualified sperm scoring experts. The results are shown in figure 4.2. This figure demonstrates the subjective nature and emphasizes the variability of SOP scores. The variation between the scores assigned by the three experts is determined. Only 41.3% of the sperm received an identical score from all three experts. Sperm received the same score from two out of the three experts 51.1% of the time. Finally, 7.6% of the sperm received a different score from each of the three experts.

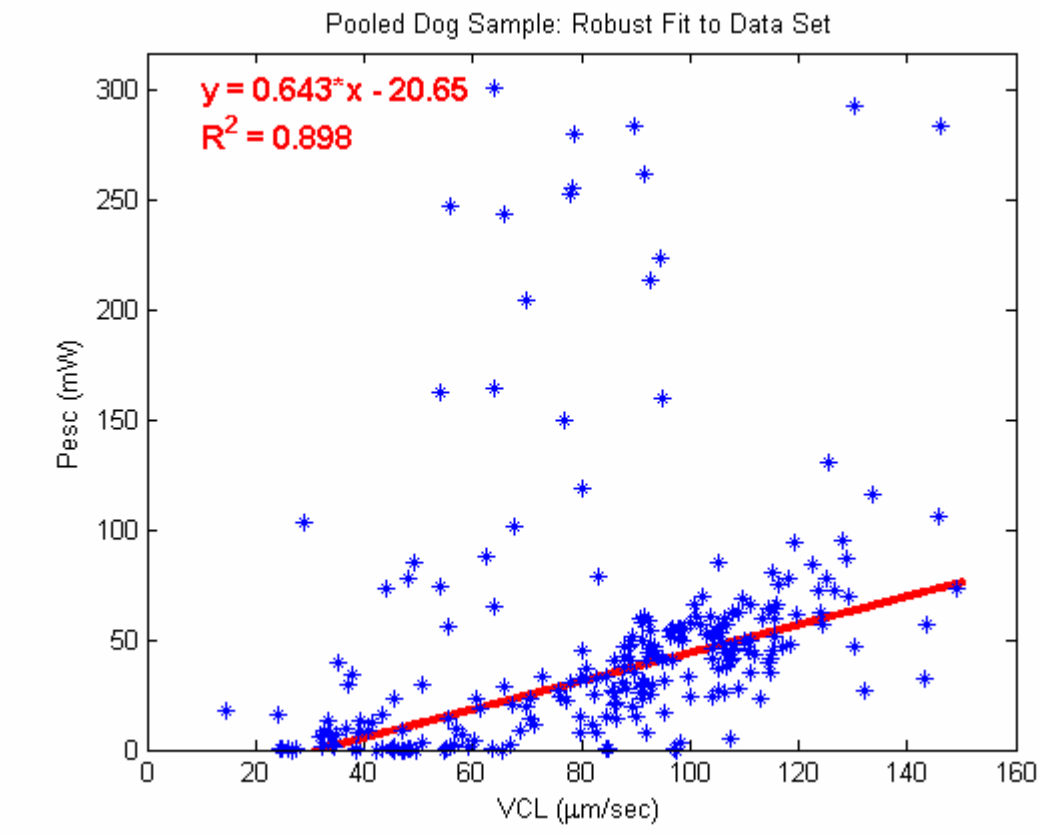

Figure 4.1: Pesc (mW) plotted against VCL (µm/sec) for pooled dog sperm sample. A robust linear regression is applied to the data set, showing a linear relationship between the two parameters. Inset in the figure is the slope, y-intercept and R^2 values for the regression.

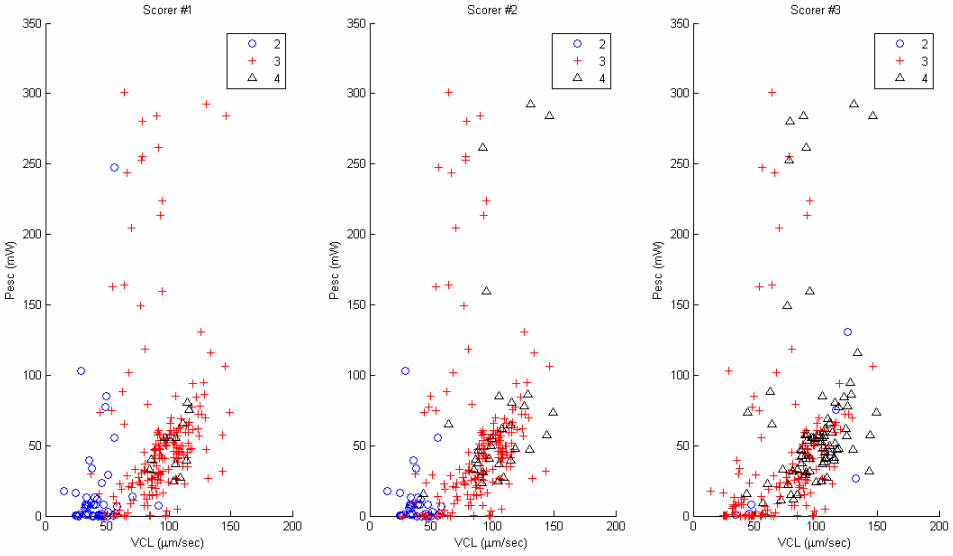

Figure 4.2: Discrepancy between SOP score assignment between individuals: Pesc vs. VCL for the pooled dog sperm sample with scores assigned by scorers #1, #2, and #3 (left to right). Sperm given an SOP score of 2 are labeled in blue circles, 3's are red crosses, and 4's are black triangles.

PC analysis consolidated 73% of the variation in the data to within the first two principle components. Table 4.1 lists the percent variability accounted for by each PC as well as the PC weights. Figure 4.3 plots PC1 vs. PC2 for the pooled sperm data.

Table 4.1: Principal Component Analysis: Percentage of variability each PC is responsible for and the PC weights for each measurement that transform the original data of pooled dog sperm samples into new data (PC space).

	PC 1	**PC 2**	**PC 3**	**PC 4**	**PC 5**
% Variability Explained	52.0663%	21.1449%	15.9962%	10.2293%	0.5633%
VCL	-0.48	0.11	-0.04	0.87	0.04
Pesc	-0.26	0.59	0.74	-0.18	-0.001
Disp	-0.58	-0.23	-0.10	-0.33	0.71
Dist Pt2Pt	-0.49	-0.55	0.23	-0.16	-0.62
Disp/ Dist Pt2Pt	-0.36	0.54	-0.62	-0.28	-0.34

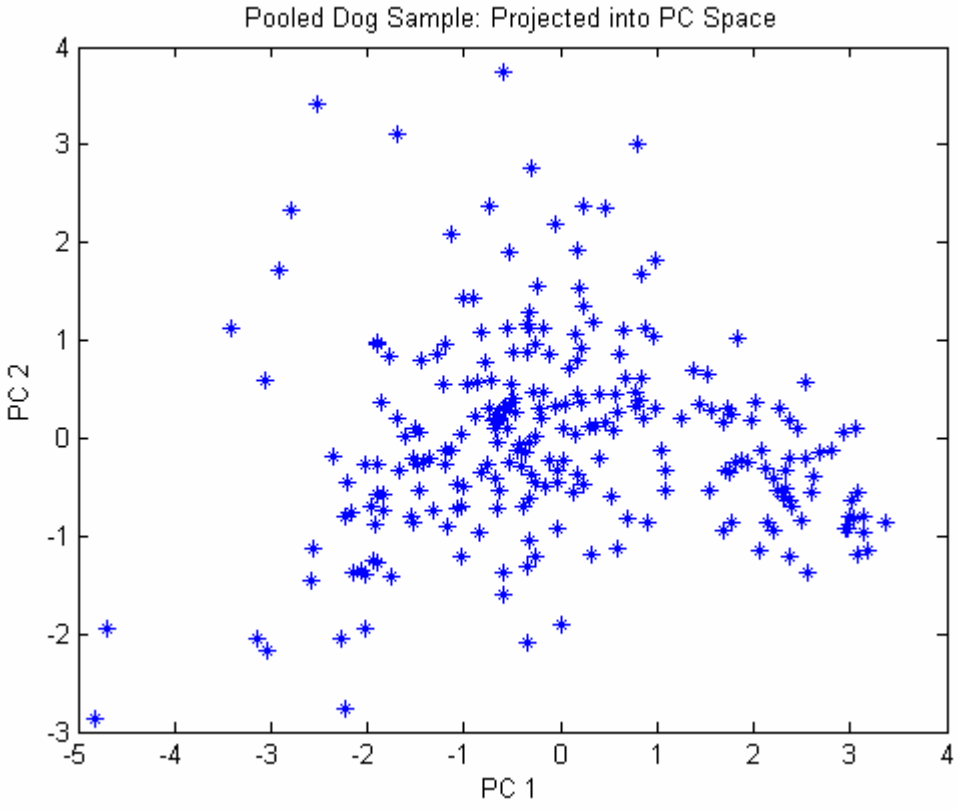

Figure 4.3: Pooled dog sperm data set in principal component (PC) space.

To test uniqueness of the SOP scores, Wilcoxon paired-sample tests (Zar 1984) for equal median (5% significance level) were performed on Pesc distributions of sperm grouped by SOP score, for each scorer. Table 4.2 summarizes the number of significantly separable groups each scorer distinguished. Two of the three scorers uniquely distinguished at most two groups of sperm, consisting of "slower" and "faster" swimmers. For the purpose of classification in PC space, modified SOP scores were constructed based on these findings: "slower" = SOP 2* and "faster" = SOP 3* (Table 4.2 maps SOP scores to modified SOP scores for each scorer).

Table 4.2: Defining sperm classes: The Wilcoxon paired-sample test applied to pooled dog sperm sample shows which scorers distinguish a separation between sperm of different SOP scores and the overall number of distinct classes each scorer can differentiate. Last two columns show how each sperm's original SOP score is reassigned to fit the new SOP* classes.

	SOP 2 vs. SOP 3	**SOP 3 vs. SOP 4**	**# Distinct Classes**	**SOP 2***	**SOP 3***
Scorer #1	Unequal Medians ($P < 0.05$)	Equal Medians ($P > 0.05$)	2	SOP 2	SOP 3 & 4
Scorer #2	Unequal Medians ($P < 0.05$)	Unequal Medians ($P < 0.05$)	3	SOP 2	SOP 3 & 4
Scorer #3	Equal Medians ($P > 0.05$)	Unequal Medians ($P < 0.05$)	2	SOP 2 & 3	SOP 4

Figure 4.4 plots the pooled dog sperm data in PC space labeled by their modified SOP scores for scorers #1 and #2. As can be seen, the region of support lies nearly along a straight line. A supervised classifier with a linear hyperplane was found to yield the lowest classification error rate (7.44%). A classifier based on scorer #3 had a misclassification error rate of 28.05% (not shown). Subsequent data analysis is based only on classifiers trained from scorers #1 and #2.

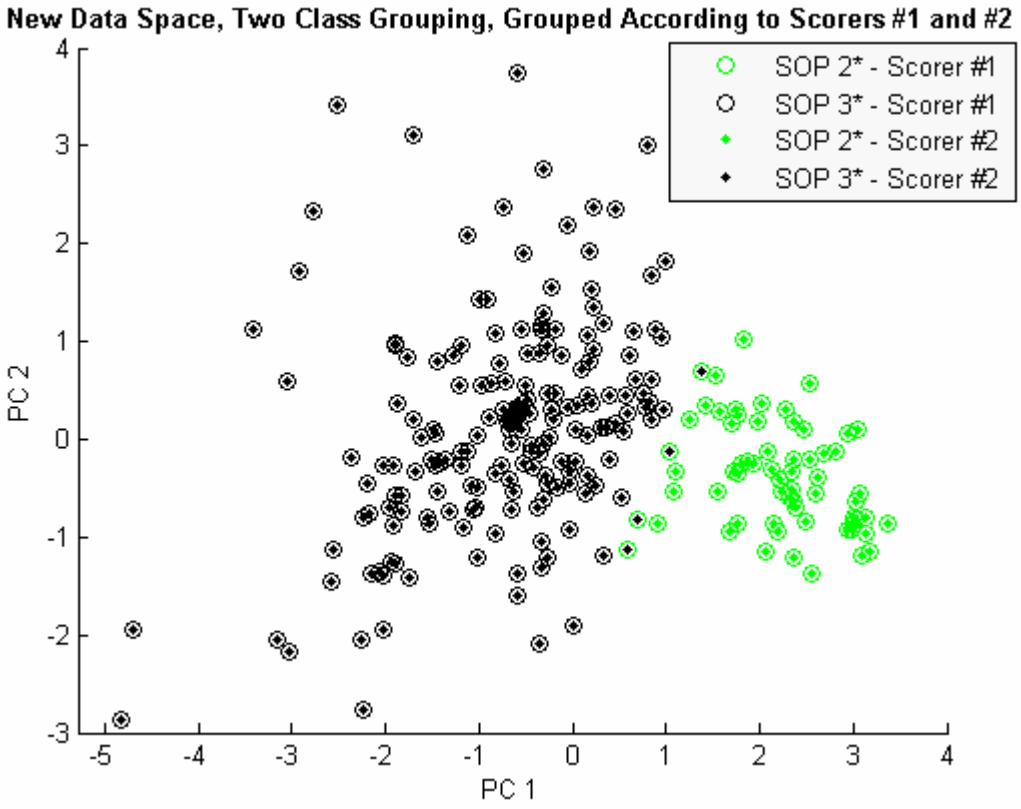

Figure 4.4: Data Variation Maximization: Pooled dog sperm data set in PC space - Optimum group division shown for two classes. Scorer #1 plotted as circles, scorer #2 plotted as dots, both showing SOP 2^* group in green and SOP 3^* group in black.

Figure 4.5 plots the data of figure 4.1 labeled by classifier output. Linear regressions with robust fitting for each group (SOP 2^*, SOP 3^*) are shown for scorer #1 and #2 (figure 4.5a and 4.5b respectively). Table 4.3 lists the slopes (m), y-intercepts and R^2 values for linear regressions applied to the original data set and applied to the classified groups, by scorer. Regressions were compared using the Student's T-test (Zar 1984). Regression parameters of the original data were statistically different from the SOP 2^* and SOP 3^* groups casting doubt on the validity of regressing the entire data set. Interestingly, SOP2^* slopes showed little to no relationship between Pesc and VCL (mean value was 0 or 0.02 for scorers #1 and #2 respectively). Both scorers revealed an SOP3^* group with equivalent non-zero slopes. This suggests the SOP 3^* group has a linear Pesc to VCL dependence.

(a)

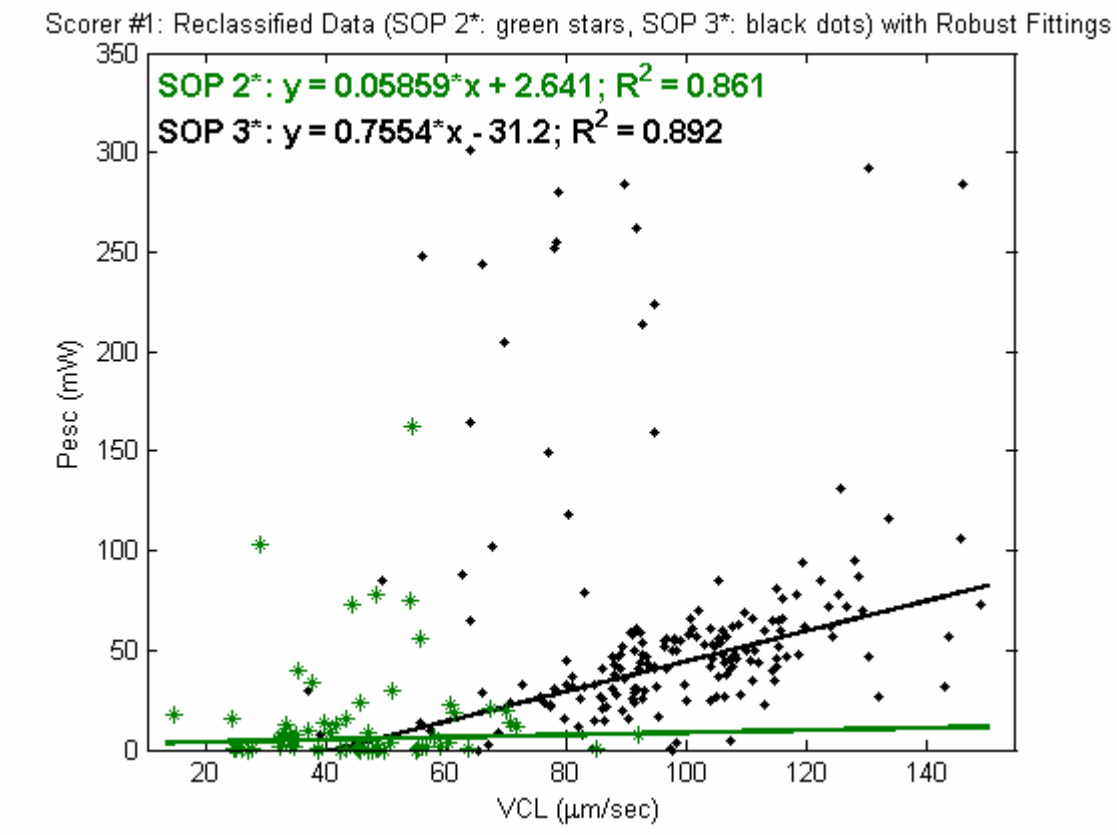

Figure 4.5: Classified data with regressions: Pesc vs. VCL for pooled dog sperm sample is plotted according to the reclassification for Scorer #1 (a) and #2 (b) with robust linear regressions applied to each sperm class.

(b)

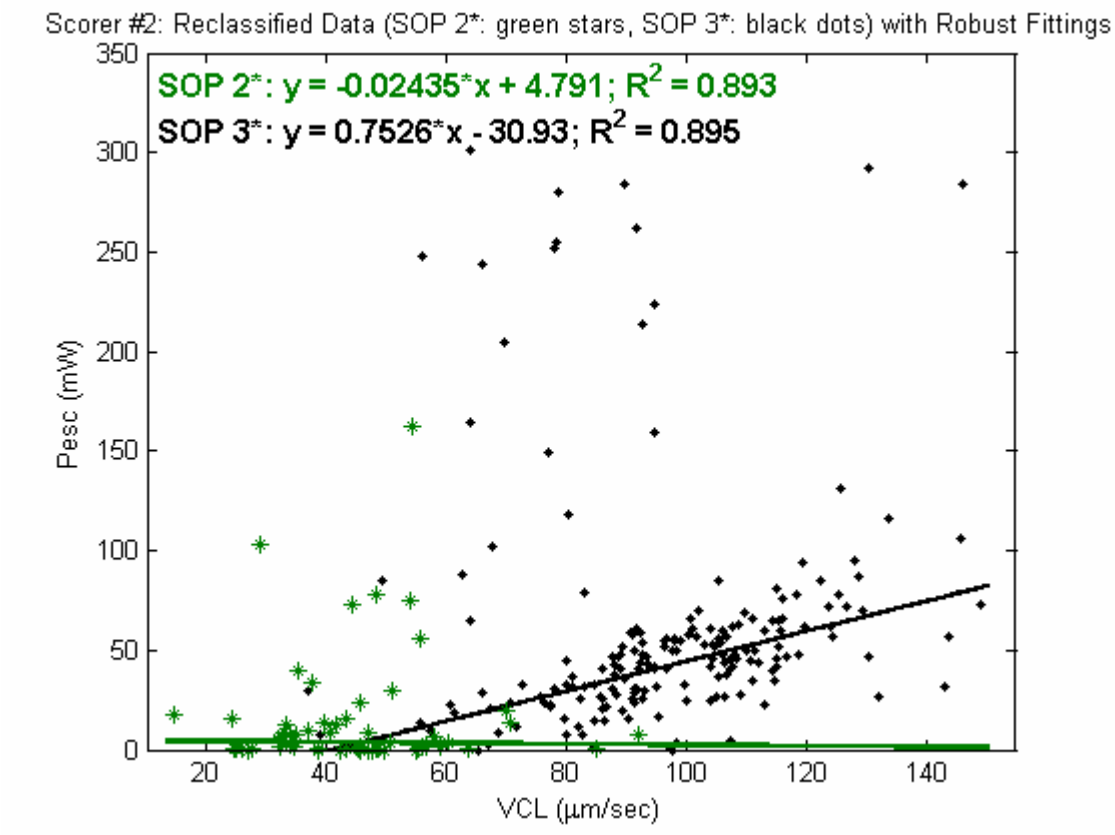

Figure 4.5 (continued): (b) Classified data with regressions for Scorer #2.

Of interest are the outlying sperm that escape the trap at higher powers than the majority of the sperm analyzed. They were neither identifiable by their SOP score (see figure 4.2), nor as an independent group using PCA and supervised classification. One possibility is that these outlier sperm are all from one specific dog within the pooled sample which has stronger swimming sperm. This theory is tested by repeating the experiment using the single dog sperm samples. Figure 4.6 plots Pesc vs. VCL for the individual dog sperm samples (dog 1 and dog 2 tested on separate

days) superimposed with the pooled dog sample data. Both individual dog sperm samples exhibit two groups of sperm, slower and faster swimming, as well as outlying sperm that escape the trap at higher trapping powers. Using the Wilcoxon rank sum test, VCL and Pesc of dog 2 were found to have equal medians ($P > 0.05$) between days one and two.

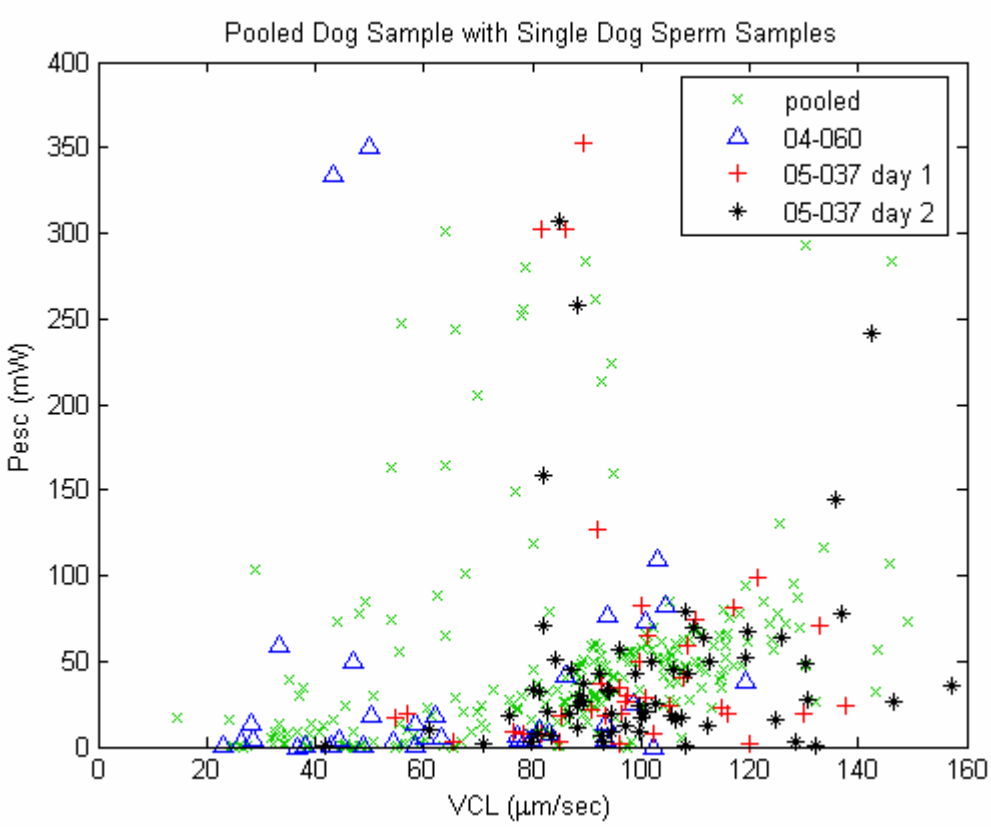

Figure 4.6: Comparison of individual samples with pooled samples: Pesc vs. VCL for individual dog sperm samples referenced with pooled dog sample. Dog 1 in blue triangles, dog 2 (day 1) in red crosses, dog 2 (day 2) in black asterisks, and pooled dog in green x's.

The individual dog sperm data sets are grouped together and transformed into PC space by the PC weights calculated with the pooled dog sperm data (figure 4.7 a – d). Figure 4.7 (a) shows the single dog sperm data set transferred into PC space (PC 2 vs. PC 1). Figure 4.7 (b) plots the single dog sperm data set in PC space in addition to the pooled dog data set in PC space. Subsequent classification (trained on the pooled dog data) had a classification error rate of 1.36%. Figure 4.7 (c) plots the single dog sperm data set in PC space classified according to the modified SOP scoring system. Figure 4.7 (d) plots this same data in addition to the classification of the pooled dog data set in PC space. Figure 4.8 plots Pesc against VCL for the classified single dog sperm data along with the linear regressions. The linear regression of the SOP 2^* group shows a near zero slope while regression of the SOP 3^* group finds a linear increase in swimming force with swimming speed. Table 4.3 summarizes the regression results.

(a)

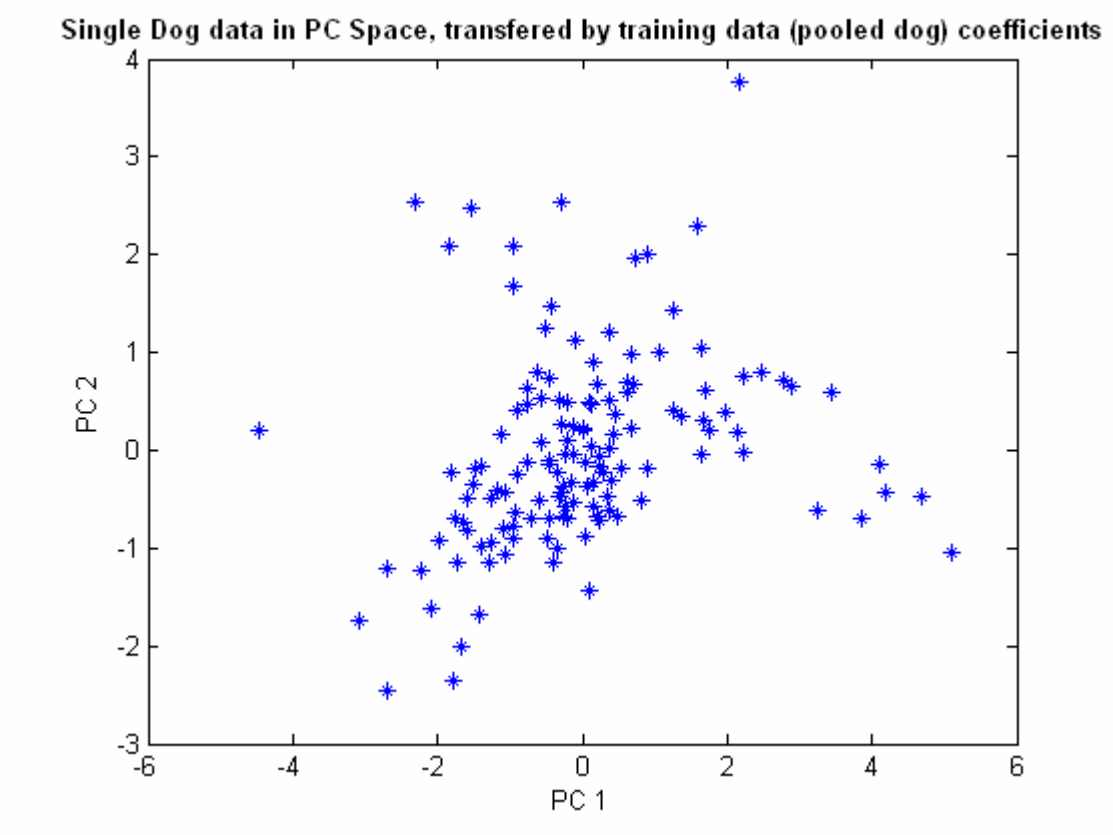

Figure 4.7: Single dog sperm data in PC space. Data is transferred into PC space using weights calculated from the training data (pooled dog data set). (a) unclassified single dog data; (b) unclassified single dog data in blue asterisks plotted with the original pooled dog data in green crosses (see figure 4.3); (c) single dog data classified according to the modified SOP scores; (d) single dog data classified according to the modified SOP scores (crosses and asterisks) plotted with the original pooled dog data classified according to the same modified SOP scores (x's) (see figure 4.4).

(b)

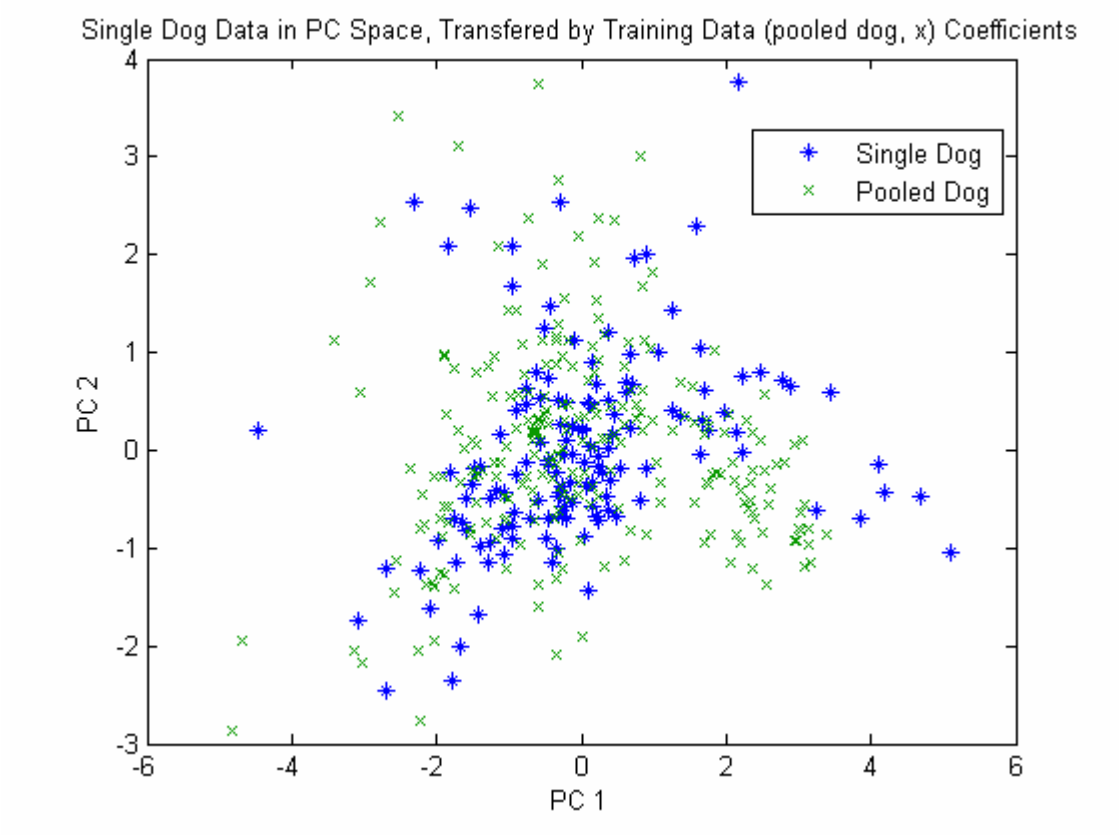

Figure 4.7 (continued): (b) Unclassified single dog data in blue asterisks plotted with the original pooled dog data in green crosses (see figure 4.3).

(c)

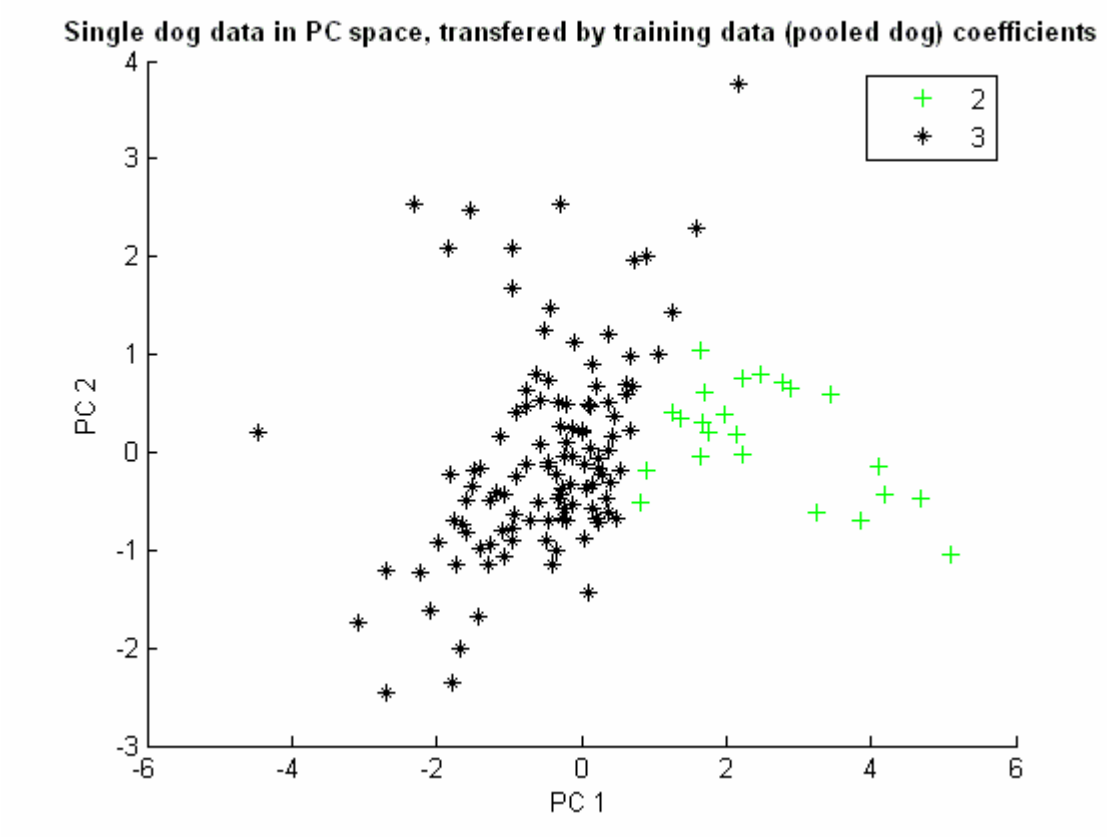

Figure 4.7 (continued): (c) Single dog data classified according to the modified SOP scores.

(d)

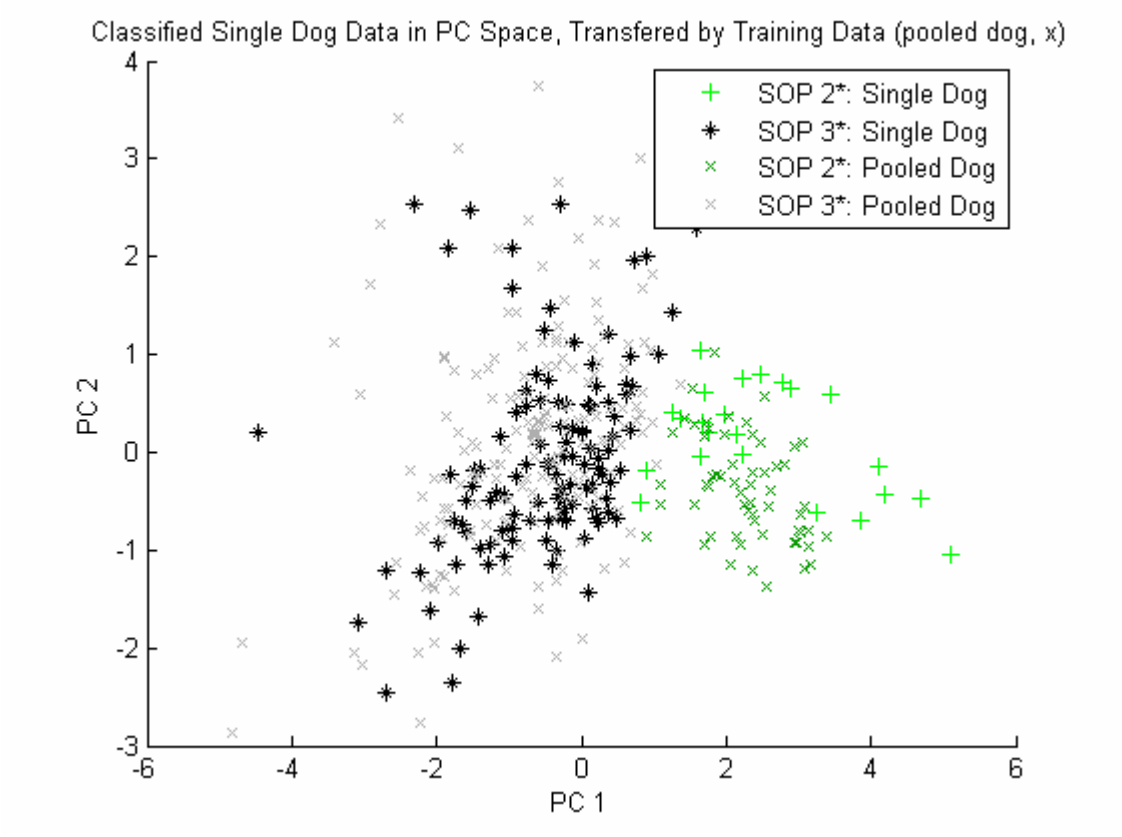

Figure 4.7 (continued): (d) Single dog data classified according to the modified SOP scores (crosses and asterisks) plotted with the original pooled dog data classified according to the same modified SOP scores (x's) (see figure 4.4).

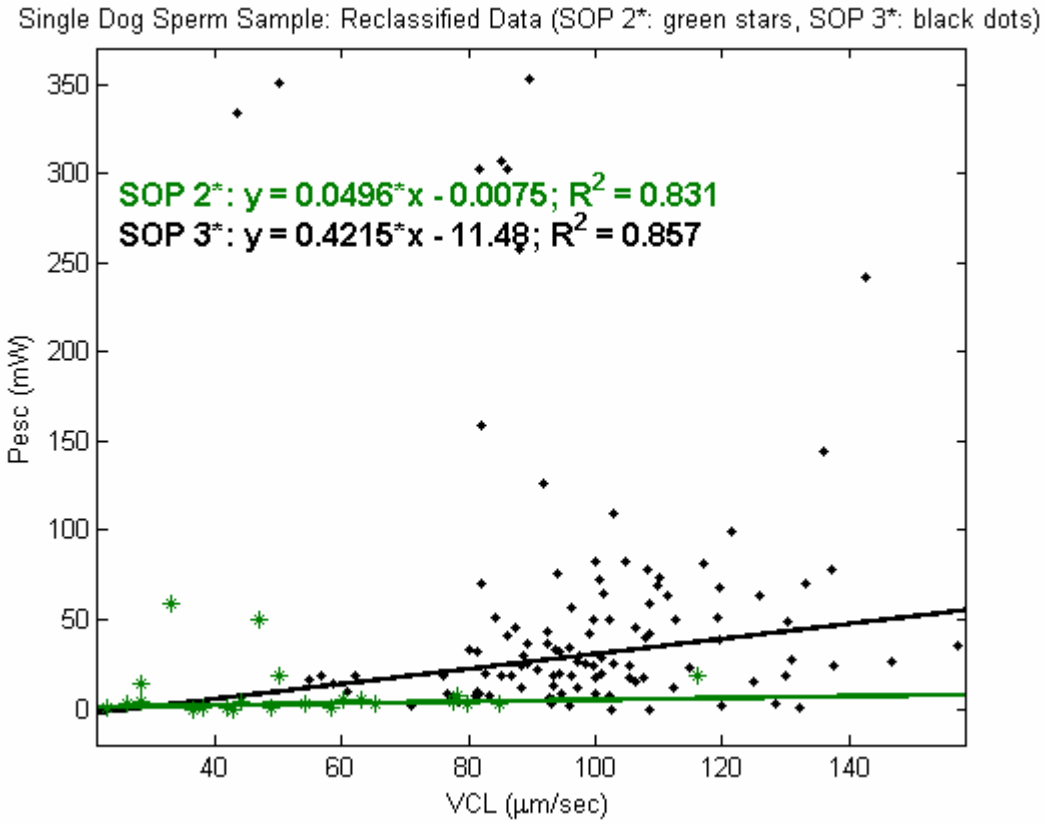

Figure 4.8: Classified single dog sperm data with regressions: Pesc vs. VCL for single dog sperm sample is plotted according to the reclassification based on the modified SOP scoring system with robust linear regressions applied to each sperm class.

Table 4.3: Unclassified vs. classified data: Comparison of regression values (slope, y-intercept and R^2) for the four sets of regressions applied to the pooled dog sperm data (original, reclassified for scorer #1, reclassified for scorer #2) and the individual dog sperm data.

	Original Data	**Scorer #1: SOP 3***	**Scorer #1: SOP 2***	**Scorer #2: SOP 3***	**Scorer #2: SOP 2***	**Individual Dog Sperm (SOP 2*)**	**Individual Dog Sperm (SOP 3*)**
Slope (m)	0.6430	0.7554	0.0586	0.7526	-0.0244	0.0496	0.4215
y-int	- 20.65	- 31.20	2.64	- 30.93	4.79	-0.0075	-11.48
R^2 Value	0.8977	0.8924	0.8610	0.8952	0.893	0.8307	0.8567

Sperm velocity distributions were found to be of equal median ($P > 0.05$) for a sample analyzed at room temperature and at 37°C. Regressions fit to escape power vs. VCL are found to be statistically equivalent ($P > 0.05$).

4.4 Discussion

Escape power plotted against VCL suggests a complicated relationship. The inclusion of standard SOP scores neither assisted in categorizing the data into non-overlapping domains, nor provided a deeper understanding of the data. The SOP scores were found to be neither independent nor mutually exclusive, requiring a modification of the SOP scores into two new SOP scores (SOP 2^* and SOP 3^*). These modified SOP scores were used to train a classifier operating on the first 2 PCs of motility measurements. This analysis revealed at least two distinct classes of sperm separated along the VCL axis of a Pesc vs. VCL plot. Linear regressions applied separately to the two sperm classes were found to be significantly different than the regression of the entire data set.

Two conclusions can be drawn from these results. The first is that the SOP 2^* and SOP 3^* sperm have significantly different dependencies of Pesc on VCL. Pesc for the SOP 2^* sperm was not found to increase with swimming speed. This could be either a biological phenomenon or an experimental bias since it is difficult to pinpoint the precise moment that a slow swimming sperm escapes from the trap. Sperm in this category require further investigation with an incrementally decreasing step function in laser power, rather than a continuous linear downward ramp. In the SOP 3^* group Pesc increased linearly with swimming speed. This is consistent with the relationship

between swimming force and viscous resistance for sperm swimming at constant thrust. Experiments are currently being conducted on other species to determine if parameters of classification and linear regression correlate to species type.

The second conclusion is that Pesc is necessary but not sufficient to distinguish SOP 2^* from SOP 3^* sperm. Figure 4.4 shows that variation in the data is primarily along the PC 1 axis where the Pesc weight is minimal. However, the hyperplane dividing the two groups is not parallel to the PC 2 axis. Therefore the PC 2 dimension nontrivially determines the sperm class. In this system escape power is a critical parameter in sperm classification since it has the largest weight in PC 2, which represents 21.14% of the variability in the data. Therefore, it is concluded that the effective use of escape power as a variable to assess sperm motility requires that it be used in conjunction with other established parameters (velocity, displacement, etc.) to characterize the sperm. This combination results in a more comprehensive evaluation of overall sperm quality.

Results from individual dog sperm samples negated the notion that outlier sperm were artifacts of experimental technique. Individual dog data also validated the classifier, which was trained on the pooled dog sperm sample. Classifier validation showed low error rates and an equivalent separation of sperm classes between the training (pooled) and testing (individual) data, suggesting we have observed a general phenomenon, and not just one confined to the pooled dog sperm.

The individual dog sperm analysis also confirmed the presence of “outlier” sperm and negated the notion that outlier sperm in the pooled dog sperm data

represented the sperm of one single dog. The existence of outliers may point to a fundamental physiological distribution in sperm phenotype. It is possible that outlier sperm are in a state of increased physiological energetics (such as at a higher rate of ATP production and/or consumption) and may respond to physical/chemical barriers in a distinctly different manner than the rest of the sample. Fluorescent probes capable of measuring energetics and metabolism should 'shed light' on the outlier sperm. If there is a subgroup of sperm within a semen sample that exhibits higher motility characteristics, their separation and study could be of considerable value in both basic and applied infertility research. The fact that a ubiquitous class of sperm can be identified using laser trapping force measurements means that a method now exists to assign "swimming force" scores directly to individual sperm. Furthermore, an overall force value can be assigned to any given semen sample. In conclusion, in this chapter I have described the use of a laser optical trap to measure the swimming force(s) of a large number of individual sperm in a semen sample, thus expanding the quantitative parameters available for assessment of sperm motility and semen quality.

Acknowledgements

The material presented in Chapter 4 is, in part, a reprint of the material as it appears in "Analysis of sperm motility using optical tweezers," by J. M. Nascimento, E. L. Botvinick, L. Z. Shi, B. Durrant, and M. W. Berns, *J. Biomed. Opt.* **11**(4), 044001 (2006). The dissertation author was the first author of the paper.

References

Araujo, E. Jr., Tadir, Y., Patrizio, P., Ord, T., Silber, S., Berns, M. W., Asch, R. H. (1994). Relative force of human epididymal sperm. *Fertil. Steril.* **62**(3), 585-590.

Ashkin, A. (1991). The study of cells by optical trapping and manipulation of living cells using infrared laser beams. *ASGSB Bull* **4**(2), 133-146.

Ashkin, A. (1998). Forces of a single-beam gradient laser trap on a dielectric sphere in ray optics regime. *Methods Cell. Biol.* **55**, 1-27.

Biggers, J. D., Whitten, W. D., Whittingham, D. G. (1971). The culture of mouse embryos in vitro. in *Methods of mammalian embryology*, San Francisco: Freeman.

Dantas, Z. N., Araujo, E. Jr., Tadir, Y., Berns, M. W., Schell, M. J., Stone, S. C. (1995). Effect of freezing on the relative escape force of sperm as measured by a laser optical trap. *Fertil. Steril.* **63**(1), 185-188.

Durrant, B. S., Harper, D., Amodeo, A., Anderson, A. (2000). Effects of freeze rate on cryosurvival of domestic dog epididymal sperm. *J. Andrology*. Suppl. 59, 21.

Harper, S. A., Durrant, B. S., Russ, K. D., Bolamba, D. (1998). Cryopreservation of domestic dog epididymal sperm: A model for the preservation of genetic diversity. *J. Andrology*. Suppl. 50, 19.

Konig, K., Svaasand, L., Liu, Y., Sonek, G., Patrizio, P., Tadir, Y., Berns, M. W., Tromberg, B. J. (1996). Determination of motility forces of human spermatozoa using an 800 nm optical trap. *Cell Mol. Biol. (Noisy-le-grand)* **42**(4), 501-509.

Liaw, L. H. and Berns, M. W. (1981). Electron microscope autoradiography on serial sections of preselected single living cells. *J. Ultrastruct* **75**, 187–194.

Olson, M. A., Yan, H., DeSheng, L., Hemin, Z., Durrant, B. (2003). Comparison of Storage Techniques for Giant Panda Sperm. *Zoo Biology* **22,** 335-345.

Patrizio, P., Liu, Y., Sonek, G. J., Berns, M. W., Tadir, Y. (2000). Effect of pentoxifylline on the intrinsic swimming forces of human sperm assessed by optical tweezers. *J. Androl.* **21**(5), 753-756.

StatSoft, Inc. *Principal Components and Factor Analysis* (2003) <http://www.statsoft.com/textbook/stfacan.html>.

Tadir, Y., Wright, W. H., Vafa, O., Ord, T., Asch, R. H., Berns, M. W. (1989). Micromanipulation of sperm by a laser generated optical trap. *Fertil. Steril.* **52**(5), 870-873.

Tadir, Y., Wright, W. H., Vafa, O., Ord, T., Asch, R. H., Berns, M. W. (1990). Force generated by human sperm correlated to velocity and determined using a laser generated optical trap. *Fertil. Steril.* **53**(5), 944-947.

Zar, J. H. (1984). *Biostatistical Analysis*, Prentice Hall, Englewood Cliffs.

V. Effects of cryopreservation on sperm swimming speed and swimming force

5.1 Introduction

Sperm cryopreservation offers many benefits in genetic improvement programs, such as selective breeding and domestication (Dong *et al.* 2005; Maxwell *et al.* 2007). Long-term cryopreservation of semen provides a means for gene preservation for endangered species and as well as livestock (Maxwell *et al.* 2007). Domestic animal semen that has been frozen can be used in artificial insemination, which helps maximize the male breeding potential (Su *et al.* 2007; Cotter *et al.* 2005). In addition, cryopreservation provides a reliable supply of sperm without seasonal limitations (Dong *et al.* 2005; Vuthiphandchai *et al.* 2007).

The effects of cryopreservation protocol, technique and types of cryoprotectants at various concentrations on sperm motility have been addressed (Dantas *et al.* 1995; Dong *et al.* 2005; Durrant *et al.* 1994 and 2000; Harper *et al.* 1998; Maxwell *et al.* 2007; Su *et al.* 2007; Vuthiphandchai *et al.* 2007). These studies are important for optimization and standardization of cryopreservation protocol to ensure sperm post-thaw are minimally/negligibly damaged. It is the purpose of this chapter to measure the effects of cryopreservation on five species (domestic dog, domestic cat, Bighorn sheep, Javan banteng, and West Caucasian tur) as assessed by sperm swimming speed and swimming force.

5.2 Materials and Methods

5.2.1 Specimen

Domestic Dog (*Canis familiaris*): A dog was neutered at a veterinary clinic. The testes were sent to the center for Conservation and Research of Endangered Species (CRES) of the Zoological Society of San Diego where the semen sample was extracted from the epididymis (sliced the epididymis into Test Yolk buffer (0% glycerol) and squeezed out with the rounded edge of a pair of curved scissors). An aliquot of the sperm in Test Yolk buffer is reserved as the "fresh" sample, and placed into 4˚C refrigerator until picked up. The rest of the sample was prepared for cryopreservation according to published protocol (Durrant *et al.* 2000; Harper *et al.* 1998).

Domestic Cat (*Felis catus*): A cat was neutered at a veterinary clinic. The testes were sent to CRES where the semen sample was extracted from the epididymis (sliced the epididymis into Test Yolk buffer (0% glycerol) and squeezed out with the rounded edge of a pair of curved scissors). An aliquot of the sperm in Test Yolk buffer is reserved as the "fresh" sample, and placed into 4˚C refrigerator until picked up. The rest of the sample was prepared for cryopreservation according to published protocol (Durrant *et al.* 2000; Harper *et al.* 1998).

Bighorn Sheep (*Ovis canadensis*): The semen sample was extracted from the epididymis of the male approximately one hour post-mortem (sliced the epididymis into Test Yolk buffer (0% glycerol) and squeezed out with the rounded edge of a pair of curved scissors). An aliquot of the sperm in Test Yolk buffer is reserved as the "fresh" sample, and placed into 4˚C refrigerator until picked up. The rest of the sample was prepared for cryopreservation according to a published protocol (Durrant

et al. 1994). Briefly, the technique used for cooling and freezing the sperm is as follows:

1. Slice the epididymis in Test Yolk buffer (0% glycerol) and squeeze out the sperm.
2. Place the sperm into cryovials (375µL extended sperm).
3. Place cryovials in a water bath with room temperature water.
4. Place the water bath into a 4˚C room for 2.5 hours.
5. After 2.5 hours, add 16% glycerol Test Yolk buffer (125µL) for a final concentration of 4% glycerol Test Yolk buffer.
6. Place the vials onto a thick styrofoam rack (2 inches) and place it on top of 3 inches of liquid nitrogen (contained inside of a box). The average rate of freeze from this method is 7˚C per minute.
7. After 15 minutes on the rack, plunge the vials into the liquid nitrogen and store the vials in liquid nitrogen.

Javan Banteng (*Bos javanicus javanicus*): The semen sample was extracted from the epididymis of the male approximately one hour post-mortem (sliced the epididymis into Test Yolk buffer (0% glycerol) and squeezed out with the rounded edge of a pair of curved scissors). An aliquot of the sperm in Test Yolk buffer is reserved as the "fresh" sample, and placed into 4˚C refrigerator until picked up. The rest of the sample was prepared for cryopreservation according to a published protocol (Durrant *et al.* 1994), using the same technique as described for bighorn sheep sperm.

West Caucasian Tur (*Capra caucasica*): The semen sample was extracted from the epididymis of the male approximately one hour post-mortem (sliced the epididymis into Test Yolk buffer (0% glycerol) and squeezed out with the rounded edge of a pair of curved scissors). An aliquot of the sperm in Test Yolk buffer is reserved as the "fresh" sample, and placed into 4˚C refrigerator until picked up. The rest of the sample was prepared for cryopreservation according to a publish protocol (Durrant *et al.* 1994), using the same technique as described for bighorn sheep sperm.

Each fresh sample is picked up from the CRES facility, brought back to the laboratory at UCSD (kept at 4^{o}C using a cool pack while in transport) and prepared for analysis. The sample is transferred to an Eppendorf centrifuge tube and centrifuged at 2000 rpm for ten minutes (centrifuge tip radius is 8.23cm). The supernatant is removed and the remaining sperm pellet is suspended in 1 milliliter (mL) of pre-warmed media (1mg of bovine serum albumin (BSA) per 1mL of Biggers, Whittens, and Whittingham (BWW), osmolarity of 270 – 300 mmol/kg water, pH of 7.2 – 7.4 (Biggers *et al.* 1971)). For the frozen sperm experiments, a sperm sample is thawed in a water bath (37^{o}C) for approximately one to two minutes before transfer to an Eppendorf tube and being centrifuged (2000rpm, 10minutes). Again, the supernatant is removed and the remaining sperm pellet is suspended in 1 mL of pre-warmed BWW.

For every experiment, final dilutions of ~30,000 sperm per mL of media are used. The specimen is loaded into a rose chamber and mounted into a microscope

stage holder (Liaw and Berns 1981). The sample is kept at 37^{o}C using an air curtain incubator (NEVTEK, ASI 400 Air Stream Incubator, Burnsville, VA).

5.2.2 Hardware, Software and Optical Design

Chapter 3 provides a detailed description (including figures) describing the optical design used for the experiments in this chapter. Briefly, a single point gradient trap was generated using a Nd:YVO4 continuous wave 1064nm wavelength laser (Spectra Physics, Model BL-106C, Mountain View, CA) coupled into a Zeiss Axiovert S100 microscope and a 40x, phase III, NA 1.3 oil immersion objective (Zeiss, Thornwood, NY) which is also used for imaging. The polarizer is used to control the laser power in the specimen plane for the power decay experiments (see chapter 3, figure 3.1 (a)). Laser power is attenuated by rotating the polarizer, which is mounted in a stepper-motor-controlled rotating mount (Newport Corporation, Model PR50PP, Irvine, CA). The mount is controlled by a custom program that allows the experimenter to set the power decay rate (rotation rate of polarizer) and record power decay parameters once the sperm escapes the trap.

The sperm are analyzed using the real-time automated tracking and trapping system (RATTS) which is described in greater detail in Shi *et al*. 2006b. Briefly, phase contrast images of swimming sperm are acquired using a CCD camera (Sony, Model XC – 75, New York City, NY, operating at 30 frames per second) coupled to a variable zoom lens system (0.33X magnification) to increase the field of view and digitized to the computer at video rate. RATTS creates a region of interest (ROI) centered about a sperm in response to a mouse click. The contrast enhancement and

multi-class image segmentation algorithms are applied to extract the tracked sperm head as it transitions in and out of focus. The nearest neighbor method is complemented with a speed-check feature to aid tracking in the presence of additional sperm or other particles. The swimming velocity (curvilinear velocity, VCL, μm/sec) is calculated based on the pixel (x, y) coordinates of the sperm's swimming trajectory:

$$VCL = \frac{\sum_{i=1}^{N}\left(\frac{\sqrt{(x_i - x_{(i-1)})^2 + (y_i - y_{(i-1)})^2}}{\Delta frame} * \frac{micron}{1.39\,pixel} * \frac{30\,frames}{\sec}\right)}{N_{frames}}$$

where *i* is the current frame. Since the sperm is tracked by the head, VCL accounts for both forward progression and lateral head movement. This measurement is the same as that made by conventional Computer Assisted Sperm Analysis (CASA) machines. After 3.33 seconds (100 frames), the average VCL is stabilized (Shi *et al.* 2006a). Therefore, RATTS automatically traps the sperm after 3.33 seconds using the laser tweezers (Shi *et al.* 2006b). Once trapped, the laser power is reduced by rotating the linear polarizer. RATTS monitors a square region, ~10μm/side, centered about the laser (x, y) coordinates. The image within this region is segmented and a size threshold is used to detect the presence or absence of the sperm. RATTS then automatically identifies when the sperm is capable of escaping the trap and records the escape laser power in Watts (Pesc, mW) (Shi *et al.* 2006b). The minimum laser power needed to hold a sperm in a trap is directly proportional to the sperm's swimming force ($F = Q \times P / c$ where F is the swimming force in pN, P is the laser power in

mW, c is the speed of light in the medium with a given index of refraction, and Q is the geometrically determined trapping efficiency parameter) (Konig *et al.* 1996).

Sperm from both fresh and frozen aliquots of every species are analyzed. Sperm swimming speed (VCL, μm/sec) and escape power (Pesc, mW) are recorded for each sperm. For each species, the VCL and Pesc distributions of the fresh sample are statistically compared to those of the frozen sample.

5.3 Results

D. Dog: Figure 5.1 plots Pesc against VCL for both the fresh (blue) and frozen (red) sperm samples analyzed. The data sets overlap, showing the sperm swim similar speed and force. The Pesc and VCL distributions of the fresh and frozen samples are statistically compared using the non-parametric Wilcoxon paired-sample test (since the distributions are not Gaussian, the statistical comparison required the use of the non-parametric test (Zar 1984)). The VCL distributions are found to be statistically equal ($P > 0.06$) as are the Pesc distributions ($P > 0.9$). (The median values for each distribution are listed in table 5.1.) Thus, the cryopreservation protocol used for dog is found to not significantly affect sperm motility.

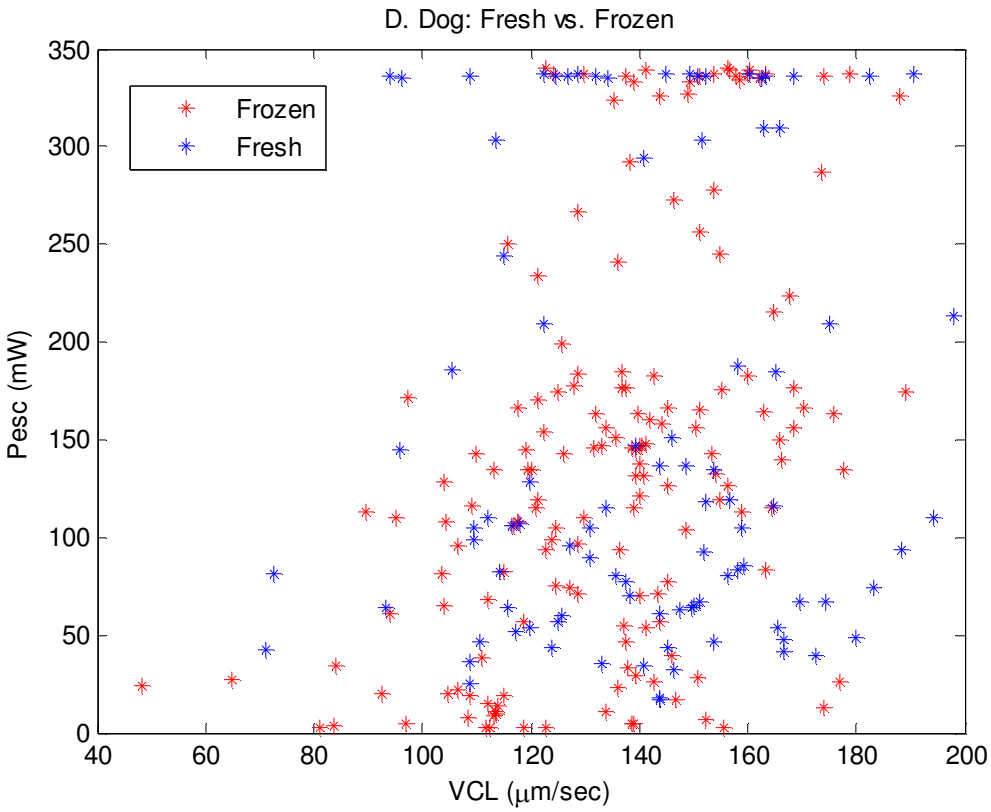

Figure 5.1: Pesc vs. VCL for dog sperm: The fresh sample (blue) is plotted with the frozen sample (red). The two data sets overlap, showing that the cryopreservation protocol used on dog sperm does not significantly affect sperm motility.

D. Cat: Figure 5.2 plots Pesc against VCL for both the fresh (blue) and frozen (red) sperm samples analyzed. The Pesc and VCL distributions of the fresh and frozen samples are statistically compared using the non-parametric Wilcoxon paired-sample test. The VCL distributions are found to be statistically different ($P < 0.01$). However, the median VCL value of the frozen sample is greater than that of the fresh sample. This could be due to the amount of time between sperm extraction and pick up/analysis of the fresh sample. The Pesc distributions, however, were found to be statistically equal ($P > 0.6$). (The median values for each distribution are listed in

table 5.1.) Thus, the cryopreservation protocol used for cat is found to not significantly affect sperm motility. More importantly, Pesc appears to be a more robust measurement of sperm motility, as it is less sensitive to time of analysis.

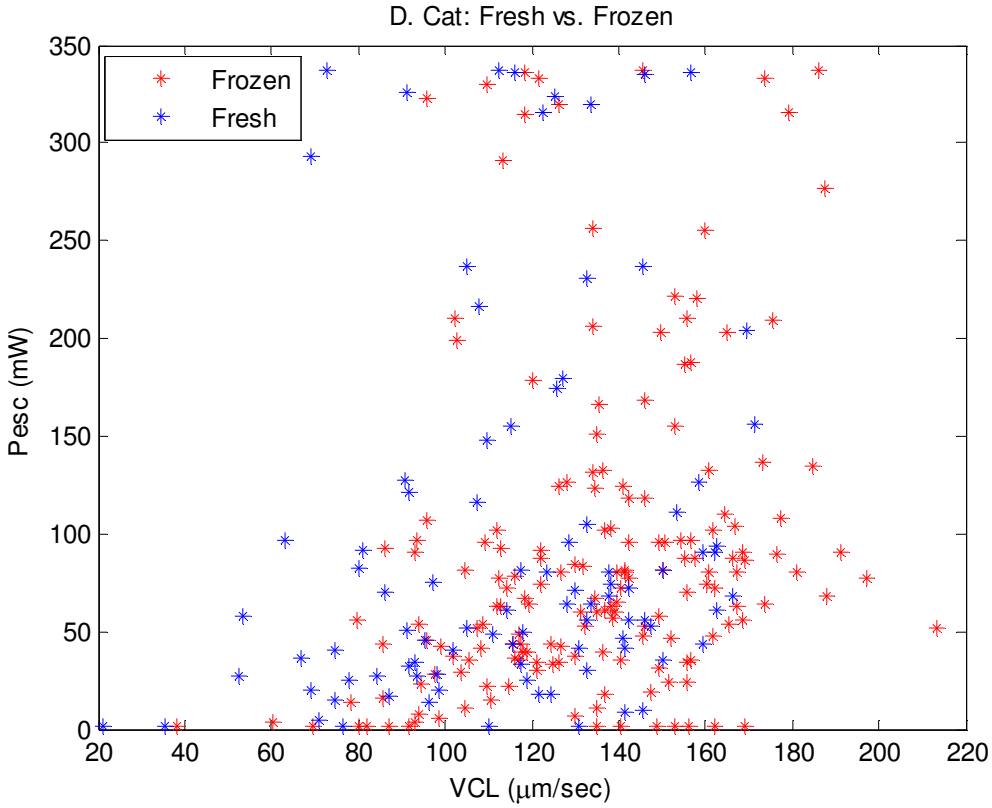

Figure 5.2: Pesc vs. VCL for cat sperm: The fresh sample (blue) is plotted with the frozen sample (red). The two data sets overlap in terms of Pesc, however the frozen sperm are faster than the fresh sperm. This shows that the cryopreservation protocol used on cat sperm does not significantly affect sperm motility, but the time between extraction and analysis does affect sperm swimming speed.

Bighorn Sheep: Figure 5.3 plots Pesc against VCL for both the fresh (blue) and frozen (red) sperm samples analyzed. The Pesc and VCL distributions of the fresh and frozen samples are statistically compared using the non-parametric Wilcoxon paired-sample test. The VCL and Pesc distributions are found to be statistically

different ($P < 0.05$). However, the median VCL and Pesc values of the frozen sample are greater than those of the fresh sample. Again, this could be due to the amount of time between sperm extraction and pick up/analysis of the fresh sample. (The median values for each distribution are listed in table 5.1.) Thus, the cryopreservation protocol used for bighorn sheep is found to not significantly affect sperm motility. More importantly, Pesc appears to be a more robust measurement of sperm motility, as it is less sensitive to time of analysis.

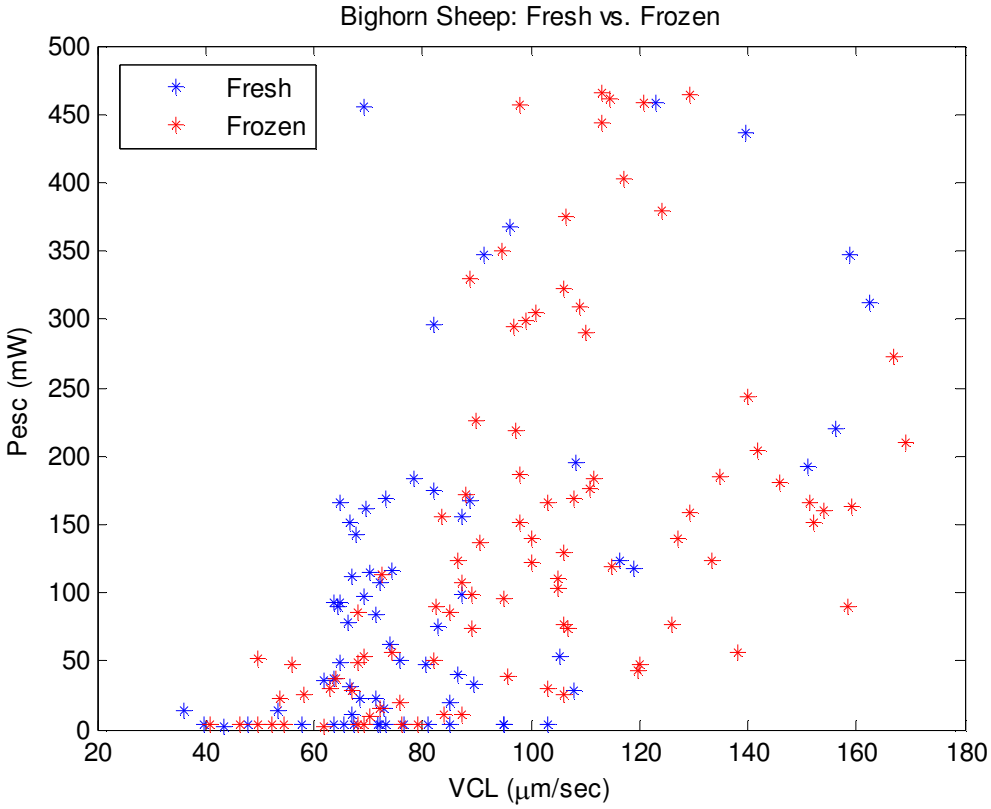

Figure 5.3: Pesc vs. VCL for bighorn sheep sperm: The fresh sample (blue) is plotted with the frozen sample (red). The two data sets overlap in terms of Pesc, however the frozen sperm are faster than the fresh sperm. This shows that the cryopreservation protocol used on bighorn sheep sperm does not significantly affect sperm motility, but the time between extraction and analysis does affect sperm swimming speed.

Javan Banteng: Figure 5.4 plots Pesc against VCL for both the fresh (blue) and frozen (red) sperm samples analyzed. The figure shows that the sperm from the fresh sample swim with faster speeds and stronger forces. The Pesc and VCL distributions of the fresh and frozen samples are statistically compared using the non-parametric Wilcoxon paired-sample test. The VCL distributions are found to be statistically different ($P < 0.001$) as are the Pesc distributions ($P < 0.001$). (The median values for each distribution are listed in table 5.1.) Thus, the cryopreservation protocol used for Javan banteng is found to significantly affect sperm motility.

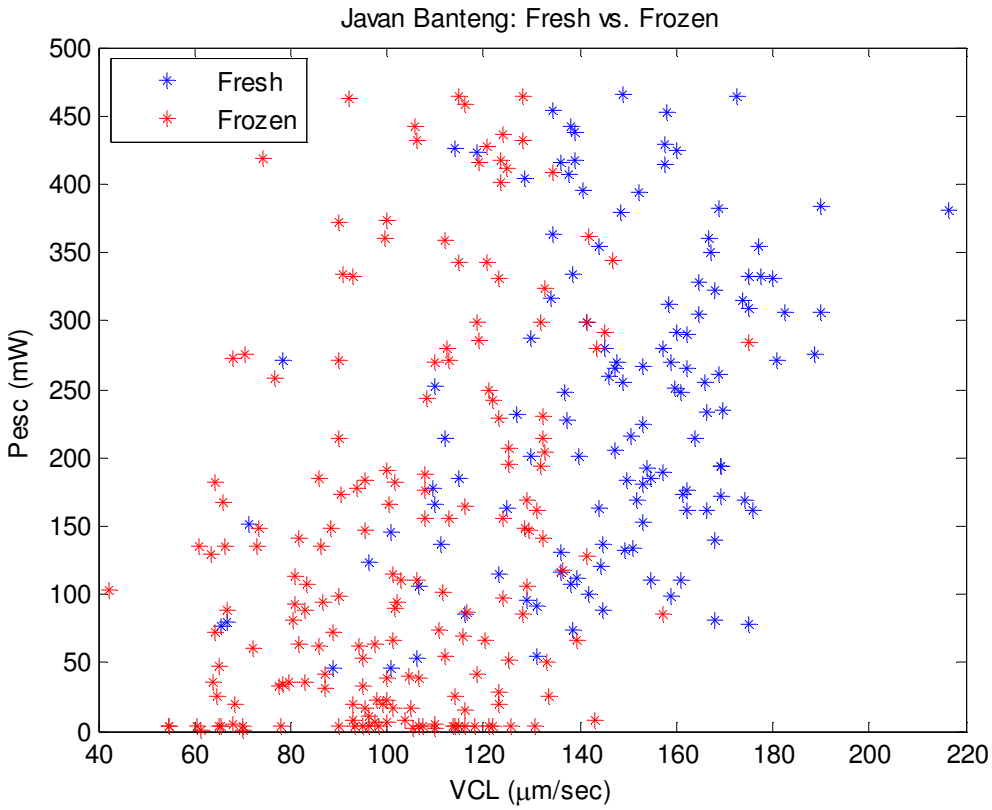

Figure 5.4: Pesc vs. VCL for Javan banteng sperm: The fresh sample (blue) is plotted with the frozen sample (red). The sperm from the fresh sample are faster and stronger than the sperm from the frozen sample. This shows that the cryopreservation protocol used on Javan banteng sperm does significantly affect sperm motility.

West Caucasian Tur: Figure 5.5 plots Pesc against VCL for both the fresh (blue) and frozen (red) sperm samples analyzed. The figure shows that the sperm from the fresh sample swim with faster speeds and stronger forces. The Pesc and VCL distributions of the fresh and frozen samples are statistically compared using the non-parametric Wilcoxon paired-sample test. The VCL distributions are found to be statistically different ($P < 0.001$) as are the Pesc distributions ($P < 0.001$). (The median values for each distribution are listed in table 5.1.) Thus, the cryopreservation protocol used for West Caucasian tur is found to significantly affect sperm motility. Interestingly, the fertility experts at the CRES facility were not able to detect a difference in motility, based on SOP scores as described in chapter 4, between the fresh and frozen samples. The quantitative approach used in this chapter is therefore a more objective and informative method to assess the effects of cryopreservation. Table 5.1 lists the median values for each distribution and summarizes the results of the statistical comparisons between fresh and frozen samples for all five species analyzed.

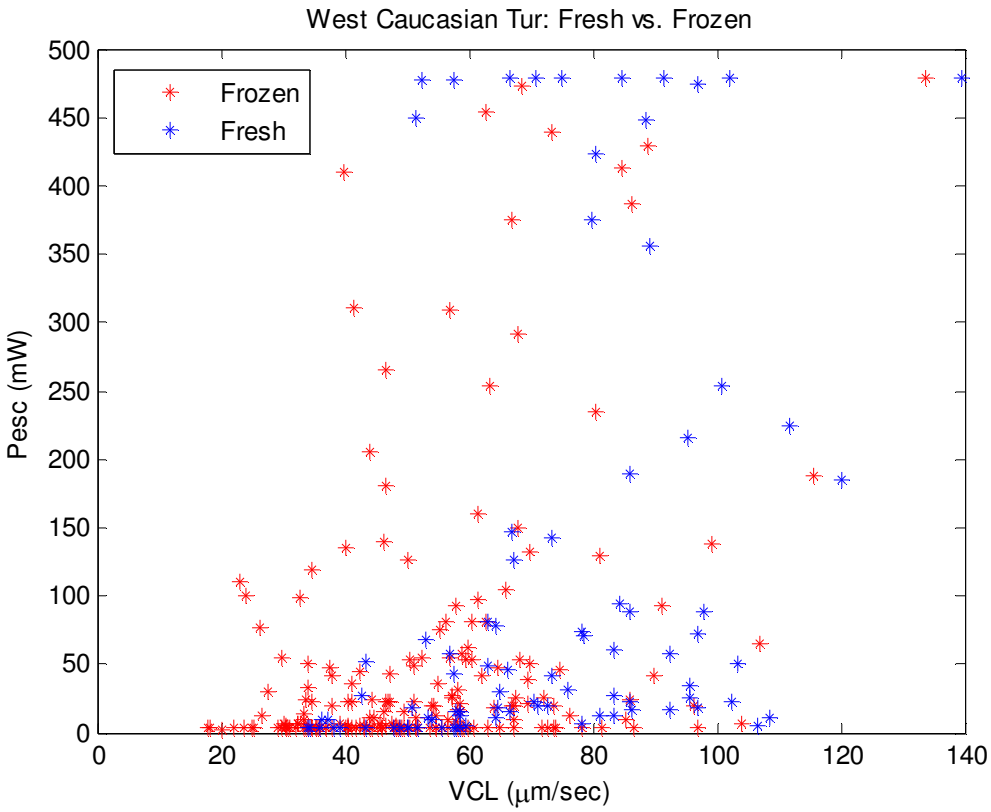

Figure 5.5: Pesc vs. VCL for West Caucasian tur sperm: The fresh sample (blue) is plotted with the frozen sample (red). The sperm from the fresh sample are faster and stronger than the sperm from the frozen sample. This shows that the cryopreservation protocol used on West Caucasian tur sperm does significantly affect sperm motility.

Table 5.1: Comparison of VCL and Pesc distributions of the fresh and frozen samples. The median values for each distribution are listed. The *P* values resulting from the statistical comparisons using Wilcoxon paired-sample test are listed. '*' indicates that the median value of the frozen sample distribution was greater than that of the fresh sample.

	VCL (μm/sec)			**Pesc (mW)**		
	Fresh	**Frozen**	**Statistical Comparison**	**Fresh**	**Frozen**	**Statistically Comparison**
D. Cat	117.77	134.94	Diff. (P < 0.05)*	62.45	72.42	Same (P > 0.6)
D. Dog	143.90	137.56	Same (P > 0.06)	105.03	134.51	Same (P > 0.9)
Bighorn Sheep	73.43	98.00	Diff. (P < 0.05)*	68.72	116.28	Diff. (P < 0.05)*
Javan Banteng	149.49	104.68	Diff. (P < 0.001)	233.13	102.30	Diff. (P < 0.001)
West Caucasian Tur	70.60	50.16	Diff. (P < 0.001)	29.92	13.49	Diff. (P < 0.001)

5.4 Discussion

In this chapter, I have demonstrated how the measurements of sperm swimming speed and swimming force can be used to assess the effects of sperm cryopreservation. For a majority of the species analyzed, the freezing technique did not negatively affect sperm motility (cat, dog, and bighorn sheep). For the cat and bighorn sheep species, frozen sperm were found to be faster and/or stronger than the fresh sperm. In these cases, the time between sperm collection and analysis of the fresh sperm probably caused the decrease in sperm motility. Future studies should measure the effects of time of analysis after collection on sperm motility.

The freezing technique used for sperm from Javan banteng and West Caucasian tur species significantly affected sperm motility (frozen sperm are found to

be statistically slower and weaker than fresh sperm). Moreover, the quantitative analysis was able to detect changes in tur sperm motility that were not detected using the SOP scoring analysis. This demonstrates the importance of using an objective system that can quantitatively assess sperm motility. Such information can be used to optimize the freezing protocol and/or freezing media used for sperm cryopreservation.

Acknowledgements

The material presented in Chapter 5 is, in part, a reprint of the material as it appears in "Real-time automated tracking and trapping system (RATTS)," by L. Z. Shi, J. M. Nascimento, C. Chandsawangbhuwana, M. W. Berns, and E. L. Botvinick *Microscopy Research and Technology* **69**(11), 894-902 (2007). The dissertation author was the second author of the paper but contributed equal amount of effort as the first author.

References

Biggers, J. D., Whitten, W. D., Whittingham, D. G. (1971). The culture of mouse embryos in vitro. in *Methods of mammalian embryology*, San Francisco: Freeman.

Cotter, P. Z., Goolsby, H. A., Prien, S. D. (2005). Preliminary Evaluation of a Unique Freezing Technology for Bovine Spermatozoa Cryopreservation. *Reprod. Dom. Anim.* **40**, 98-99.

Dantas, Z. N., Araujo, E. Jr., Tadir, Y., Berns, M. W., Schell, M. J., Stone, S. C. (1995). Effect of freezing on the relative escape force of sperm as measured by a laser optical trap. *Fertil. Steril.* **63**(1), 185-188.

Dong, Q., Huang, C., Eudeline, B., Tiersch, T. R. (2005). Systematic factor optimization for the cryopreservation of shipped sperm samples of diploid Pacific Oysters, *Crassostrea gigas*. *Cryobiology* **51**, 176-197.

Durrant, B.S., Burton, M., Patton, M.L., Pratt, N.C. (1994). Effects of pre-freeze cooling and post-thaw treatment on the cryosurvival of Tonkin Sika deer sperm. *Biol. Reprod.* 50 Suppl. 1, 182.

Durrant, B. S., Harper, D., Amodeo, A., Anderson, A. (2000). Effects of freeze rate on cryosurvival of domestic dog epididymal sperm. *J. Andrology* Suppl. 59, 21.

Harper, S. A., Durrant, B. S., Russ, K. D., Bolamba, D. (1998). Cryopreservation of domestic dog epididymal sperm: A model for the preservation of genetic diversity. *J. Andrology*. Suppl. 50, 19.

Konig, K., Svaasand, L., Liu, Y., Sonek, G., Patrizio, P., Tadir, Y., Berns, M. W., Tromberg, B. J. (1996). Determination of motility forces of human spermatozoa using an 800 nm optical trap. *Cell. Mol. Biol. (Noisy-le-grand)* **42**(4), 501-509.

Liaw, L. H. and Berns, M. W. (1981). Electron microscope autoradiography on serial sections of preselected single living cells. *J. Ultrastruct* **75**, 187–194.

Maxwell, W. M. C., Parrilla, I., Caballero, I., Garcia, E., Roca, J., Martinez, E. A., Vazquez, J. M., Rath, D. (2007). Retained Functional integrity of Bull Spermatozoa after Double Freezing and Thawing Using PureSperm® Density Gradient Centrifugation. *Reprod. Dom. Anim.* **42**, 489-494.

Shi, L. Z., Nascimento, J., Berns, M. W., Botvinick, E. (2006a). Computer-based tracking of single sperm. *J. Biomed. Opt.* **11**(5), 054009.

Shi, L. Z., Nascimento, J. M., Chandsawangbhuwana, C., Berns, M. W., Botvinick, E. (2006). Real-time automated tracking and trapping system (RATTS). *Microscopy Research and Technology* **69**(11), 894-902.

Su, L., Li, X., Quan, J., Yang, S., Li, Y., He, X., Tang, X., (2007). A comparison of the protective action of added egg yolks from five avian species to the cryopreservation of bull sperm. *Anim. Reprod. Sci.* doi: 10.1016/j.anireprosci.2007.06.019.

Vuthiphandchai, V., Nimrat, S., Kotcharat, S., Bart, A. N. (2007). Development of a cryopreservation protocol for long-term storage of black tiger shrimp (*Penaeus monodon*) spermatophores. *Theriogenology* doi: 10.1016/j.theriogenology.2007.08.024.

Zar, J. H. (1984). in *Biostatistical Analysis,* 2nd end. pp. 150-161 and pp. 292-305. Prentice Hall, Englewood Cliffs.

VI. Species-specific relationship between sperm swimming force and swimming speed

6.1 Introduction

In chapter 4, a relationship was found between sperm swimming speed (VCL, μm/sec) and swimming force (in terms of escape laser power, Pesc, mW) for domestic dog sperm. In general, swimming speed linearly increased with swimming force. A more detailed analysis of the data showed that there are two statistically separable groups, each with its own relationship between the two parameters. More importantly, the work done in chapter 4 showed that in addition to common sperm motility measurements, such as swimming velocity and lateral head movement, the quantitative measurement of sperm swimming force is a useful parameter for assessing sperm quality.

A major limitation of that study, however, was low throughput. The user had to manually trap the sperm and use an offline program (Shi *et al.* 2006a) to calculate the swimming speed of each sperm analyzed. A three hour experiment could take the user a week to analyze the data. The challenges thus were (1) to catch a sperm and measure its swimming force and velocity all automatically and (2) to repeat this process for many sperm (>150) during a period of approximately 3 hours (period during which sperm preparation was viable).

In chapter 5, we introduced the real-time automated tracking and trapping system (Shi *et al.* 2006b). This combination of laser tweezers and computer/robotic technology solved the problem of low throughput and created a system that can be

used to assess sperm from a variety of species. In this chapter, RATTS is used to measure the swimming speed and swimming force of eleven species. The relationship between the two parameters for each species is quantified and compared to that of the other ten species. For each species, swimming speed is found to linearly increase with swimming force. Additionally, the regression relating swimming speed to swimming force is, in general, unique for each species.

6.2 Materials and Methods

6.2.1 Specimen

Domestic Cat (*Felis catus*): A cat was neutered at a veterinary clinic. The testes were sent to CRES where the semen sample was extracted from the epididymis (sliced the epididymis into Test Yolk buffer (0% glycerol) and squeezed out with the rounded edge of a pair of curved scissors). An aliquot of the sperm in Test Yolk buffer is reserved as the "fresh" sample, and placed into 4˚C refrigerator until picked up. The rest of the sample was prepared for cryopreservation according to a published protocol (Durrant *et al.* 2000; Harper *et al.* 1998). The escape laser power distributions of the fresh and frozen samples were found to be statistically equal. The swimming speed distributions of the fresh and frozen samples were found to be statistically different; however, the fresh sperm were slower than the frozen sample. (See chapter 5 for details.) Therefore, the two distributions are pooled together for analysis in this chapter.

Domestic Dog (*Canis familiaris*): Semen samples collected from several dogs were pooled and cryopreserved according to a published protocol (Durrant *et al.* 2000; Harper *et al.* 1998).

Domestic Horse (*Equus caballus*): The semen sample was collected and cryopreserved by Select Breeders Services (Thousand Oaks, CA) according to their proprietary protocol (examples of published protocols for equine sperm can be found in Vidament *et al.* 2001 and Vidament 2005).

Bighorn Sheep (*Ovis canadensis*): The semen sample was extracted from the epididymis of the male approximately one hour post-mortem (sliced the epididymis into Test Yolk buffer (0% glycerol) and squeezed out with the rounded edge of a pair of curved scissors). An aliquot of the sperm in Test Yolk buffer is reserved as the "fresh" sample, and placed into 4˚C refrigerator until picked up. The rest of the sample was prepared for cryopreservation according to a published protocol (Durrant *et al.* 1994). The swimming speed and escape laser power distributions are found to be statistically different ($P < 0.05$). However, the median swimming speed and escape laser power values of the frozen sample are greater than those of the fresh sample. (See chapter 5 for details.) Therefore, the two distributions are pooled together for analysis in this chapter.

Nubian Ibex (*Capra nubiana*): The semen sample was extracted from the epididymis of the male approximately thirty minutes post-mortem (sliced the epididymis into Test Yolk buffer (0% glycerol) and squeezed out with the rounded

edge of a pair of curved scissors) and prepared for cryopreservation according to a published protocol (Durrant *et al.* 1994).

Debrazza's Guenon (*Cercopithecus neglectus*): The semen sample collected from an electroejaculation and prepared for cryopreservation according to a modified published protocol (Durrant *et al.* 1999). Briefly, the modifications are as follows:

1. The ejaculate was extended in a mix of 0% Test Yolk Buffer and Tyrodes media
2. It was cooled "Fast" (0.59^{o}C per minute)
3. It was frozen "Sideways" (7^{o}C per minute)

Schmidt's Spot-Nosed Guenon (*Cercopithecus ascanius schmidti*): The semen sample was extracted from the epididymis of the male approximately one hour post-mortem (sliced the epididymis into Test Yolk buffer (0% glycerol) and squeezed out with the rounded edge of a pair of curved scissors) and prepared for cryopreservation according to a published protocol (Durrant *et al.* 1999). Briefly, the technique used for cooling and freezing the sperm is as follows:

1. Slice the epididymis in Test Yolk Buffer (0% glycerol) and squeeze out the sperm.
2. Place the extended sperm into cryovials (375µL extended sperm) then add the 16% glycerol/Test yolk buffer (125µL) for a final concentration of 4% glycerol.
3. Place cryovials in a water bath with room temp water.
4. Place the water bath into a 4˚C room for 30 minutes.

5. Place the vials onto a thick styrofoam rack (2 inches) and place it on top of 3 inches of liquid nitrogen (contained inside of a box). The average rate of freeze from this method is 7˚C per minute.
6. After 15 minutes on the rack, plunge the vials into the liquid nitrogen and store the vials in liquid nitrogen.

Chimpanzee (*Pan troglodytes*): Chimpanzee sperm were collected from four males at the Primate Foundation of Arizona, courtesy of Jo Fritz, using an artificial vagina. Sperm samples were allowed to liquefy at room temperature for 30 minutes then added to 10mL of Biggers, Whittens, and Whittingham (BWW) with Penicillin and Streptomycin and transported in a cooler at 10°C. Samples were washed with BWW (21mM HEPES, 21.5mM Lactic acid, 91.06 mM NaCl, 4.78 mM KCl, 1.71 mM CaCl, 1.71 mM KH2PHO4, 2.44 mM MgSO4, 5.55 mM Glucose, 4mM NaHCO3, 0.25 mM Napyruvate, 1% bovine serum albumin (BSA), pH 7.5, filter sterilized over 22µm filter, osmolarity 295 mOsm/kg water, kept at 4ºC and warmed to room temperature prior to use) by spinning at 600g for 6 minutes. These samples were received within 24 hours of ejaculation and analyzed within 48 hours.

Rhesus Macaque (*Macaca mulatta*): Fresh rhesus macaque semen samples were prepared for cooled (5^{o}C) storage as follows: 4mL of media (0.5 mg of BSA per 1mL of BWW) was added to the semen and rotated for 5 minutes on a rocker. The coagulum was pulled up onto the side of the tube and left to sit for 10 minutes. The top 3.5mL of sperm supernatant was transferred into a new tube (sperm motility and concentration were checked). The sample was centrifuged at 300g for 10 minutes then

suspended at 50 x 10^6/mL in a commercial nonfat dry skim milk semen diluent (Animal Reproduction Systems, Chino, CA). The sample was loaded into Whirl-Pak® bags (Nasco, Fort Atkinson, WI) ensuring minimal air space then placed in an Equitainer® semen transporter (Hamilton Research, Inc, South Hamilton, MA) and shipped overnight to the lab. The samples arrived at approximately 24 hours and were analyzed after warming the sample (37°C) for 5-10 minutes. Frozen rhesus macaque semen samples were prepared using a programmable freezer utilizing a Tes-Tris egg yolk-containing medium in addition to 3% glycerol (freezing curve: 22°C – 8°C at 0.2°C/min followed by cooling to -110°C at -17°C/min and plunging in liquid nitrogen), and were thawed in 37°C water bath for approximately one minute before analysis. The data sets from the fresh and frozen groups are pooled together.

Human (*Homo sapiens*): Human sperm from two males were collected by masturbation after 3 days of abstinence and prepared as follows: samples were allowed to liquefy at room temperature for 30 minutes then added to 10mL of Biggers, Whittens, and Whittingham (BWW) with Penicillin and Streptomycin and transported in a cooler at 10°C. Samples were washed with BWW (same as that used for chimpanzee sperm) by spinning at 600g for 6 minutes. These samples were received within 24 hours of ejaculation and analyzed within 48 hours. Human semen samples from two males (different than those analyzed fresh) were frozen according to a published protocol (DiMarzo *et al.* 1990; Ethics Committee of the American Fertility Society 1986; Serfini and Marrs 1986) and prepared for analysis using a twice wash

protocol (DiMarzo and Rakoff 1986; Toffle *et al.* 1985). The data sets from the fresh and frozen groups are pooled together.

Gorilla (*Gorilla gorilla*): Gorilla sperm from male Ivan at Zoo Atlanta, courtesy of Tara Stoinski, was collected opportunistically after the animal masturbated in his cage. The sample was allowed to liquefy at room temperature for 30 minutes then added to 10mL of Biggers, Whittens, and Whittingham (BWW) with Penicillin and Streptomycin and transported in a cooler at 10°C. The sample was washed with BWW (same as that used for chimpanzee sperm) by spinning at 600g for 6 minutes. The sample was received within 24 hours of ejaculation and analyzed within 48 hours. Gorilla sperm from a different male at the Henry Doorly Zoo, Center for Conservation and Research, Omaha, Nebraska, were frozen according to a published protocol (O'Brien *et al.* 2002) and thawed for eight seconds in 50^{o}C water bath before analysis. The data sets from the fresh and frozen groups are pooled together.

6.2.2 Hardware, Software and Optical Design

Chapter 3 provides a detailed description (including figures) describing the optical design used for the experiments in this chapter. Briefly, a single point gradient trap was generated using a Nd:YVO4 continuous wave 1064nm wavelength laser (Spectra Physics, Model BL-106C, Mountain View, CA) coupled into a Zeiss Axiovert S100 microscope and a 40x, phase III, NA 1.3 oil immersion objective (Zeiss, Thornwood, NY). Laser power in the specimen plane is attenuated by rotating a polarizer (see chapter 3, figure 3.1 (a)) at a user-defined rate (linear power decay within ten seconds, see results from chapter 3).

Chapter 5 provides a detailed description of how the sperm are analyzed using the real-time automated tracking and trapping system (RATTS) (Shi *et al*. 2006 a, b). Briefly, phase contrast images of swimming sperm are acquired using a CCD camera (Sony, Model XC – 75, New York City, NY, operating at 30 frames per second) coupled to a variable zoom lens system (0.33X magnification) to increase the field of view and digitized to the computer at video rate. Individual sperm are selected by the user and then automatically tracked and trapped. The swimming velocity (curvilinear velocity, VCL, μm/sec) is calculated based on the pixel (x, y) coordinates of the sperm's swimming trajectory. Once trapped, the laser power is attenuated until the sperm is capable of escaping the trap. RATTS automatically identifies this event and records the escape laser power in Watts (Pesc, mW) (Shi *et al.* 2006b).

6.3 Results

Figures 6.1 through 6.11 plot Pesc (mW) against VCL (μm/sec) for cat, dog, horse, bighorn sheep, Nubian ibex, Debrazza's guenon, spot-nosed guenon, chimpanzee, rhesus macaque, human and gorilla sperm, respectively. A linear regression (robust fit) is applied to each scatter plot. The regression equation, including slope and y-intercept, as well as the R^2 value are listed in each figure. Table 6.1 summarizes the regression information (slope, y-intercept and R^2 value) for each species. The median values and the extent of the data of the swimming speed and escape laser power distributions for each species are also listed in table 6.1.

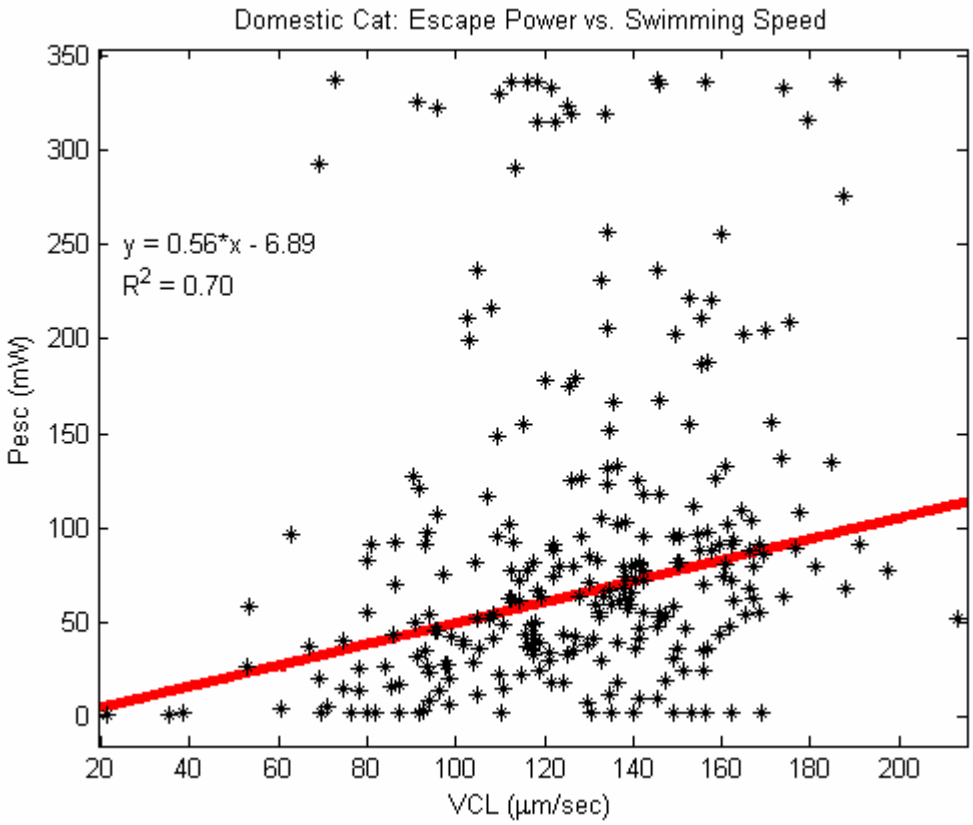

Figure 6.1: Domestic Cat – Pesc (mW) vs. VCL (µm/sec) with linear regression

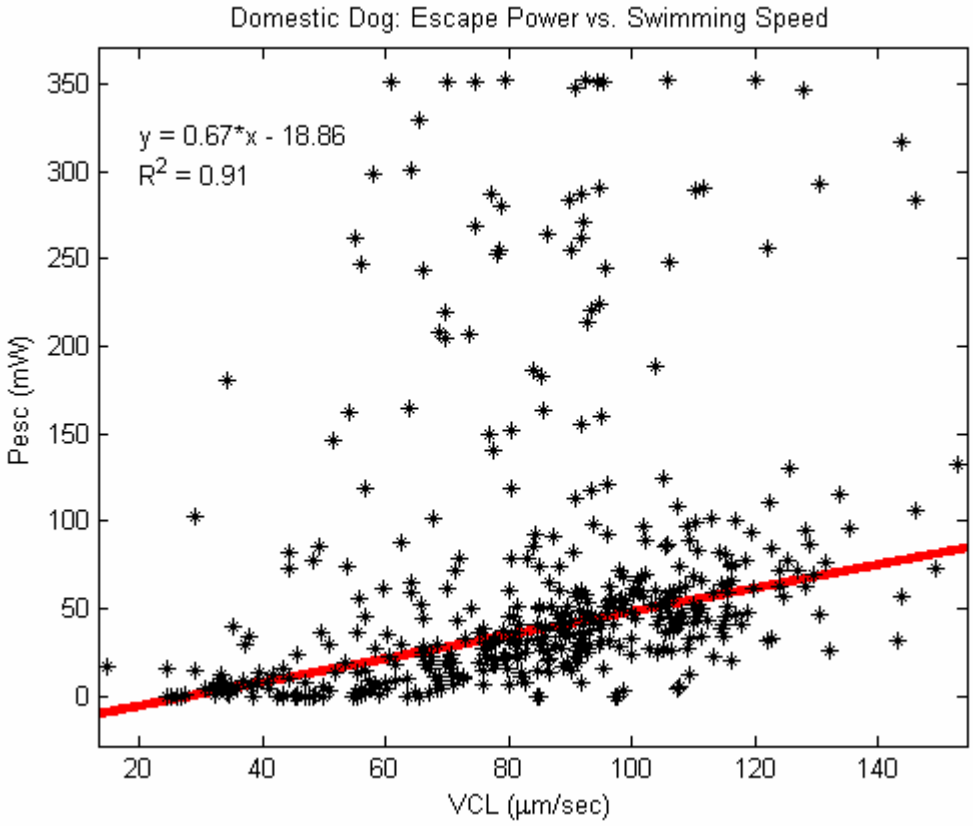

Figure 6.2: Domestic Dog – Pesc (mW) vs. VCL (µm/sec) with linear regression

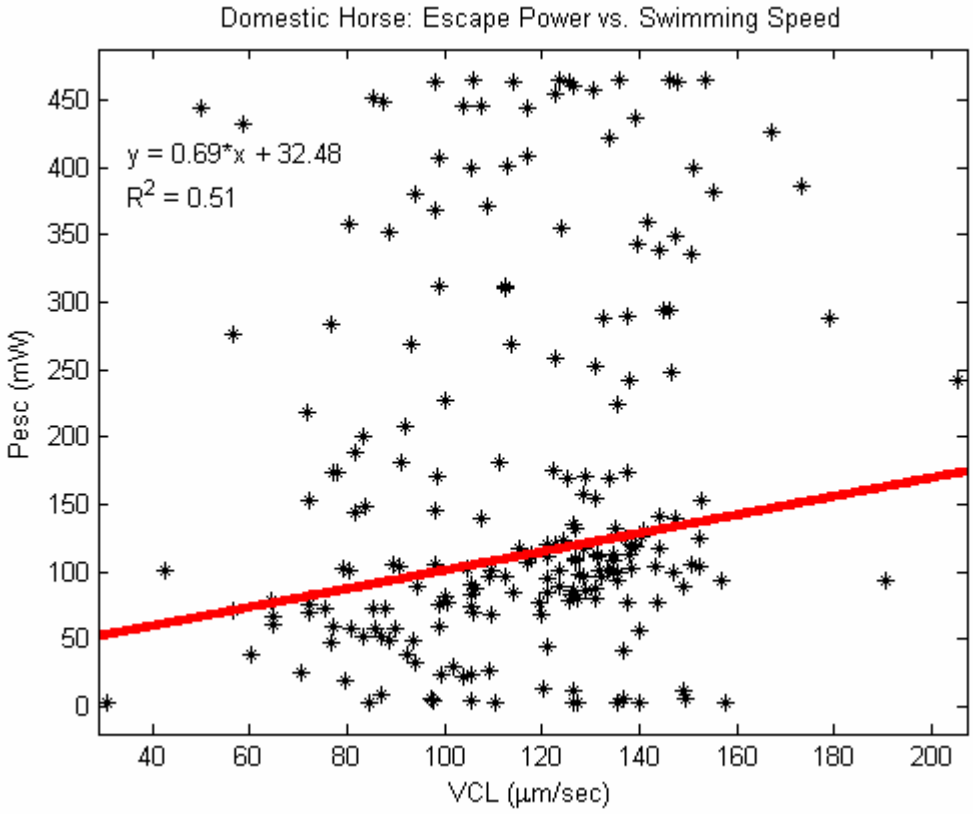

Figure 6.3: Domestic Horse – Pesc (mW) vs. VCL (µm/sec) with linear regression

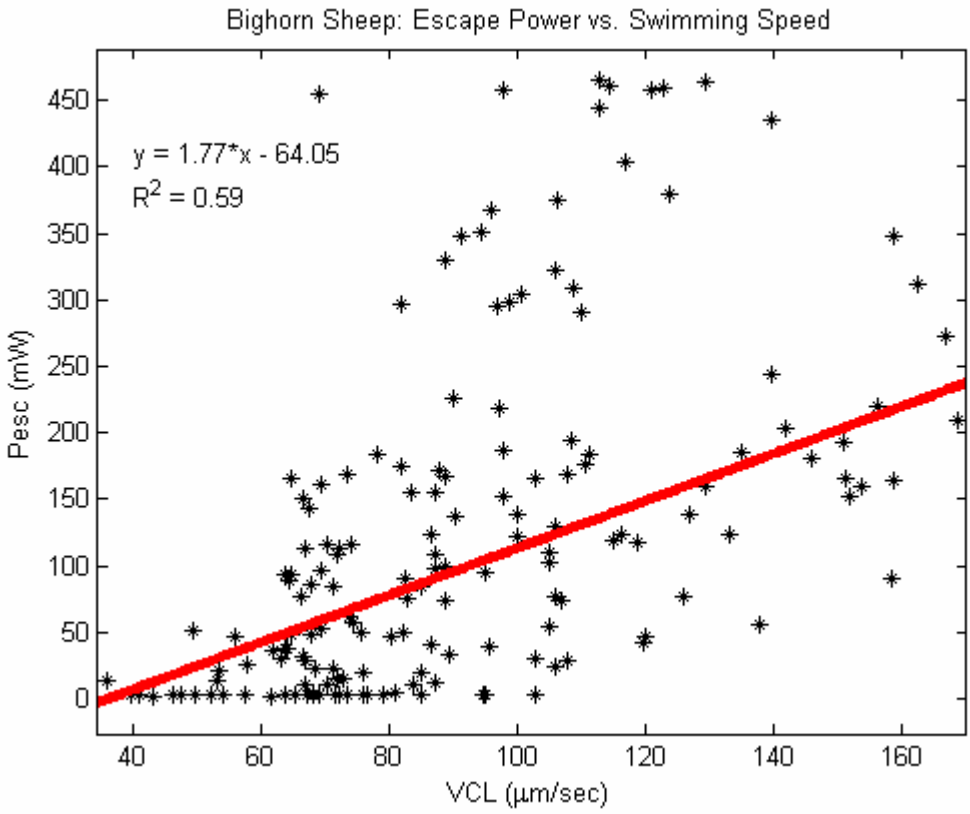

Figure 6.4: Bighorn Sheep – Pesc (mW) vs. VCL (µm/sec) with linear regression

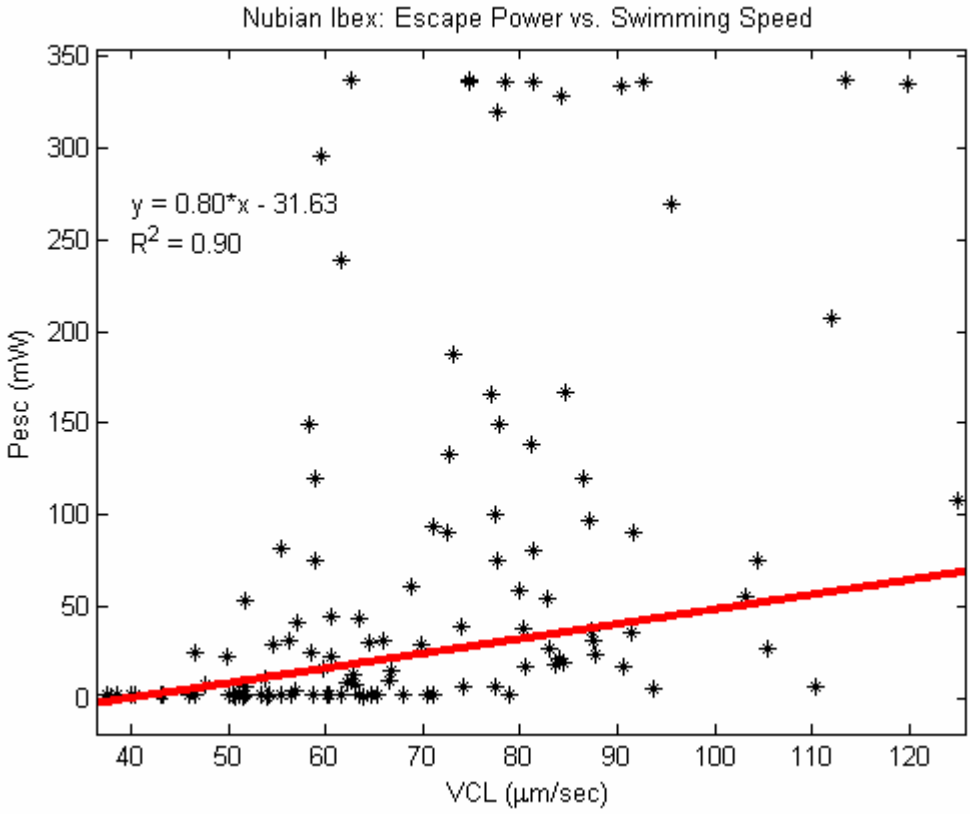

Figure 6.5: Nubian Ibex – Pesc (mW) vs. VCL (µm/sec) with linear regression

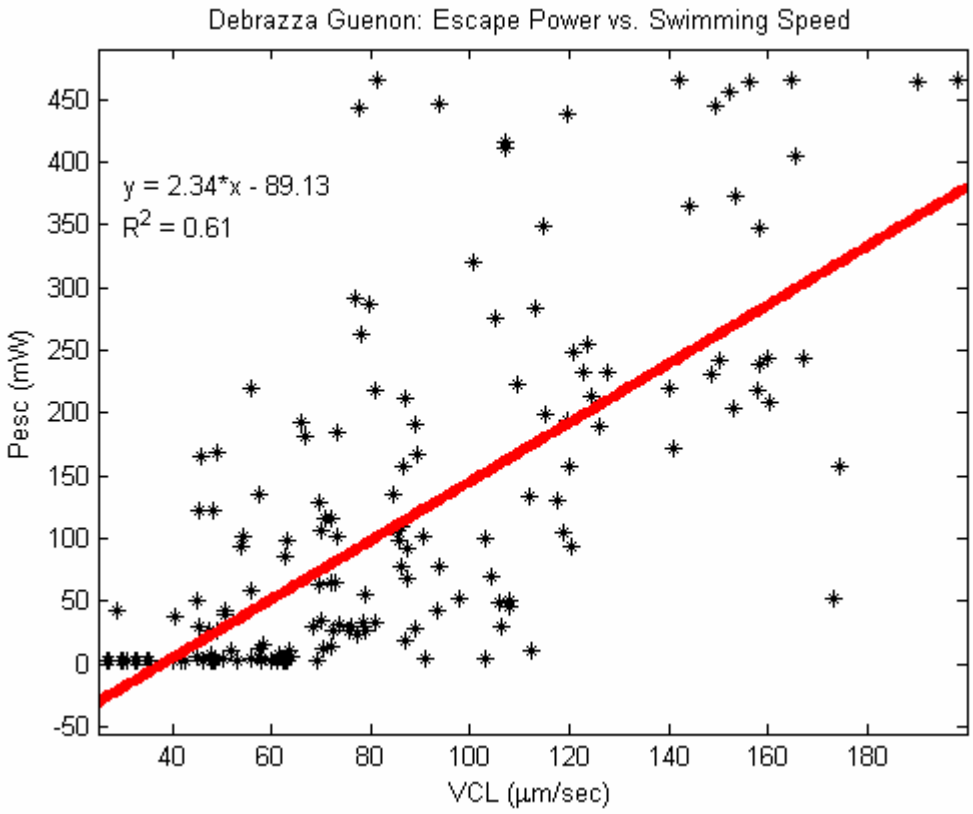

Figure 6.6: Debrazza's Guenon – Pesc (mW) vs. VCL (µm/sec) with linear regression

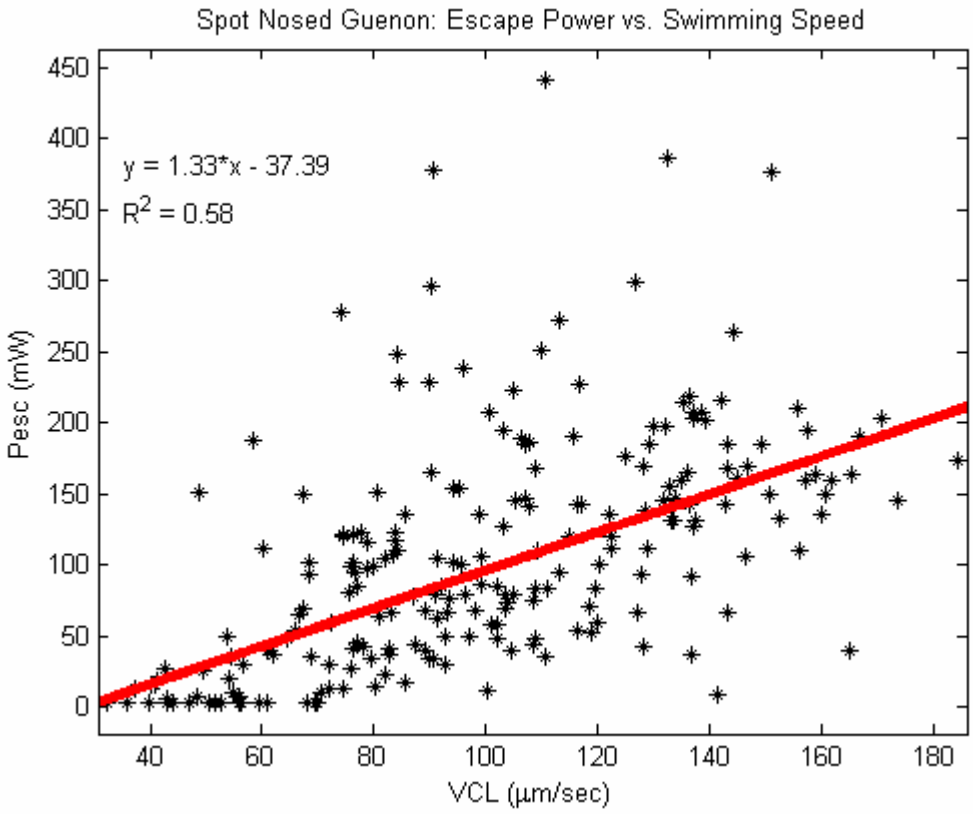

Figure 6.7: Spot-Nosed Guenon – Pesc (mW) vs. VCL (µm/sec) with linear regression

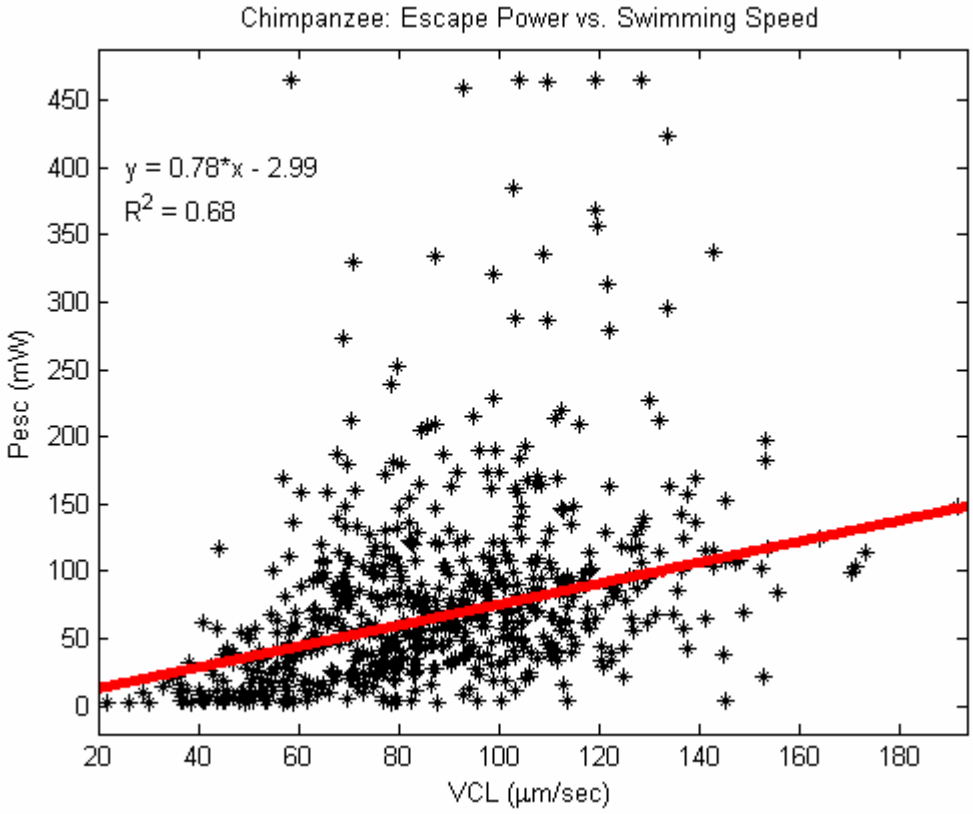

Figure 6.8: Chimpanzee – Pesc (mW) vs. VCL (µm/sec) with linear regression

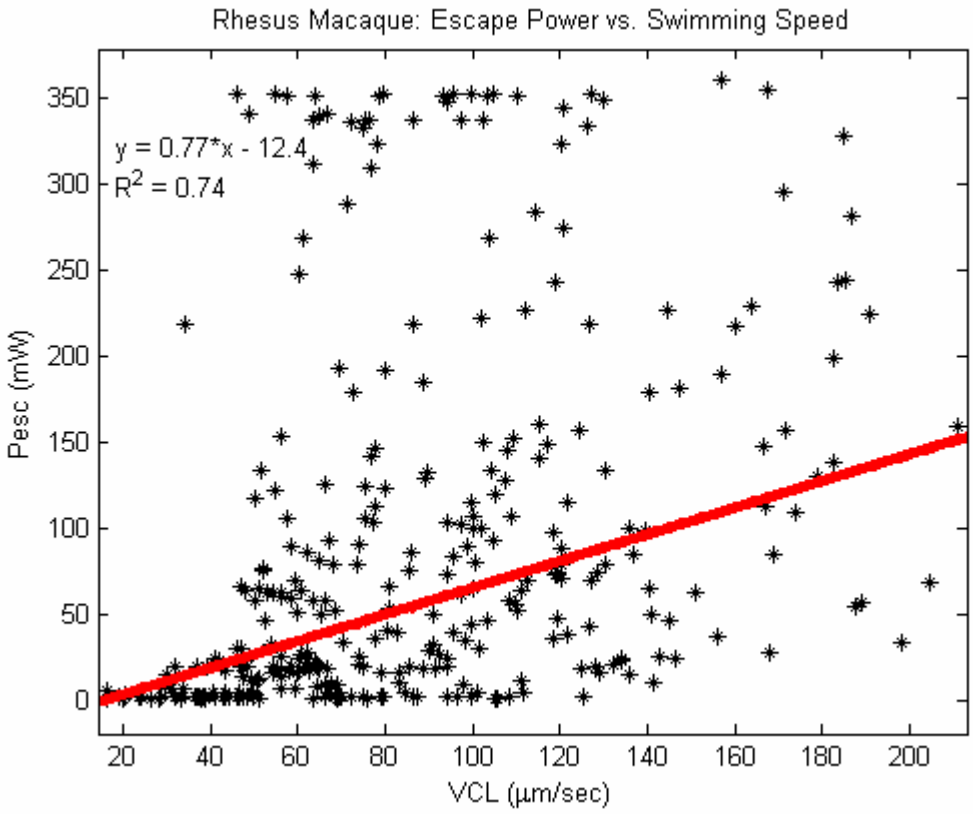

Figure 6.9: Rhesus Macaque – Pesc (mW) vs. VCL (µm/sec) with linear regression

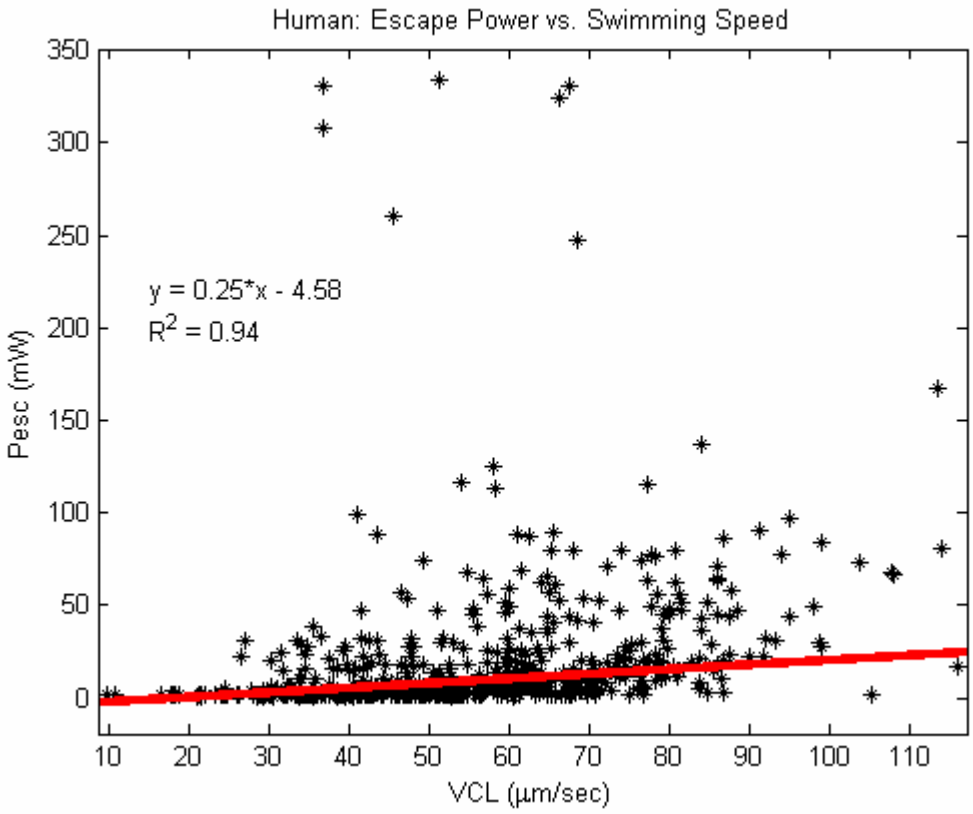

Figure 6.10: Human – Pesc (mW) vs. VCL (µm/sec) with linear regression

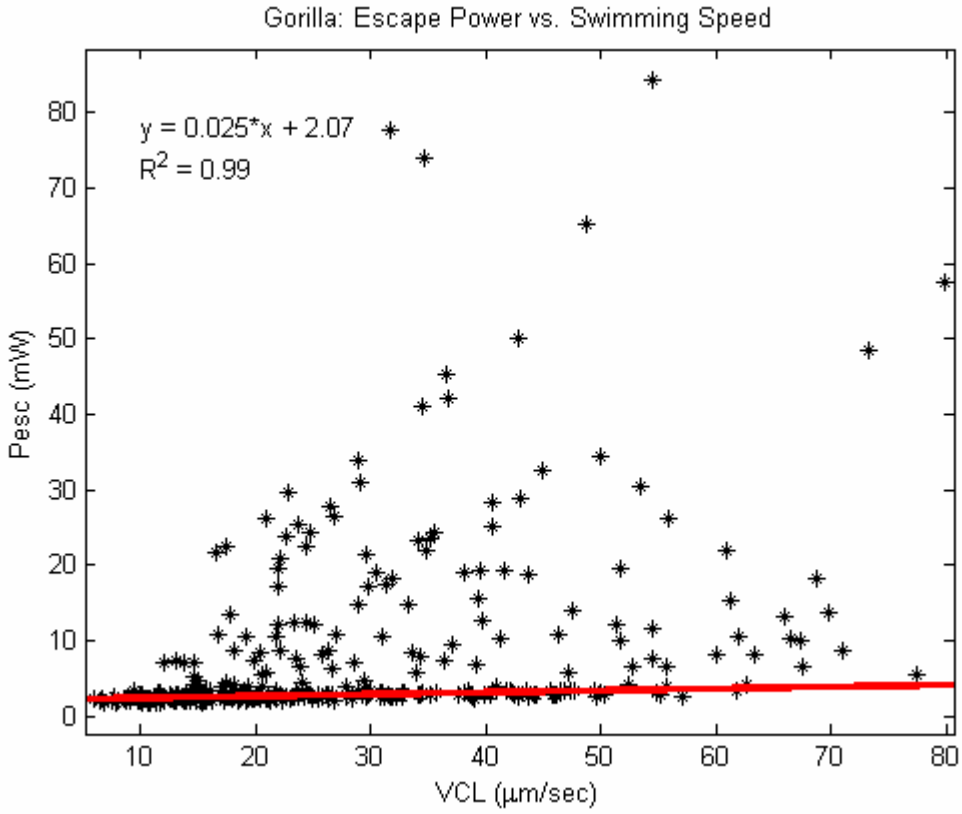

Figure 6.11: Gorilla – Pesc (mW) vs. VCL (µm/sec) with linear regression

Table 6.1: Median values and data range (minimum/maximum values in brackets) of the swimming speed (VCL) and escape laser power (Pesc) distributions for all eleven species analyzed. Regression information (slope, y-intercept and R^2 value) are also listed for each species.

	VCL (μm/sec)	**Pesc (mW)**	**Slope**	**y – int**	**R^2**
D. Cat (N = 266)	129.99 [21.18 - 213.33]	68.03 [1.22 - 337.15]	0.56	-6.89	0.7
D. Dog (N = 433)	86.63 [14.60 - 152.93]	41.60 [1.25 - 351.73]	0.67	-18.86	0.91
D. Horse (N = 211)	120.16 [30.64 - 205.35]	109.74 [3.17 - 465.06]	0.69	32.48	0.51
Bighorn Sheep (N = 160)	87.19 [35.95 - 168.96]	94.31 [1.68 - 465.07]	1.77	-64.05	0.59
Nubian Ibex (N = 118)	66.60 [37.41 - 125.06]	22.77 [0.83 - 337.17]	0.8	-31.63	0.9
Debrazza's Guenon (N = 163)	76.77 [26.73 - 198.26]	69.51 [3.15 - 465.08]	2.34	-89.13	0.61
Spot-Nosed Guenon (N = 219)	96.49 [32.18 - 184.52]	96.83 [3.11 - 440.81]	1.33	-37.39	0.58
Chimp (N = 622)	85.35 [21.49 - 191.69]	65.52 [2.57 - 465.08]	0.78	-2.99	0.68
Rhesus Macaque (N = 324)	77.54 [16.23 - 211.15]	50.11 [0.97 - 359.99]	0.77	-12.4	0.74
Human (N = 549)	54.60 [9.62 - 116.05]	7.94 [0.64 - 333.88]	0.25	-4.58	0.94
Gorilla (N = 338)	23.69 [5.92 - 79.87]	2.87 [1.74 - 84.33]	0.025	2.07	0.99

The regressions for each species are statistically compared (Zar 1984). The regressions for dog and cat are statistically equal ($P > 0.1$); however both are statistically different than that for any other species ($P < 0.05$). The regression for horse is found to be statistically equal to those of Nubian ibex, Bighorn sheep and

Debrazza's guenon ($P > 0.05$), but different than all other species ($P < 0.001$). The regression for Bighorn sheep is statistically equal to those of horse and Debrazza's guenon ($P > 0.05$), but different than all other species ($P < 0.02$). The regression for Nubian ibex is statistically equal to those of horse, spot-nosed guenon, chimpanzee, and rhesus macaque ($P > 0.05$), but different than all other species ($P < 0.02$). Interestingly, the regressions for Nubian ibex and Bighorn sheep are found to be statistically different ($P < 0.02$), even though both species are in the subfamily *Caprinae*. Within the six primate species, each regression is found to be statistically different ($P < 0.05$), except that of the rhesus macaque which is equal to that of the spot-nosed guenon ($P > 0.5$).

6.4 Discussion

This chapter demonstrates the utility and versatility of the custom system, RATTS. The combination of laser tweezers and computer/robotic technology not only significantly increased throughput compared to previous methods (see chapters 3 and 4) but also was able to analyze sperm from a wide variety of species. This achievement, combined with the fact that sperm swimming force has been shown to be a useful parameter for assessing sperm quality (Nascimento *et al.* 2006; chapter 4), is considerably valuable for both basic and applied infertility research.

The relationships between sperm swimming speed and swimming force for eleven species were quantified. The data show that for each species, swimming speed linearly increases with swimming force. This is consistent with previous work done on human (Tadir *et al.* 1990) and dog (Nascimento *et al.* 2006; chapter 4) sperm. The

results also show that, in general, the regression relating swimming speed to swimming force is unique for each species. This may be a reflection of the different mating habits, as will be discussed further in chapter 7. In addition, some regressions give better R^2 values than others, meaning some regressions fit the data set better than others. This could be due to the low number of males per species (in some cases, only one male is representing an entire species). Future work will need to analyze sperm from more males of each of these species. Another possibility could be due to the quality of sperm analyzed. Sperm from some of the species, such as domestic horse and Nubian ibex, were analyzed frozen-thawed without being compared to fresh samples. Cryopreservation, as was shown in chapter 5, can significantly affect sperm motility. Therefore, future work should compare "fresh" vs. "frozen" sperm to quantify the effects of cryopreservation for some of the species analyzed in this chapter (horse, Nubian ibex, Debrazza's guenon, spot-nosed guenon and gorilla). It may prove that the distribution does not change with the addition of more data, in which case biological and/or environmental factors would most likely be the cause for variation among different species. Nonetheless, these data sets provide baseline measurements for each species that can be used for analysis of sperm from other males. Future work should also expand the study to sperm from other species.

References

DiMarzo, S. J., Huang, J., Kennedy, J. F., Villanueva, B., Hebert, S. A., Young, P. E. (1990). Pregnancy rates with fresh versus computer-controlled cryopreserved semen for artificial insemination by donor in a private practice setting. *Am. J. Obstet. Gynecol.* **162**(6), 1483-1490.

DiMarzo, S. J., Rakoff, J. S. (1986). Intrauterine insemination with husband's washed sperm. *Fertil. Steril.* **46**, 470-475.

Durrant, B.S., Burton, M., Patton, M.L., Pratt, N.C. (1994). Effects of pre-freeze cooling and post-thaw treatment on the cryosurvival of Tonkin Sika deer sperm. *Biol. Reprod.* 50 Suppl. 1, 182.

Durrant, B.S., Cammidge, L., Wiley, S., Carlsson, I.B., Wesche, P., Russ, K.D. (1999) Cryopreservation of semen from the drill baboon (*Mandrillus leucophaeus*). *Biol. Reprod*, 60 Suppl. 1, 103.

Durrant, B. S., Harper, D., Amodeo, A., Anderson, A. (2000). Effects of freeze rate on cryosurvival of domestic dog epididymal sperm. *J. Andrology* Suppl. 59, 21.

The Ethics Committee of the American Fertility Society, from the New Guidelines for the use of Semen for Donor Insemination (1986). *Fertil. Steril.* **6**(Suppl), 85.

Harper, S. A., Durrant, B. S., Russ, K. D., Bolamba, D. (1998). Cryopreservation of domestic dog epididymal sperm: A model for the preservation of genetic diversity. *J. Andrology*. Suppl. 50, 19.

Nascimento, J. M., Botvinick, E. L., Shi, L. Z., Durrant, B., Berns, M. W. (2006). Analysis of sperm motility using optical tweezers. *J. Biomed. Opt.* **11**(4), 044001.

O'Brien, J. K., Crichton, E. G., Evans, K. M., Schenk, J. L., Stojanov, T., Evans, G., Maxwell, W. M. C., Loskutoff, N. M. (2002). Sex ratio modification using sperm sorting and assisted reproductive technology – a population management strategy. In *Proceedings of the Second International Symposium on Assisted Reproductive Technology for the Conservation and Genetic Management of Wildlife* (Omaha's Henry Doorly Zoo), pp. 224-231.

Serfini, P., Marrs, R. P. (1986). Computerized staged-freezing technique improves sperm survival and preserves penetration of zona-free hamster ova. *Fertil. Steril.* **45**, 854-858.

Shi, L. Z., Nascimento, J., Berns, M. W., Botvinick, E. (2006a). Computer-based tracking of single sperm. *J. Biomed. Opt.* **11**(5), 054009.

Shi, L. Z., Nascimento, J. M., Chandsawangbhuwana, C., Berns, M. W., Botvinick, E. (2006b). Real-time automated tracking and trapping system (RATTS). *Microscopy Research and Technology* **69**(11), 894-902.

Tadir, Y., Wright, W. H., Vafa, O., Ord, T., Asch, R. H., Berns, M. W. (1990). Force generated by human sperm correlated to velocity and determined using a laser generated optical trap. *Fertil. Steril.* **53**(5), 944-947.

Toffle, R. C., Nagel, T. C., Tagatz, G. E., Phansey, S. A., Okagaki, T., Wavrin, C. A. (1985). Intrauterine insemination: The University of Minnesota Experience. *Fertil. Steril.* **43**(5), 743-747.

Vidament, M., Yvon, J. M., Couty, I., Arnaud G., Nguekam-Feugang, J., Noue, P., Cottron, S., Le Tellier, A., Noel, F., Palmer, E., Magistrini, M. (2001). Advances in cryopreservation of stallion semen in modified INRA82. *Animal Reproduction Science* **68**, 201-218.

Vidament, M. (2005). French field results (1985–2005) on factors affecting fertility of frozen stallion semen. *Animal Reproduction Science* **89**, 115-136.

Zar, J. H. (1984). Comparing Simple Linear Regression Equations *in* Biostatistical Analysis, Prentice Hall, Englewood Cliffs, pp 292-295.

VII. Effects of mating pattern on sperm evolution

7.1 Introduction

Single spot, gradient force laser tweezers were first used to manipulate single cells in the 1980's (Ashkin *et al.* 1987) and soon thereafter were applied to sub-cellular organelles, such as chromosomes on the mitotic spindle (Berns *et al.* 1989). Since then, laser tweezers have been used to study many aspects of cell behavior and physiology (Ashkin 1991; Berns 1998; Ozkan *et al.* 2003; Shao *et al.* 2006). In particular, laser tweezers have been used to trap sperm cells to study laser-sperm interactions and to quantify sperm motility by measuring sperm swimming forces (Konig *et al.* 1996; Araujo *et al.* 1994; Dantas *et al.* 1995; Patrizio *et al.* 2000; Tadir *et al.* 1989 and 1990). These studies found that the minimum laser power needed to hold a sperm in a trap is directly proportional to the sperm's swimming force ($F = Q \times P / c$ where F is the swimming force, P is the laser power, c is the speed of light in the medium with a given index of refraction, and Q is the geometrically determined trapping efficiency parameter) (Konig *et al.* 1996).

Recent studies found a correlation between sperm swimming forces and swimming speeds (Tadir *et al.* 1990; Nascimento *et al.* 2006). For domestic dog sperm, it was found that for a subset of the sperm population, swimming force linearly increased with swimming speed (Nascimento *et al.* 2006). The study showed that in addition to common measurements of sperm motility, such as swimming velocity and lateral head movement, the quantitative measurement of sperm swimming force is a useful parameter for assessing sperm motility and quality. However, in that study, a

major problem was low throughput. The user had to manually trap the sperm and use an offline program to calculate the swimming speed of each sperm analyzed. The challenges thus were (1) to catch a sperm and measure its swimming force and velocity all automatically and (2) to repeat this process for many sperm (>150) during a period of approximately 3 hours (period during which sperm preparation was viable). These problems have been solved through a combination of laser tweezers and computer/robotic technology (Shi *et al.* 2006b), creating a system that can be used to assess sperm from a variety of species.

In primate species where the mating pattern is polygamous (multimale-multifemale), several different males copulate with a single female within a short time-frame. As a result, strong competition for fertilization between the sperm from the rival males occurs within the female reproductive tract (Dixson 1998). Evidence indicates that sexual selection through sperm competition has directly affected sperm morphology, sexual behavior, and the structure of accessory sexual organs. Sexual selection has been shown to result in the evolution of larger testis relative to body weight in males where the level of sperm competition is high (Harcourt *et al.* 1981). Males from multi-partner mating mammals were shown to have high sperm production rates, large sperm reserves, and large numbers of sperm per ejaculate (Moller 1989). In addition, the vas deferens is shorter and has a thicker muscular structure in males from multi-partner mating systems than in males from single partner mating systems (Anderson *et al.* 2004). Morphological analysis of individual sperm showed that sperm from males of multi-partner mating systems have larger

midpiece volumes compared to those from males of single partner mating systems (Anderson and Dixson 2002).

In this chapter, a combination of laser trapping, computer tracking software and robotics is used to study the question of sperm evolution in relation to the mating patterns of different primates. Sperm swimming force and swimming speed, as well as the relationship between these two parameters are measured and compared for four primate species: chimpanzee, rhesus macaque, human and gorilla. The results are supportive of sperm competition during the evolution of primates. Additionally, the swimming speed and swimming force distributions of mice species with known mating patterns (including single-partner and multi-partner mating systems) are analyzed.

7.2 Materials and Methods

7.2.1 Specimen

Semen samples were collected from four primates: chimpanzee (*Pan troglodytes verus*, four males, fresh samples), rhesus macaque (*Macaca mulatta*, two males, fresh and frozen samples), human (*Homo sapiens*, four males, fresh and frozen samples), and western lowland gorilla (*Gorilla gorilla*, two males, fresh and frozen samples). Although it is difficult to do a comparative study where semen samples from each species are prepared using different methods, the procedures used have undergone a great deal of optimization by the laboratories specializing in studying sperm of each respective species. In addition, since prior studies have shown that properly freezing, storing, and thawing sperm has no significant effect on the escape

force of human sperm (Dantas *et al.* 1995), frozen-thawed and fresh semen samples in the present study are considered comparable.

Sperm preparation protocol for fresh chimpanzee (collected using an artificial vagina), fresh human (collected by masturbation after 3 days of abstinence) and fresh gorilla (collected opportunistically after animal masturbated in cage) samples is as follows: samples were allowed to liquefy at room temperature for 30 minutes then added to 10mL of Biggers, Whittens, and Whittingham (BWW) with Penicillin and Streptomycin and transported in a cooler at 10°C. Samples were washed with BWW (21mM HEPES, 21.5mM Lactic acid, 91.06 mM NaCl, 4.78 mM KCl, 1.71 mM CaCl, 1.71 mM KH2PHO4, 2.44 mM MgSO4, 5.55 mM Glucose, 4mM NaHCO3, 0.25 mM Napyruvate, 1% bovine serum albumin (BSA), pH 7.5, filter sterilized over 22µm filter, osmolarity 295 mOsm/kg water, kept at 4ºC and warmed to room temperature prior to use) by spinning at 600g for 6 minutes. These samples were received within 24 hours of ejaculation and analyzed within 48 hours. Fresh rhesus macaque semen samples were prepared for cooled (5^{o}C) storage as follows: 4mL of media (0.5 mg of BSA per 1mL of BWW) was added to the semen and rotated for 5 minutes on a rocker. The coagulum was pulled up onto the side of the tube and left to sit for 10 minutes. The top 3.5mL of sperm supernatant was transferred into a new tube (sperm motility and concentration were checked). The sample was centrifuged at 300g for 10 minutes then suspended at 50 x 10^{6}/mL in a commercial nonfat dry skim milk semen diluent (Animal Reproduction Systems, Chino, CA). The sample was loaded into Whirl-Pak® bags (Nasco, Fort Atkinson, WI) ensuring minimal air space then placed

in an Equitainer® semen transporter (Hamilton Research, Inc, South Hamilton, MA) and shipped overnight to the lab. The samples arrived at approximately 24 hours and were analyzed after warming the sample (37°C) for 5-10 minutes. Frozen rhesus macaque semen samples were prepared using a programmable freezer utilizing a Tes-Tris egg yolk-containing medium in addition to 3% glycerol (freezing curve: 22°C – 8°C at 0.2°C/min followed by cooling to -110°C at -17°C/min and plunging in liquid nitrogen), and were thawed in 37°C water bath for approximately one minute before analysis. Frozen human semen samples were frozen according to published protocol (DiMarzo *et al.* 1990; Ethics Committee of the American Fertility Society 1986; Serfini and Marrs 1986) and prepared for analysis using a twice wash protocol (DiMarzo and Rakoff 1986; Toffle *et al.* 1985). Frozen gorilla samples were frozen according to published protocol (O'Brien *et al.* 2002) and thawed for eight seconds in 50°C water bath before analysis.

All primate samples, except human, were suspended in BWW+BSA (1mg of BSA per 1mL of BWW) for analysis. Human sperm were suspended in modified Human Tubal Fluid (mHTF) HEPES buffered (osmolarity 272 – 288 mOsm/kg water, pH of 7.3 – 7.5) with 5% Serum Substitute Supplement (SSS) filtered through 0.2um syringe filter, first five drops were disposed (Irvine Scientific, Santa Ana, Ca). Sperm samples of 30,000 sperm per mL of media dilutions were loaded into rose chambers and mounted into a microscope stage holder and kept at 37°C using an air curtain incubator (NEVTEK, ASI 400 Air Stream Incubator, Burnsville, VA) interfaced with

a thermocouple feed-back system. A total of 622 chimpanzee sperm, 324 rhesus macaque sperm, 549 human sperm, and 338 gorilla sperm were analyzed.

7.2.2 Hardware, Software, and Optical Design

The optical design used to create the laser tweezers, hardware and sperm tracking software, experimental procedure and analysis of sperm have been described in greater detail in Nascimento *et al.* 2006, Shi *et al.* 2006a and 2006b. Briefly, an optical trap was generated using a 1064nm wavelength laser, coupled into a Zeiss Axiovert S100 microscope with a 40x phase III, NA 1.3, oil immersion objective (Zeiss, Thornwood, NY). (See chapter 3 figure 3.1 for optical schematic.)

Phase contrast images of swimming sperm are digitized to the computer at video rate. The real-time automated tracking and trapping system, RATTS, creates a region of interest (ROI) centered about a sperm in response to a mouse click. The contrast enhancement and multi-class image segmentation algorithms are applied to extract the tracked sperm head as it transitions in and out of focus. The nearest neighbor method is complemented with a speed-check feature to aid tracking in the presence of additional sperm or other particles. The swimming velocity (curvilinear velocity, VCL, μm/sec) is calculated based on the pixel (x, y) coordinates of the sperm's swimming trajectory:

$$VCL = \frac{\sum_{i=1}^{N}\left(\frac{\sqrt{(x_i - x_{(i-1)})^2 + (y_i - y_{(i-1)})^2}}{\Delta frame} * \frac{micron}{1.39\,pixel} * \frac{30\,frames}{\sec}\right)}{N_{frames}}$$

where *i* is the current frame. Since the sperm is tracked by the head, VCL accounts for both forward progression and lateral head movement. This measurement is the same

as that made by conventional Computer Assisted Sperm Analysis (CASA) machines. After 3.33 seconds (100 frames), the average VCL is stabilized (Shi *et al.* 2006a). Therefore, RATTS automatically traps the sperm after 3.33 seconds using the laser tweezers (Shi *et al.* 2006b). Once trapped, the laser power is reduced by rotating a linear polarizer set in a rotating mount (Newport Corporation, Model PR50PP, Irvine, CA). RATTS monitors a square region, ~10μm/side, centered about the laser (x, y) coordinates. The image within this region is segmented and a size threshold is used to detect the presence or absence of the sperm. RATTS then automatically identifies when the sperm is capable of escaping the trap and records the escape laser power in Watts (Pesc, mW) (Shi *et al.* 2006b).

7.3 Results

Semen samples from chimpanzee, rhesus macaque, human and gorilla are analyzed. The mating systems for both the chimpanzee and rhesus macaque are multimale-multifemale (females of these species mate with more than one male within a short period of time). Gorillas are polygynous, defined here as one male – multiple females. That is, the single dominant male mates with the females in the "harem" unit (Dixson 1998), and therefore, from the female point of view, the gorilla is strictly monogamous. Human mating patterns are variable, differing across cultures but can be considered to be predominantly polygynous (83% of societies), more rarely monogamous (16%) and only very occasionally polyandrous (<1%) (Dixson 1998). Therefore, the sperm analyzed in this study come from primates that represent a variety mating patterns, ranging from strictly polygynous (gorilla) to multimale-

multifemale (chimpanzee and rhesus macaque). The level of sperm competition respectively ranges from absent to very intense.

Sperm swimming forces and swimming speeds are measured for the four primate species. Slight variation in VCL and Pesc distributions between males within a species were found (data not shown). However, in general, there is a clustering of average swimming speed and average swimming force for males within a species, thus data sets from different males per species were pooled together to represent the larger population. Figure 7.1 shows the box plots for distributions of (a) sperm swimming speed (curvilinear velocity, VCL, μm/sec) and (b) sperm escape power (Pesc, mW) for the four primates. Each box plot graphically displays the following parameters for a given distribution: (a) median (center line of box), (b) lower and upper quartile values (bottom and top line of box, respectively), (c) the range of the data (dashed lines extending from the top and bottom of box), and (d) the data points lying outside three times the interquartile range (labeled as '+' marks). Notches in the box represent an estimate of the uncertainty about the median value. If notches on the box plots of two groups do not overlap, it can be concluded with 95% confidence that the two medians differ. Inset in figure 7.1 (b) is an expanded view of the human and gorilla Pesc box plots to emphasize the difference in medians between the two species. Data points lying outside three times the interquartile range are present only in the swimming force distributions. These "outliers" represent a small percentage of the sperm population (2.57% of chimpanzee population, 0% of rhesus macaque population, 3.46% of human population, and 7.69% of gorilla population). Each species

swimming speed and escape force distributions are found to be statistically different ($P < 0.05$) using the Wilcoxon rank sum test for equal medians (Zar 1984) (VCL and Pesc distributions for all primates are found not to be normally distributed using Lilliefors test (Zar 1984), thus requiring the use of the non-parametric Wilcoxon test). The medians of both measurements, VCL and Pesc, show that rhesus macaque and chimpanzee sperm swim with the fastest speeds and the strongest forces, while gorilla sperm swim with the slowest speeds and weakest forces. Human sperm swimming speeds and swimming forces lie between these two extremes.

(a)

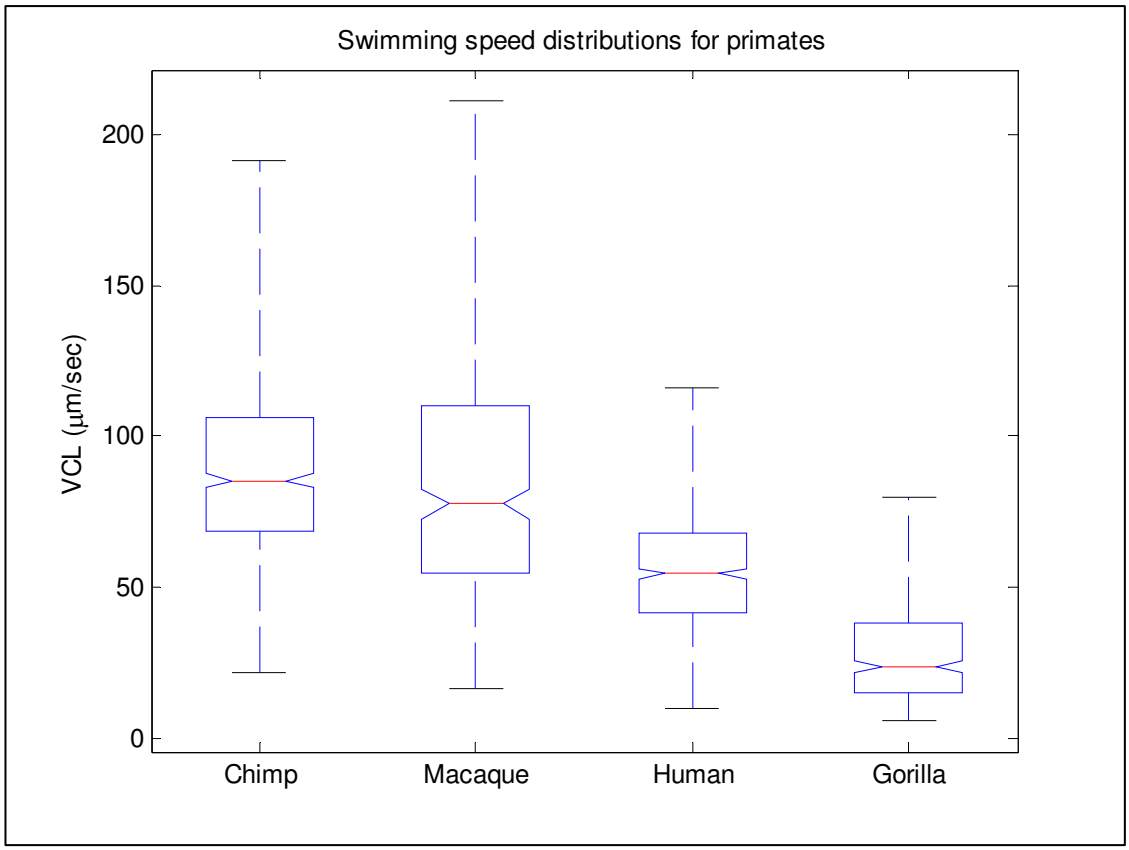

Figure 7.1: Swimming Speed and Escape Power Distributions. Box plots of the distributions of (a) swimming speed (VCL, µm/sec) and (b) escape power (Pesc, mW) for all four primates. Inset in figure (b) shows a magnified view of human and gorilla distributions to emphasize the difference in median values. All distributions are found to be statistically significantly different ($P < 0.05$).

(b)

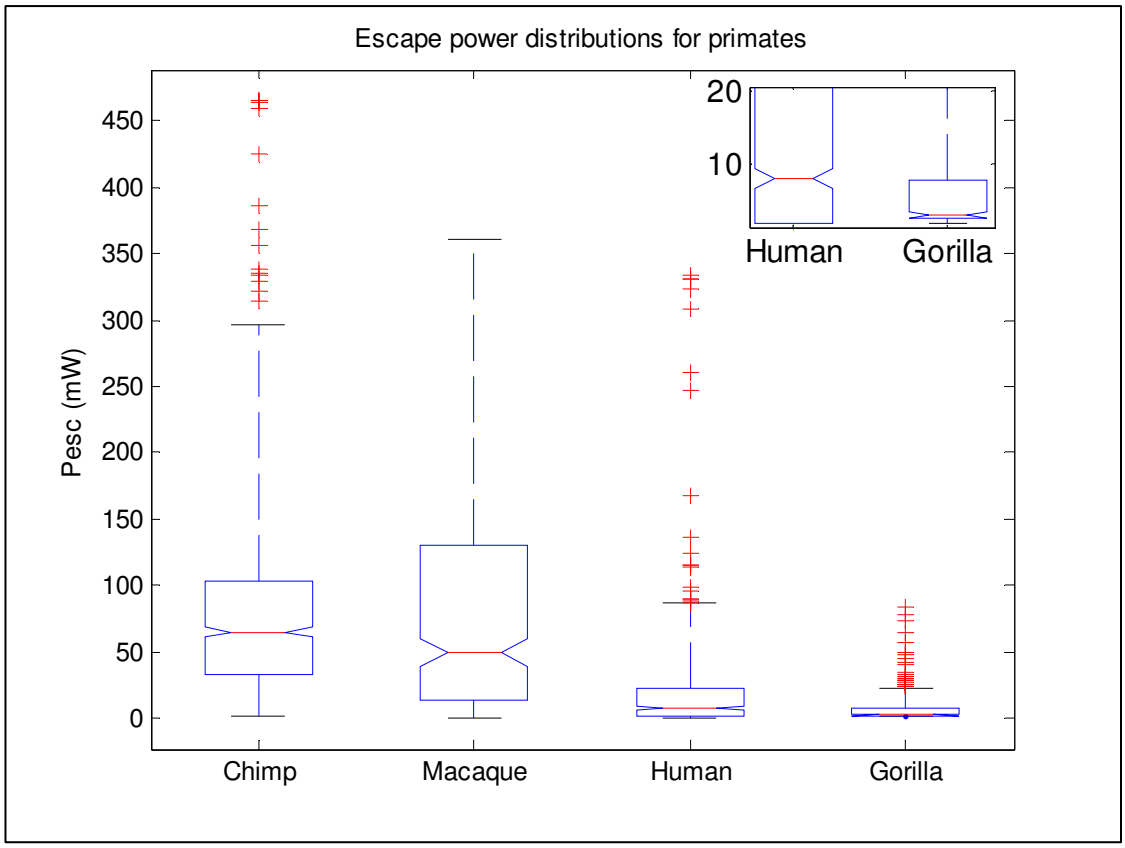

Figure 7.1 (continued): (b) Box plots of the escape power (Pesc, mW) distributions for all four primates. Inset in figure (b) shows a magnified view of human and gorilla distributions to emphasize the difference in median values. All distributions are found to be statistically significantly different ($P < 0.05$).

Relationships between the two measurements, Pesc and VCL, for each species have also been identified. Figure 7.2 overlaps the plots of Pesc (mW) vs. VCL (μm/sec) for each primate species analyzed. This figure reflects the range in sperm competition, showing that as the level of competition increases, the swimming speed distribution increases to faster velocities and the escape force distribution increases to stronger swimming forces. Figure 7.3 shows the data of Pesc vs. VCL with robust

linear regressions applied to the scatter plots for the four different primates. Inset in each graph of figure 7.3 are the regression equations, giving the slopes, y-intercepts, and R^2 values. Each linear regression relating VCL and Pesc was found to be statistically different, using a linear regression comparison test (Zar 1984), for all four primates ($P < 0.05$).

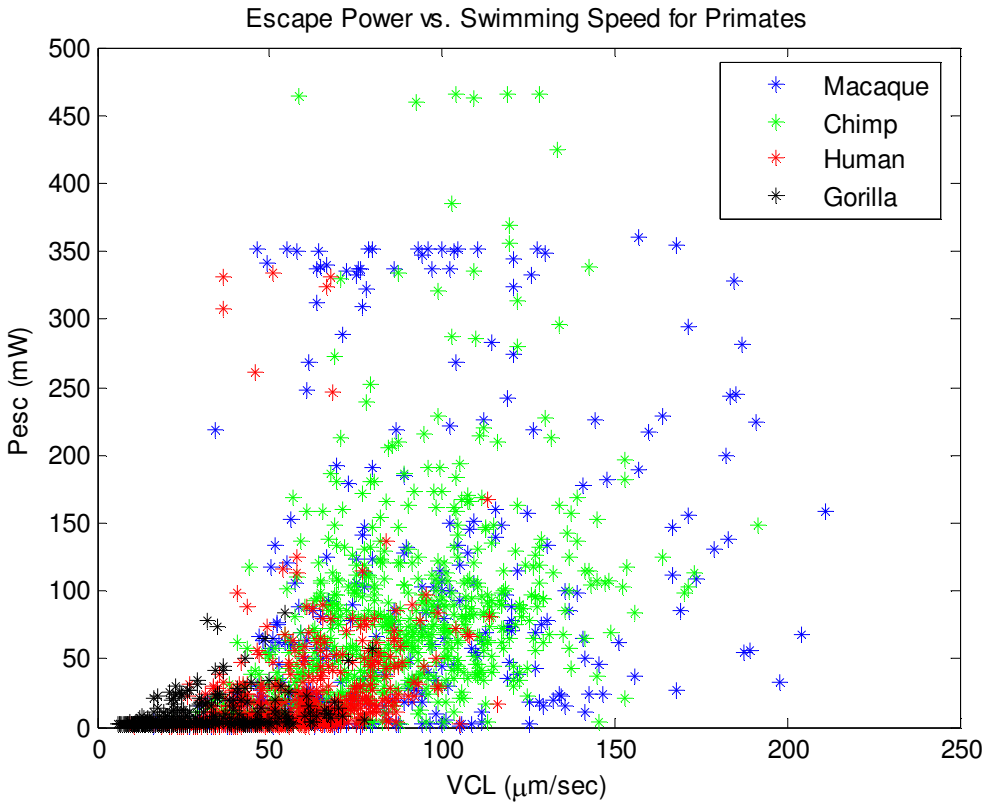

Figure 7.2: Escape Power vs. Swimming Speed. All four primates (chimpanzee, rhesus macaque, human, gorilla) overlapping to show that as level of sperm competition increases, so does sperm swimming speed and force.

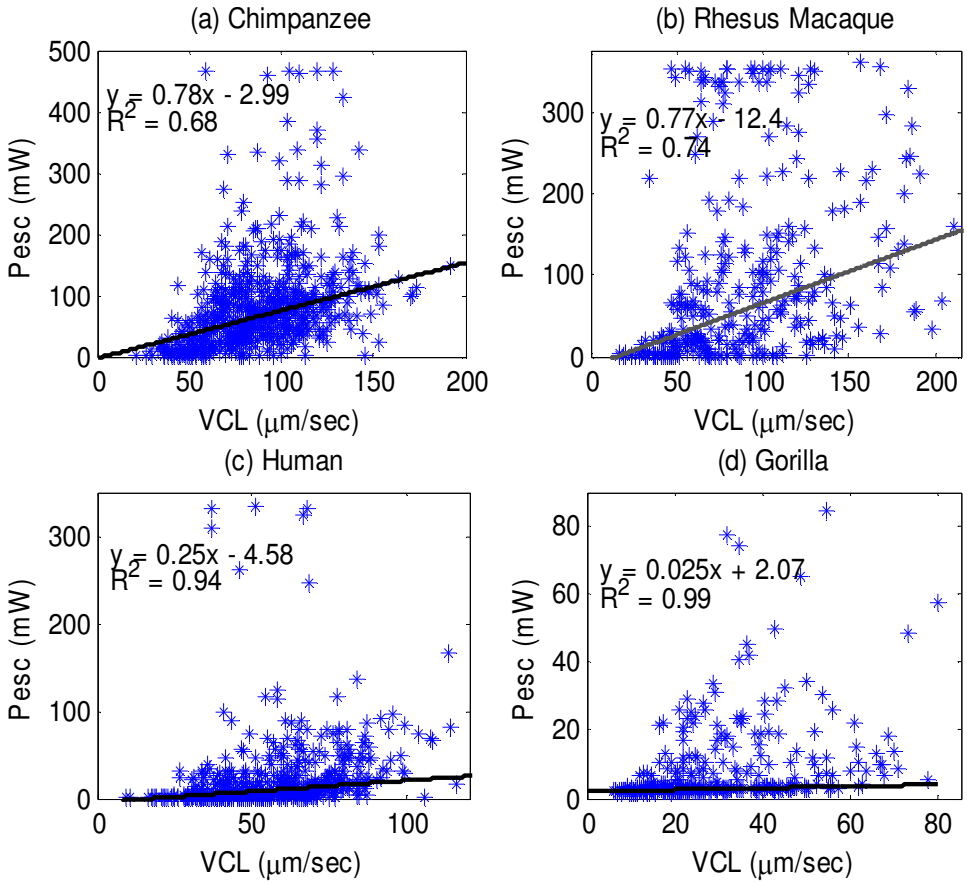

Figure 7.3: Escape Power vs. Swimming Speed with Regressions. Pesc (mW) vs. VCL (μm/sec) with linear regressions for four primate species: (a) Chimpanzee, (b) Rhesus Macaque, (c) Human, (d) Gorilla. Inset on each graph gives the regression equation (slope and y-intercept) as well as the R^2 value to show goodness of fit. Each regression is found statistically significantly different ($P < 0.05$).

7.4 Discussion

The results shown in figure 7.1 compare the median escape power and swimming speeds between primate species. The data show a relatively wide variation in the distributions of both VCL and Pesc for all four species. This same wide

variation is found for each male within a species as well (data not shown). Notwithstanding these variations, the data demonstrate that escape force and swimming speed increase as the level of sperm competition increases. These results support the theory that sperm from primates that are polygamous have experienced high competitive pressures and thus have evolved to swim both stronger and faster than sperm from primates that have not been under such high competitive pressures.

Relationships between escape force and swimming speed for each species were also identified. The results in figure 7.3 demonstrate that for each species, faster sperm swim with stronger forces, confirming the relationship found between the two parameters in previous studies using domestic dog semen (Nascimento et al. 2006). However, the slope of the linear regression becomes steeper as the level of sperm competition increases. Specifically, comparing gorilla to chimpanzee and rhesus macaque, the slope approximately increases by a factor of thirty. In addition, the two multi-partner mating primates have lower R^2 values for the regressions, whereas the other two primates, human and gorilla, have regressions with a much higher R^2 value. The regressions therefore fit the data much better for the human and gorilla than they do for the multi-partner mating primates. The lower R^2 values for the chimpanzee and rhesus macaque reflect the spread in the escape force distribution, as seen in figure 7.1b, and indicate that for these polygamous species, sperm swimming speed is a poor predictor of the sperm's escape power. Explanation and speculation about the difference in the slopes and the R^2 values must await further studies that examine

larger populations of sperm from a larger number of males for each primate species studied (as discussed in chapter 6).

In conclusion, I have used a custom-designed real-time automated tracking and trapping system (RATTS) to measure sperm escape power and swimming speed. These results support the theory of sperm competition. The data presented here are intriguing and appear to demonstrate a correlation between sperm motility and mating type. Furthermore, this combination of physics (optics and lasers) and engineering (automated computer tracking) principles should be applicable to other problems of sperm motility as well as to the study of cell behavior in other motile cell systems.

Acknowledgements

The material presented in Chapter 7 is a reprint of the material as it appears in "The use of optical tweezers to study sperm competition and motility in primates," by J. M. Nascimento, L. Z. Shi, S. Meyers, P. Gagneux, N. M. Loskutoff, E. L. Botvinick, and M. W. Berns, *J. R. Soc. Interface* doi:10.1098/rsif.2007.1118 (Online), 2007. The dissertation author was the first author of the paper.

References

Anderson, M. J., Dixson, A. F. (2002). Motility and the midpiece in primates. *Nature* **416**, 496.

Anderson, M. J., Nyholt, J., Dixson, A. (2004). Sperm competition affects the structure of the mammalian vas deferens. *J. Zool. Lond.* **264**, 97-103.

Araujo, E. Jr., Tadir, Y., Patrizio, P., Ord, T., Silber, S., Berns, M. W., Asch, R. H. (1994). Relative force of human epididymal sperm. *Fertil. Steril.* **62**(3), 585-590.

Ashkin, A., Dziedzic, J. M., Yamane, T. (1987). Optical trapping and manipulation of single cells using infrared laser beams *Nature* **330**:769-771.

Ashkin, A. (1991). The study of cells by optical trapping and manipulation of living cells using infrared laser beams. *ASGSB Bull.* **4**, 133-146.

Berns, M. W. (1998). Laser scissors and tweezers. *Scientific American (International Edition)* **278**, 52-57.

Berns, M. W., Wright, W.H., Tromberg, B. J., Profeta, G.A., Andrews, J. J., Walter, R.J. (1989). Use of a laser-induced optical force trap to study chromosome movement on the mitotic spindle. *PNAS* **86**(12): 4539-43.

Dantas, Z. N., Araujo, E. Jr., Tadir, Y., Berns, M. W., Schell, M. J., Stone, S. C. (1995). Effect of freezing on the relative escape force of sperm as measured by a laser optical trap. *Fertil. Steril.* **63**(1), 185-188.

DiMarzo, S. J., Huang, J., Kennedy, J. F., Villanueva, B., Hebert, S. A., Young, P. E. (1990). Pregnancy rates with fresh versus computer-controlled cryopreserved semen for artificial insemination by donor in a private practice setting. *Am. J. Obstet. Gynecol.* **162**(6), 1483-1490.

DiMarzo, S. J., Rakoff, J. S. (1986). Intrauterine insemination with husband's washed sperm. *Fertil. Steril.* **46**, 470-475.

Dixson, A. F. (1998). *Primate Sexuality: Comparative Studies of the Prosimians, Monkeys, Apes, and Human Beings,* Oxford University Press, Oxford.

The Ethics Committee of the American Fertility Society, from the New Guidelines for the use of Semen for Donor Insemination (1986). *Fertil. Steril.* **6**(Suppl), 85.

Harcourt, A. H., Harvey, P. H., Larson, S. G., Short, R. V. (1981). Testis weight, body weight and breeding system in primates. *Nature* **293**, 55-57.

Konig, K., Svaasand, L., Liu, Y., Sonek, G., Patrizio, P., Tadir, Y., Berns, M. W., Tromberg, B. J. (1996). Determination of motility forces of human spermatozoa using an 800 nm optical trap. *Cell. Mol. Biol. (Noisy-le-grand)* **42**(4), 501-509.

Moller, A. P. (1989). Ejaculate quality, testes size and sperm production in mammals. *Funct. Eco.* **3**(1), 91-96.

Nascimento, J. M., Botvinick, E. L., Shi, L. Z., Durrant, B., Berns, M. W. (2006). Analysis of sperm motility using optical tweezers. *J. Biomed. Opt.* **11**(4), 044001.

O'Brien, J. K., Crichton, E. G., Evans, K. M., Schenk, J. L., Stojanov, T., Evans, G., Maxwell, W. M. C., Loskutoff, N. M. (2002). Sex ratio modification using sperm sorting and assisted reproductive technology – a population management strategy. In *Proceedings of the Second International Symposium on Assisted Reproductive Technology for the Conservation and Genetic Management of Wildlife* (Omaha's Henry Doorly Zoo), pp. 224-231.

Ozkan, M., Wang, M. M., Ozkan, C., Flynn, R. A., Esener, S. (2003). Optical manipulation of objects and biological cells in microfluidic devices. *Biomedical Microdevices* **5**, 47-54.

Patrizio, P., Liu, Y., Sonek, G. J., Berns, M. W., Tadir, Y. (2000). Effect of pentoxifylline on the intrinsic swimming forces of human sperm assessed by optical tweezers. *J. Androl.* **21**(5), 753-756.

Serfini, P., Marrs, R. P. (1986). Computerized staged-freezing technique improves sperm survival and preserves penetration of zona-free hamster ova. *Fertil. Steril.* **45**, 854-858.

Shao, B., Zlatanovic, S., Ozkan, A., Birkbeck, A., Esener, S. C. (2006). Manipulation of microspheres and biological cells with multiple agile VCSEL traps. *Sensors and Actuators, B. Chem.* **113**(2), 866-874.

Shi, L. Z., Nascimento, J., Berns, M. W., Botvinick, E. (2006a). Computer-based tracking of single sperm. *J. Biomed. Opt.* **11**(5), 054009.

Shi, L. Z., Nascimento, J. M., Chandsawangbhuwana, C., Berns, M. W., Botvinick, E. (2006b). Real-time automated tracking and trapping system (RATTS). *Microscopy Research and Technology* **69**(11), 894-902.

Tadir, Y., Wright, W. H., Vafa, O., Ord, T., Asch, R. H., Berns, M. W. (1989). Micromanipulation of sperm by a laser generated optical trap. *Fertil. Steril.* **52**(5), 870-873.

Tadir, Y., Wright, W. H., Vafa, O., Ord, T., Asch, R. H., Berns, M. W. (1990). Force generated by human sperm correlated to velocity and determined using a laser generated optical trap. *Fertil. Steril.* **53**(5), 944-947.

Toffle, R. C., Nagel, T. C., Tagatz, G. E., Phansey, S. A., Okagaki, T., Wavrin, C. A. (1985). Intrauterine insemination: The University of Minnesota Experience. *Fertil. Steril.* **43**(5), 743-747.

Zar, J. H. (1984). in *Biostatistical Analysis,* 2nd end. pp. 150-161 and pp. 292-305. Prentice Hall, Englewood Cliffs.

VIII. Sperm Mitochondrial Respiration

8.1 Introduction

Quantitative and objective techniques are important for assessing sperm quality. Computer Assisted Sperm Analysis (CASA) systems have been developed to measure parameters such as curvilinear velocity, amplitude of lateral head movement, and percent of motile sperm, providing quantitative information about the overall motility of a sperm population (Amann and Katz 2004; Mortimer 1994). In addition, flow cytometry in combination with fluorescent probes has been used to monitor mitochondrial membrane potential (MMP) in sperm cells (Marchetti *et al.* 2002 and 2004; Gallon *et al.* 2006; Kasai *et al.* 2002). MMP, given by the Nernst equation, is dependent upon the distribution of hydrogen ions across the inner mitochondrial membrane. This electrochemical proton gradient drives the synthesis of ATP that is used for energy by the cell. Therefore, the fluorescence intensity of cyanine dyes, such as 3,3'-diethyloxacarbocyanine iodide ($DiOC_2(3)$), which increases as the magnitude of MMP increases, is an indicator of the energetic state of the cell. Studies have demonstrated that high MMP in sperm correlates with increased motility (Marchetti *et al.* 2002) as well as high fertility (Marchetti *et al.* 2004; Gallon *et al.* 2006; Kasai *et al.* 2002). Several fluorescent probes are available, and comparisons between probes have been performed (Marchetti *et al.* 2004; Novo *et al.* 1999). Specifically, Novo *et al.* (1999) showed that the ratiometric technique for estimation of MMP using $DiOC_2(3)$ was an accurate indicator of bacterial MMP.

Single spot, gradient force laser tweezers is another tool that has been used to study sperm motility by measuring sperm swimming force. It has been shown that the minimum laser power needed to hold a sperm in the optical trap (threshold escape power) is directly proportional to the sperm's swimming force ($F = Q \times P / c$ where F is the swimming force in picoNewtons, P is the laser power in milliWatts, c is the speed of light in the medium with a given index of refraction, and Q is the geometrically determined trapping efficiency parameter) (Konig *et al.* 1996). Previous studies have demonstrated a positive correlation between sperm swimming speed and escape laser power (Tadir *et al.* 1990; Nascimento *et al.* 2006 and 2007. Optical traps have also been used in combination with the fluorescent probe JC-1 (5, 5', 6, 6' -tetra-chloro-1, 1', 3, 3'-tetraethylbenzimidazolyl-carbocyanine iodide) (Mei *et al.* 2005). That study measured MMP as the sperm were held in the laser trap. A major drawback, however, was the inability to determine not only the MMP of the individual sperm before or after it was exposed to the laser tweezers, but also the sperm's swimming speed and/or swimming force.

Computer tracking software and robotics were combined with the laser tweezers system to automate sperm trapping experiments (Shi *et al.* 2006a and 2006b). This custom-designed real-time, automated, tracking and trapping system, or RATTS, presents itself as a potentially useful tool, in addition to CASA systems and flow cytometric MMP measurements, to assist in the overall assessment of sperm quality. RATTS has been modified to measure MMP (prior to, during and post trapping) in

conjunction with swimming speed and swimming force of individual sperm (Shi *et al.* 2007).

In this chapter, I first describe the modification of RATTS to analyze domestic dog sperm labeled with the fluorescent probe, $DiOC_2(3)$. The effects of the probe on sperm motility are determined. The ability to monitor changes in MMP is quantified for the probe as well as the system. The effects of prolonged exposed to the laser tweezers on VCL and MMP are analyzed. In these three studies, the system's capabilities are demonstrated by simultaneously measuring VCL, Pesc and MMP for individual sperm. The results show that the combination of laser tweezers, robotics, and fluorescence imaging creates an integrated system capable of providing a detailed description of individual sperm.

The second part of the chapter uses this tool to study the role of two potential sources of ATP: oxidative phosphorylation which occurs in the mitochondria located in the sperm midpiece and glycolysis which occurs along the length of the sperm tail. Oxidative phosphorylation is a more efficient means of generating ATP than glycolysis (the metabolism of sugars in mitochondria can produce fifteen times more ATP than glycolysis (Alberts *et al.* 2002)). However, there is some doubt that ATP can sufficiently diffuse from the midpiece down to the distal segments of the tail (Turner 2003; Ford 2006). Recent studies suggest glycolysis is an important pathway for ATP generation in sperm. Analysis of the flagellum has shown that several glycolytic enzymes are localized to the fibrous sheath in mouse and human sperm (Krisfalusi *et al.* 2006; Kim *et al.* 2007) as well as an ADP/ATP carrier protein in

human sperm (Kim *et al.* 2007). Having energy production and translocation mechanisms localized to the sperm tail suggests that sperm rely upon glycolytic generation of ATP for motility (Kim *et al.* 2007). Other studies have demonstrated the importance of glucose for sperm motility. Williams *et al.* (2001) showed that the percent of motile human sperm as well as their smoothed path velocity was statistically greater when incubated in media containing glucose. Mukai *et al.* (2004), who measured the beat frequency of mouse sperm flagella, showed that the beat frequency was significantly reduced for sperm in media without glucose and that exposure to an electron transport chain inhibitor (antimycin A) did not affect flagellum beat frequency so long as the media contained glucose. Similarly, Krzyzosiak *et al.* (1999) found that bull sperm were motile in the presence of both antimycin A and rotenone (another electron transport chain inhibitor) only when suspended in media that contained glucose. Miki *et al.* (2004) found that motility (measured by CASA) was reduced in sperm from mice lacking a sperm-specific glycolytic enzyme (glyceraldehyde 3-phosphate dehydrogenase-S, GAPDS) compared to the wild type. These studies build a case for glycolysis as a major source of energy for sustained sperm motility. However, experimental proof of this is necessary.

In the second half of this chapter, the relationships between mitochondrial membrane potential (i.e. oxidative phosphorylation) and sperm swimming force and swimming speed are analyzed for domestic dog, human and gorilla species. The effects of different media, the presence/absence of glucose in the media, and both oxidative phosphorylation and glycolytic inhibitors on human sperm motility (VCL,

Pesc) and MMP are studied. The results provide quantitative evidence supporting the theory that glycolysis is a critical pathway for the generation of energy (ATP) for human sperm motility.

8.2 Materials and Methods

8.2.1 Specimen

Domestic dog: Semen samples collected from several domestic dogs are cryogenically frozen according to a standard protocol (Durrant *et al.* 2000; Harper *et al.* 1998). Studies on human sperm have shown that properly freezing, storing, and thawing sperm has no significant effect on escape force (Dantas *et al.* 1995). In addition, we compared frozen-thawed and fresh dog sperm from the same semen sample and found that the swimming speed and escape laser power distributions were statistically the same (swimming speed: $P > 0.06$; escape power: $P > 0.9$, data not shown). Therefore, frozen-thawed semen samples in this study are considered comparable to fresh samples. (See chapter five for more details.)

For each experiment, a sperm sample is thawed in a water bath (37^{o}C) for approximately one minute and its contents are transferred to an Eppendorf centrifuge tube. The sample is centrifuged at 2000 rpm for ten minutes (centrifuge tip radius is 8.23cm). The supernatant is removed and the remaining sperm pellet is suspended in 1 milliliter (mL) of pre-warmed media (1mg of bovine serum albumin (BSA) per 1mL of Biggers, Whittens, and Whittingham (BWW), osmolality of 270 – 300 mmol/kg water, pH of 7.2 – 7.4 (Biggers *et al.* 1971)).

Primates: Frozen western lowland gorilla samples are frozen according to published protocol (O'Brien *et al.* 2002) and thawed for eight seconds in 50^{o}C water bath before analysis. Gorilla sperm are suspended in BWW+BSA for analysis. Frozen human semen samples are frozen according to published protocol (DiMarzo *et al.* 1990; Ethics Committee of the American Fertility Society 1986; Serfini and Marrs 1986) and prepared for analysis using a twice wash protocol (DiMarzo and Rakoff 1986; Toffle *et al.* 1985). To study the relationship between MMP and both Pesc and VCL, the human sperm are suspended in modified Human Tubal Fluid (mHTF) HEPES buffered (osmolarity 272 – 288 mOsm/kg water, pH of 7.3 – 7.5) with 5% Serum Substitute Supplement (SSS) filtered through 0.2um syringe filter, first five drops were disposed (Irvine Scientific, Santa Ana, Ca). (A different preparation method described in detail below is used for the study of the effects of glucose and inhibitors.)

Final dilutions of ~30,000 sperm (dog, human and gorilla) per mL of media are used in the experiments. The diluted sperm suspension is loaded into a 3mL Rose tissue culture chamber and mounted into a microscope stage holder according to previously described methods (Liaw and Berns 1981). The sample is kept at 37^{o}C using an air curtain incubator (NEVTEK, ASI 400 Air Stream Incubator, Burnsville, VA). A thermocouple is attached to the Rose chamber to insure temperature stability.

MMP Assessment: To monitor the voltage potential across the inner membrane of the mitochondria, sperm are labeled with $DiOC_2(3)$ (3,3'-dithyloxacarbocyanine, 30nM final dye concentration for all experiments, Molecular Probes, Invitrogen Corp.,

Carlsbad, CA). $DiOC_2(3)$ is a cationic cyanine dye that primarily accumulates in the mitochondria of a cell in response to the electrochemical proton gradient, or membrane potential. The probe emits both a red and green fluorescence. The ratiometric parameter (red/green intensity) is a size-independent measure of MMP, as the green fluorescence varies with size and red fluorescence is dependent on both size and MMP (Novo *et al.* 2000). After the dye is added, the cells are incubated for 20 minutes in a 37^{o}C water bath and then centrifuged for 10 minutes (2000rpm). The pellet is suspended in the media by 'flicking' the tube according to the protocol for the MitoProbe assay kit (Invitrogen Corp.) for flow cytometry.

8.2.2 Hardware, Software and Optical Design

The optical system, shown in figure 8.1a, is adapted after Nascimento, *et al.* (2006). A single point gradient trap is generated using an Nd:YVO_4 continuous wave 1064 nm wavelength laser (Spectra Physics, BL-106C, Mountain View, CA), coupled into a Zeiss Axiovert S100 microscope equipped with a phase III, 40x, NA 1.3, oil immersion objective (Zeiss, Thornwood, NY). Laser power in the specimen plane is attenuated by rotating the polarizer, which is mounted in a stepper-motor-controlled rotating mount (Newport Corporation, Model PR50PP, Irvine, CA).

The imaging setup is shown in figure 8.1b. Two dual video adapters are used to incorporate the laser into the microscope and simultaneously image the sperm in phase contrast and fluorescence. The laser beam enters the side port of the first dual video adapter and is transmitted to the microscope. A filter (Chroma Technology Corp., Model E700SP-2P, Rockingham, VT) is used to prevent back reflections of IR

laser light from exiting the top port of the adapter but allow reflected visible light coming from the specimen to pass to the second video adapter. The specimen is viewed in phase contrast using red light filtered from the halogen lamp (Chroma Technology Corp., Model D680/60 X) and in fluorescence using the arc lamp (Zeiss FluoArc). The fluorescence filter cube contains an HQ 500/20 nm excitation filter and a dichroic beam splitter with a 505 nm cut-on wavelength. The second dual video adapter attached to the top port of the first video adapter uses a filter cube to separate the phase information (reflects > 670nm) from the fluorescence (transmits 500-670 nm). The phase contrast images are filtered through a filter (Chroma Technology Corp., Model HQ 675/50M) and acquired by a CCD camera (Cohu, Model 7800, San Diego, CA, operating at 40 frames per second) coupled to a variable zoom lens system (0.33 – 1.6 X magnification) to increase the field of view. For the fluorescent images, a Dual-View system (Optical-Insights, Tucson, AZ) splits the red and green fluorescent light emitted by the specimen to produce a copy of the image for each color. Fluorescent emission filters are placed in this emission-splitting system (green fluorescence emitter: HQ 535/40nm M filter; red fluorescence emitter: HQ 605/50nm M filter, Chroma Technology Corp.). The Dual-View system is coupled to a digital camera (Quantix 57, Roper Scientific Inc., Tucson, AZ) that captures the fluorescent images.

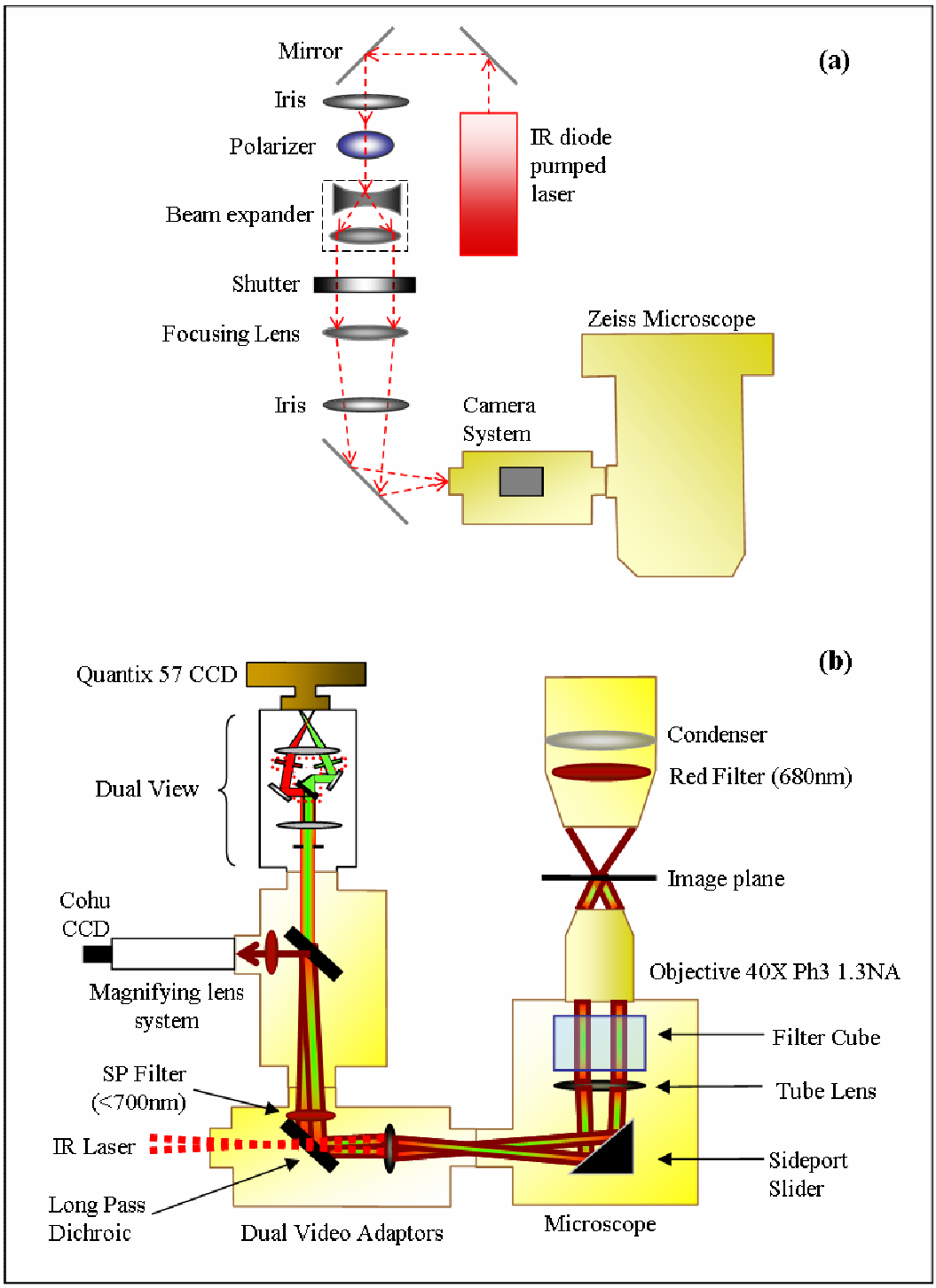

Figure 8.1: (a) Optical schematic showing the optical components used to generate and control the laser tweezers. (b) Imaging setup showing the illumination sources, filters, and cameras used to image the sperm in both phase contrast and fluorescence.

The hardware and software to perform the experiments in this paper are described in greater detail elsewhere (Shi *et al.* 2007). Briefly, two computers are networked together. An upper level computer that acquires and displays the phase images from the Cohu CCD is responsible for tracking and trapping the sperm of interest. The lower level computer is prompted by the upper level computer to acquire the fluorescent images of the sperm's mitochondria from the Quantix CCD. From the image, the lower level computer calculates the MMP ratio (red/green) value. A sample of a raw fluorescent image is shown in figure 8.2a. The image processing logic in the subroutine is as follows:

(1) Two square regions are extracted from the raw image centered about the laser trap in both the right (red) half and the left (green) half of the image as shown in figure 8.2b and 8.2c respectively.

(2) The two images are enhanced separately by subtracting background (estimated as the summation of the most frequent intensity and the standard deviation of pixel intensities) as shown in figure 8.2d for right channel and figure 8.2e for the left channel. Any negative pixel values are set to zero.

(3) A four class threshold analysis is performed on each image. Binary images are created using the lower level of the third class as the threshold value.

(4) The binary red image undergoes a morphological transformation (dilation), creating the "red mask."

(5) The binary green image is multiplied by the red mask in order to eliminate any extraneous background noise. Since both images prior multiplication

are in binary format, the particle in the resulting image is size limited by the green image. This ensures that the channel with lower signal to noise MMP ratio (green channel) governs particle size. The resulting image is the "green mask."

(6) The green mask is applied to the images found as a result of step (2). This ensures the particle size is identical in both the left and right channels and avoids division by zero.

The MMP ratio of the red image to the green image is calculated. The maximum, minimum, and mean intensity pixel values of the MMP ratio, red and green images are written in real-time to a data file.

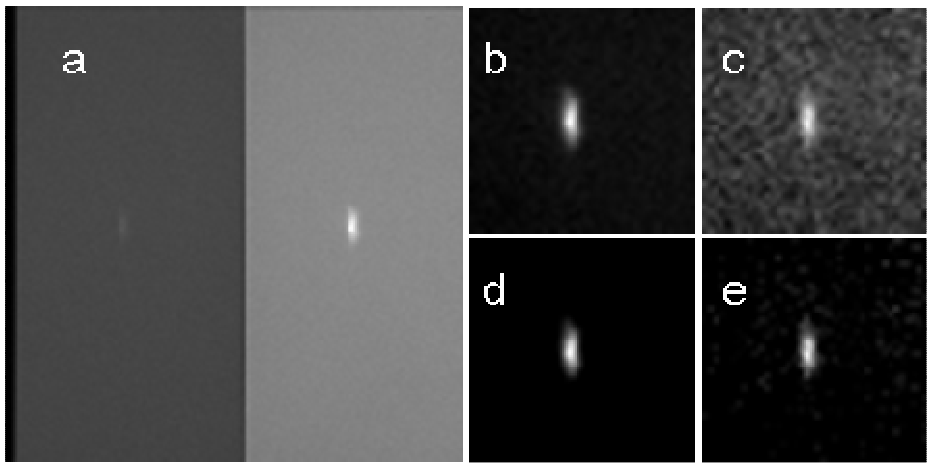

Figure 8.2: Image processing of fluorescent images: (a) The raw image taken by the Quantix camera showing both channels (green in the left, red in the right) simultaneously; (b) and (c) The enlarged partial image of the right and left channels respectively; (d) and (e) The partial images of the right and left channels respectively after background subtraction.

Once the user selects the sperm of interest, the upper level computer tracks the sperm and calculates the curvilinear velocity (VCL, μm/sec) in real-time. During this tracking phase, the microscope stage moves the sperm to the center of the field of view if it nears the edge. In addition, the sperm is relocated to a defined (x, y) coordinate every second and a command is sent to the lower level computer to acquire a fluorescent image. For track-and-trap experiments, the sperm is relocated to the laser trap coordinates after being tracked and fluorescently imaged for 5 seconds. Once the sperm is successfully trapped by the laser tweezers, the lower level computer continuously acquires fluorescent images. Laser power is either kept constant (see section 8.2.5) or is attenuated (see section 8.2.6). If the power is attenuated, the power at which the sperm is capable of escaping the trap (Pesc, mW) is recorded by the upper level computer. The sperm is tracked and fluorescently imaged for an additional 5 seconds once it is released from or escapes the optical trap. For each tracked sperm, data, including (x, y) trajectory coordinates in the field of view, stage movement, instantaneous VCL and average VCL, for each time point is saved to a file on the upper level computer. The fluorescent data, including the average, maximum and minimum MMP ratio values, for each image is saved to a file on the lower level computer.

8.2.3 Probe's effect on sperm motility

The effects of $DiOC_2(3)$ on sperm motility are assessed. The swimming speed (VCL, μm/sec) distribution of sperm exposed to $DiOC_2(3)$ is compared to that of sperm not exposed to the probe (control). Sperm from each group are analyzed during

the same time intervals. During the first time interval, both groups are viewed in phase contrast microscopy only. During the second time interval, again, both groups are viewed in phase contrast microscopy. However, the test group exposed to $DiOC_2(3)$ are also illuminated with excitation light (500nm) from the arc lamp.

8.2.4 Sensitivity to changes in MMP

The ability to measure changes in MMP as well as the ability to detect and report changes in MMP is tested. An aliquot of dog sperm are exposed to the proton ionophore CCCP (carbonyl cyanide 3-chlorophenylhydrazone, 50μM final concentration, Molecular Probes, Invitrogen Corp., Carlsbad, CA), which is known to decrease the magnitude of the MMP (Novo *et al.* 1999; Guzman-Grenfell *et al.* 2000). The test sperm group are exposed to both CCCP (50μM) and $DiOC_2(3)$ simultaneously, whereas the control sperm group are labeled only with $DiOC_2(3)$. Both groups are incubated for 20 minutes after being labeled (see section 8.2.1). Sperm are loaded onto the microscope and tracked for 10 seconds. A fluorescent image is acquired every second. The MMP ratio value and VCL distributions of the test and control groups are compared.

8.2.5 Track, trap (constant power and constant duration), and fluorescently image

Sperm labeled with $DiOC_2(3)$ are tracked and trapped under constant power (460mW) for a constant duration (90 seconds). For each sperm analyzed, fluorescent images are acquired approximately once every second during the 5 seconds prior to and post trapping and acquired continuously once the sperm is in the trap. Effects of

prolonged exposure to the laser tweezers on MMP and swimming speed (VCL, μm/sec) are assessed.

8.2.6 Track, trap (decaying laser power), and fluorescently image

Sperm labeled with $DiOC_2(3)$ are tracked and trapped under decaying power. Again, for each sperm, fluorescent images are acquired once every second during the 5 seconds prior to and post trapping and acquired continuously once the sperm is in the trap. VCL pre-trap and the average of the five ratio values calculated before trapping are used as swimming speed and MMP measurements respectively. Examples of the various responses the sperm have to the optical trap are demonstrated. The relationships between (a) VCL and MMP and (b) Pesc and MMP are addressed for dog, human and gorilla species.

8.2.7 Effects of glucose on VCL, Pesc and MMP for human sperm

After thawing, human sperm are centrifuged and washed with BWW+BSA without glucose (0mM). The sperm are divided into three aliquots of equal size and centrifuged a second time. Aliquot 1 is washed with BWW+BSA without glucose (0mM), aliquot 2 is washed with BWW+BSA with glucose (5.55mM), and aliquot 3 is washed with HTF+SSS (also with glucose, 2.78mM). Sperm from each aliquot are labeled with $DiOC_2(3)$ according to the protocol explained above. Sperm are further diluted for analysis in the appropriate media (#1: BWW+BSA without glucose, #2: BWW+BSA with glucose, and #3: HTF), loaded into the Rose chamber and onto the microscope, and analyzed (VCL, Pesc and MMP are recorded). The distributions of the three measured parameters are statistically compared (based on 5% significance).

8.2.8 Effects of glycolytic and oxidative phosphorylation inhibitors on VCL, Pesc and MMP for human sperm

Effects of 2-deoxy-D-glucose (DOG): DOG, an anti-metabolite of glucose, is used to inhibit the glycolytic pathway (Mukai and Okuno 2004). After thawing, human sperm are centrifuged and washed with BWW+BSA media lacking glucose. The sperm are divided into three aliquots of equal size and centrifuged a second time. Two aliquots are washed with BWW+BSA media lacking glucose and one is washed with BWW+BSA media containing glucose (5.55mM). The sperm in the BWW+BSA media containing glucose are exposed to DOG (6mM) and $DiOC_2(3)$ simultaneously. One of the sperm groups in the BWW+BSA media lacking glucose is also exposed to DOG (6mM) and $DiOC_2(3)$ simultaneously while the other sperm group in the media lacking glucose remains the control (labeled with $DiOC_2(3)$ only). All groups are incubated for 20 minutes after being labeled. Sperm are further diluted for analysis in the appropriate media (that with which it was washed the second time: BWW+BSA with or without glucose), loaded into the Rose chamber and onto the microscope, and analyzed (VCL, Pesc and MMP are recorded). (The experiment is repeated three times to verify results. Data from the three experiments is pooled together.) The distributions of the three measured parameters are statistically compared.

Effects of Antimycin A: Antimycin A is used to inhibit the oxidative phosphorylation pathway via the electron transport chain (inhibits the oxidation of ubiquinol in complex III) (Mukai and Okuno 2004; Miki *et al.* 2004). After thawing, human sperm are centrifuged and washed with BWW+BSA media lacking glucose.

The sperm are divided into four aliquots of equal size and centrifuged a second time. Two aliquots are washed with BWW+BSA media lacking glucose, one is washed with BWW+BSA media containing glucose (5.55mM) and the final aliquot is washed with HTF+SSS (also contains glucose, 2.78mM). The sperm groups in the BWW+BSA media containing glucose and HTF+SSS are exposed to antimycin A (40μM) and $DiOC_2(3)$ simultaneously. One of the sperm groups in the BWW+BSA media lacking glucose is also exposed to antimycin A (40μM) and $DiOC_2(3)$ simultaneously while the other sperm group in the media lacking glucose remains the control (labeled with $DiOC_2(3)$ only). All groups are incubated for 20 minutes after being labeled. Sperm are further diluted for analysis in the appropriate media (that with which it was washed the second time: BWW+BSA without glucose, BWW+BSA with glucose, or HTF), loaded into the Rose chamber and onto the microscope, and analyzed (VCL, Pesc and MMP are recorded). (The experiment is repeated three times to verify results. Data from the three experiments is pooled together.) The distributions of the measured parameters are statistically compared.

Effects of Rotenone: Rotenone is used to inhibit the oxidative phosphorylation pathway via the electron transport chain (inhibits the transfer of electrons from the iron-sulfur centers to ubiquinone in complex I) (Miki *et al.* 2004). After thawing, human sperm are centrifuged and washed with BWW+BSA media lacking glucose. The sperm are divided into four aliquots of equal size and centrifuged a second time. Two aliquots are washed with BWW+BSA media lacking glucose, one is washed with BWW+BSA media containing glucose (5.55mM) and the final aliquot is washed with

HTF+SSS (also containing glucose, 2.78mM). The sperm groups in the BWW+BSA media containing glucose and HTF+SSS are exposed to rotenone (40μM) and $DiOC_2(3)$ simultaneously. One of the sperm groups in the BWW+BSA media lacking glucose is also exposed to rotenone (40μM) and $DiOC_2(3)$ simultaneously while the other sperm group in the media lacking glucose remains the control (labeled with $DiOC_2(3)$ only). All groups are incubated for 20 minutes after being labeled. Sperm are further diluted for analysis in the appropriate media (that with which it was washed the second time: BWW+BSA without glucose, BWW+BSA with glucose, or HTF), loaded into the Rose chamber and onto the microscope, and analyzed (VCL, Pesc and MMP are recorded). (The experiment is repeated three times to verify results. Data from the three experiments is pooled together.) The distributions of the measured parameters are statistically compared.

8.3 Results

8.3.1 Probe's effect on sperm motility

The swimming speed (VCL, μm/sec) distribution of dog sperm cells exposed to $DiOC_2(3)$ is compared to that of the control sperm using the Wilcoxon paired-sample test (the distributions are found not to be Gaussian, thus requiring the non-parametric test). The VCL distributions are found to be statistically equal, even when the probe is activated by the arc lamp (without arc lamp illumination: $P > 0.3$, $N_{control} = 24$, $N_{DiOC2(3)} = 37$, with arc lamp illumination: $P > 0.2$, $N_{control} = 23$, $N_{DiOC2(3)} = 19$). Thus, $DiOC_2(3)$ does not adversely affect sperm motility.

8.3.2 Sensitivity to changes in MMP

Since the probe used in this study is typically applied in flow cytometry experiments, we needed to verify that our custom system and method of analysis is sensitive to changes in MMP. In addition, we wanted to verify that this probe reports changes in MMP. Figure 8.3 shows the ratio value over a 10 second interval for dog sperm from the test group (with CCCP) and control group (without CCCP). The figure demonstrates that CCCP does indeed cause a decrease in MMP and that both the probe and the system are capable of reporting such a decrease. The average ratio value of sperm exposed to CCCP (3.74 +/- 0.75, $N_{DiOC2(3)} = 33$) versus that of the control sperm (5.82 +/- 0.41, $N_{control} = 36$) is found to be statistically significantly different ($P << 0.001$) using the Student's T-test (distributions are found to be Gaussian). The velocity of each sperm was also measured. The average VCL value of sperm exposed to CCCP (67.15 +/- 20.77) versus that of the control sperm (70.39 +/- 24.70) is found to be statistically the same ($P > 0.56$) using the Student's T-test (distributions are found to be Gaussian).

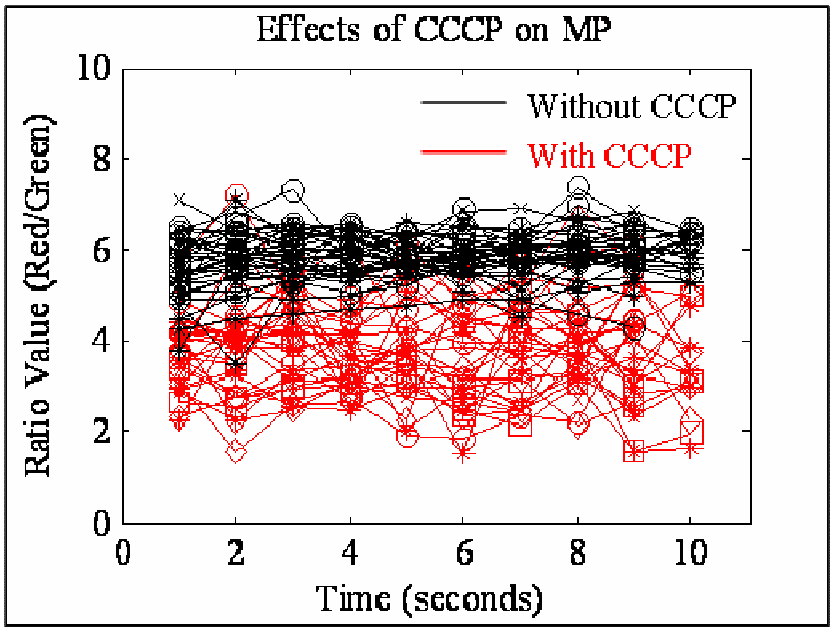

Figure 8.3: Effects of CCCP on mitochondrial membrane potential: Ratio value (red/green) is plotted against time (seconds). Ratio values are measured over a 10 second interval for test dog sperm group (with CCCP) and control dog sperm group (without CCCP). Each track represents an individual sperm.

8.3.3 Track, trap (constant power and constant time), and fluorescently image

Figure 8.4 shows the MMP ratio value prior to trapping, during trap, and after trapping plotted over time for two different dog sperm. For sperm (a) there is an overall decline in ratio value over time as the sperm is held in the trap. Once released from the optical trap, the sperm's MMP ratio value does increase, however it does not fully recover within 5 seconds to the original pre-trap value. Similarly, the sperm's swimming speed, VCL, does not recover to its pre-trapping value. For sperm (b) there is a slight decrease in ratio value while the sperm is in the trap. Again, neither swimming speed nor MMP ratio value fully recover to the pre-trapping values.

Previous work had shown that trapping sperm for 15 seconds at a constant power of 420mW in the focal volume had a negative effect on sperm motility (Nascimento *et al.* 2006; chapter 3). The results reported here are consistent with these findings.

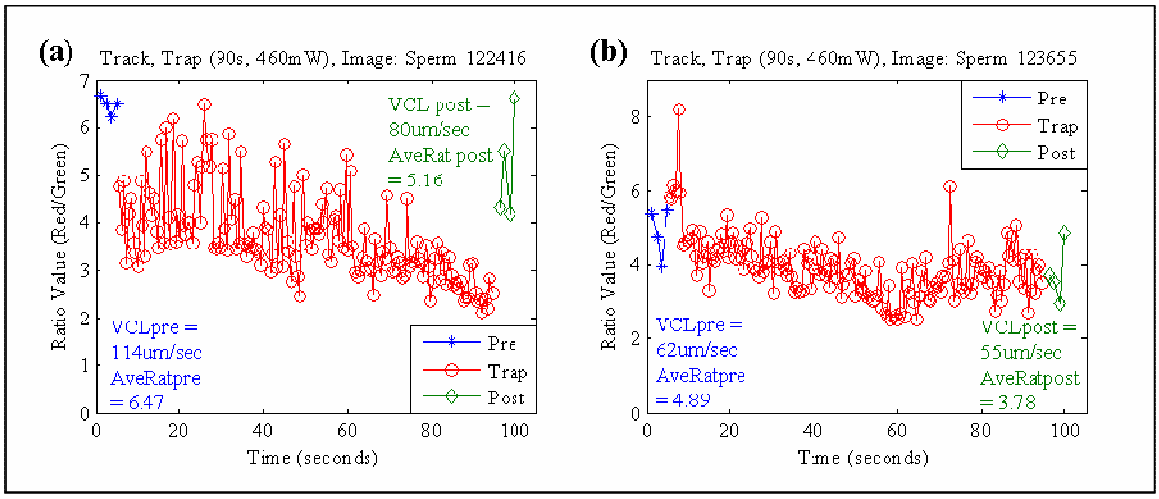

Figure 8.4: Track, trap (constant power, constant duration) and fluorescently image: MMP ratio value (red/green) is plotted against time (seconds) for the three different phases: prior trapping (blue asterisks), during trap (red open-circles) and after trapping (green diamonds). Both the average MMP ratio value (AveRat) and VCL prior to (pre) and post trapping are inset in the figure for each sperm (a and b). A trap duration of 90 seconds has a negative effect on sperm motility and energetics.

8.3.4 Track, trap (decaying laser power), and fluorescently image

For dog sperm, Pesc was plotted against VCL (data not shown) and found to give the same positive correlation between the two parameters as found in previous studies (regressions applied to data sets found to be statistically equal, $P > 0.2$) (Nascimento *et al.* 2006; chapter 4). Figure 8.5 plots the MMP ratio value over time

for four dog sperm for the three different phases: prior to trapping, during trap, and after trapping. These four examples demonstrate the various responses the sperm have to the optical trap. Sperm (a) did not escape the trap. After 10 seconds, the trapping power reaches the minimum 3.8mW, at which point the trap turns off. This sperm's VCL slightly increased after being trapped, but the average MMP ratio value decreased. Sperm (b) escaped the trap at 55mW and had an approximate 18% increase in VCL after trapping. However, the average MMP ratio value was nearly the same after trapping as it was prior to trapping. Sperm (c), although it escaped at a relatively high power, had a significant decrease in VCL, yet the average MMP ratio value increased slightly. Sperm (d) escaped the trap at 26mW, had a decrease in VCL and an increase in average MMP ratio value.

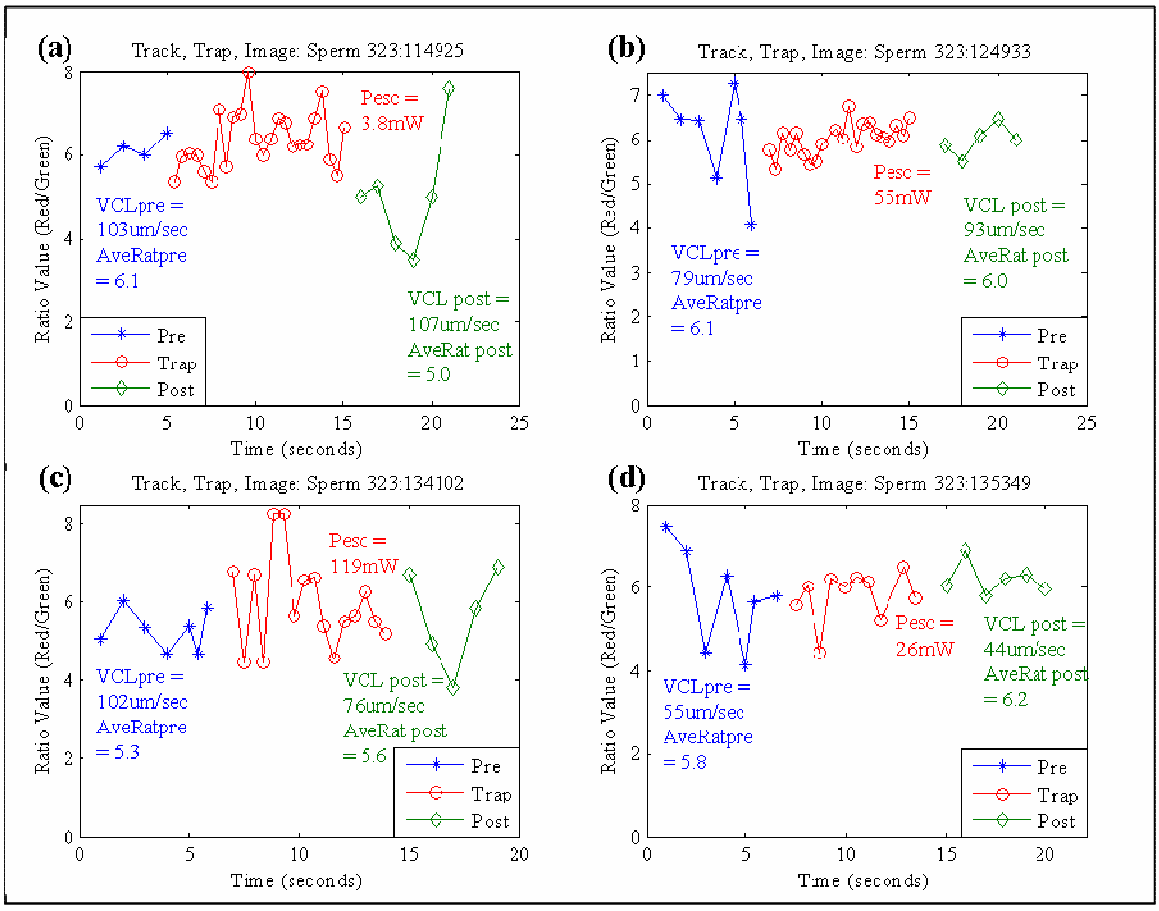

Figure 8.5: Track, trap (decaying laser power) and fluorescently image: MMP ratio value (red/green) is plotted against time (seconds) for the three different phases: prior trapping (blue asterisks), during trap (red open-circles) and after trapping (green diamonds). Various escape powers and swimming speeds are represented by the four sperm. The average MMP ratio value (AveRat) and VCL prior to (pre) and post trapping, as well as Pesc, are inset in the figure for each sperm (a – d).

A total of 309 dog sperm are analyzed. VCL and Pesc are both plotted against average MMP ratio value prior to being trapped (figure 8.6 (a) and (b) respectively). No relationship between either set of parameters is found.

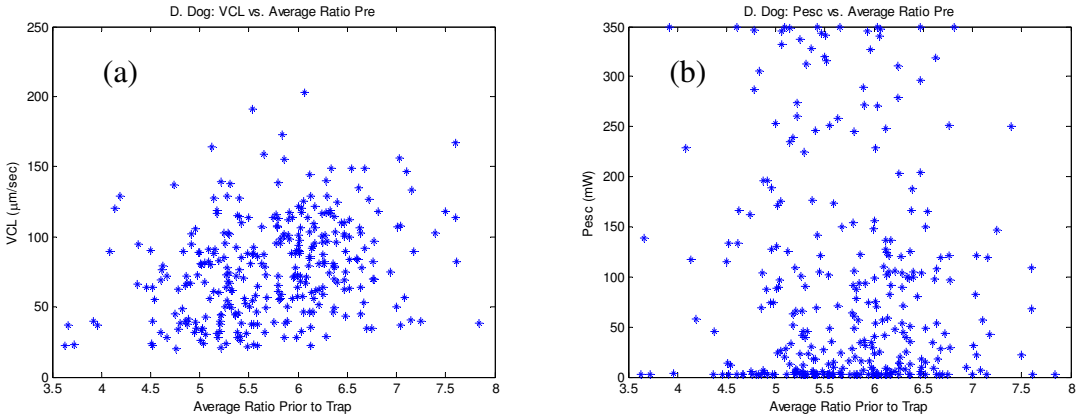

Figure 8.6: Dog - Swimming Speed and Escape Power vs. MMP Ratio Pre-Trap: (a) VCL and (b) Pesc are plotted against the average MMP ratio value prior to being trapped for dog sperm. No relationship found between sperm motility and mitochondrial respiration.

A total of 255 human sperm are analyzed. VCL and Pesc are both plotted against average ratio value prior to being trapped (figure 8.7 (a) and (b) respectively). No relationship between either set of parameters is found.

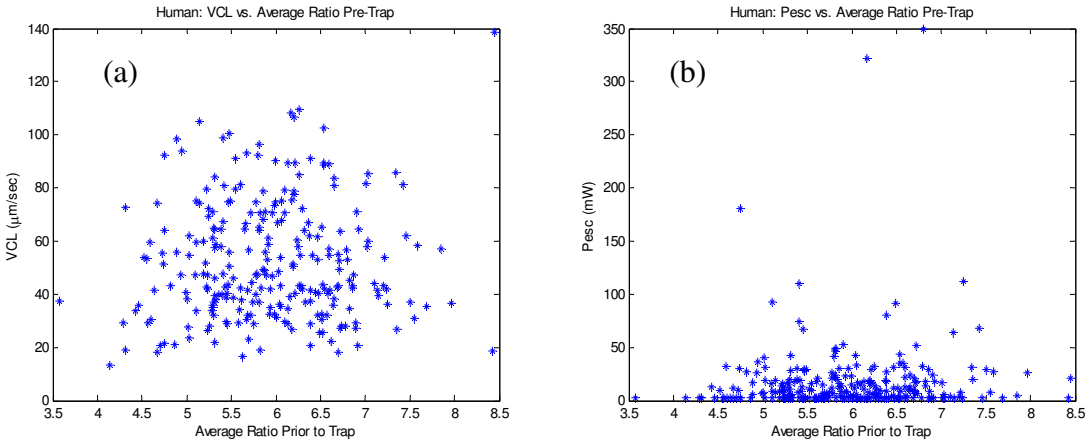

Figure 8.7: Human - Swimming Speed and Escape Power vs. MMP Ratio Pre-Trap: (a) VCL and (b) Pesc are plotted against the average MMP ratio value prior to being trapped for human sperm. No relationship found between sperm motility and mitochondrial respiration.

A total of 108 gorilla sperm are analyzed. VCL and Pesc are both plotted against average ratio value prior to being trapped (figure 8.8 (a) and (b) respectively). No relationship between either set of parameters is found. The results for the dog, human and gorilla demonstrate a lack of relationship between sperm motility and mitochondrial respiration.

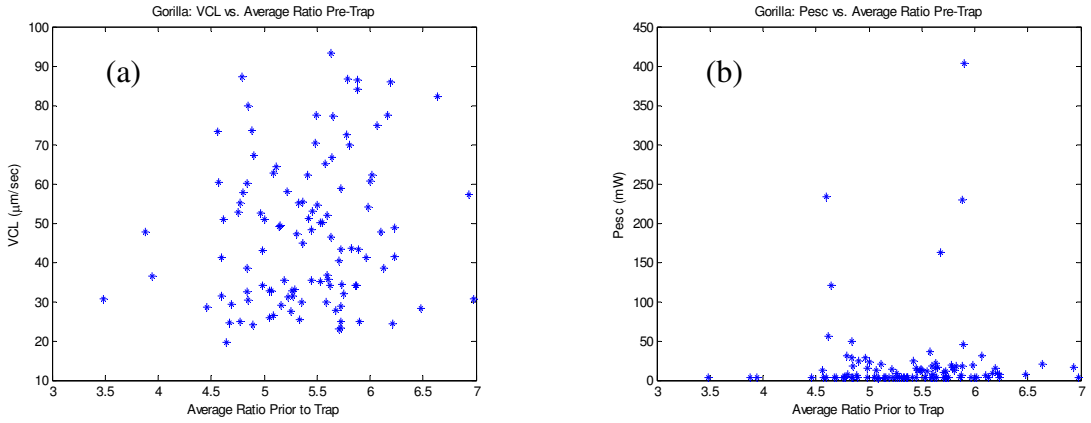

Figure 8.8: Gorilla - Swimming Speed and Escape Power vs. MMP Ratio Pre-Trap: (a) VCL and (b) Pesc are plotted against the average MMP ratio value prior to being trapped for gorilla sperm. No relationship found between sperm motility and mitochondrial respiration.

8.3.5 Effects of glucose on VCL, Pesc and MMP for human sperm

The velocity, escape power and MMP ratio value (pre-trap) distributions of the human sperm in the three different media are statistically compared using the non-parametric Wilcoxon paired-sample test (since the distributions are not Gaussian, statistical comparison requires a non-parametric test). Box plot distributions for VCL, Pesc and MMP are shown in figure 8.9 (a), (b), and (c) respectively as the blue "Glucose" set of data. Each box plot graphically displays the following parameters for a given distribution: (a) median (center line of box), (b) lower and upper quartile values (bottom and top line of box, respectively), (c) the range of the data (dashed lines extending from the top and bottom of box), and (d) the data points lying outside three times the interquartile range (labeled as '+' marks). Notches in the box represent an estimate of the uncertainty about the median value. If notches on the box plots of

two groups do not overlap, it can be concluded with 95% confidence that the two medians differ. For VCL and Pesc, the two media containing glucose (BWW+BSA and HTF) are found to be statistically equal ($P > 0.05$). The sperm in the media lacking glucose (BWW+BSA) are found to be statistically slower and weaker. However, the MMP distributions of sperm from all three groups are found to be statistically equal ($P > 0.05$). Therefore, the different concentrations of glucose (5.55mM in BWW vs. 2.78mM in HTF) do not affect sperm motility or MMP. The absence of glucose affects sperm motility but not MMP.

8.3.6 Effects of glycolytic and oxidative phosphorylation inhibitors on VCL, Pesc and MMP for human sperm

DOG: The velocity, escape power and MMP ratio value (pre-trap) distributions of the human sperm in the three different groups are statistically compared using the non-parametric Wilcoxon paired-sample test. Distributions for VCL, Pesc and MMP are shown in figure 8.9 (a), (b), and (c) respectively as the red "DOG" set of data. Sperm in BWW media containing glucose even in the presence of DOG are found to be both faster and stronger than sperm in either media lacking glucose (control group) or media lacking glucose but containing DOG (test group). Sperm in the media lacking glucose (control group) and in the media lacking glucose but containing DOG (test group) are found to be statistically equal in terms of VCL and Pesc ($P > 0.05$). All three groups are found to have equal MMP distributions ($P > 0.05$). Therefore, the presence of DOG does not affect sperm mitochondrial MMP.

Antimycin A: Human sperm in the media lacking glucose exposed to antimycin A are found to be immotile (marked as an 'X' in figure 8.9 a-c) and therefore were not measured. The velocity, escape power and MMP ratio value (pre-trap) distributions of the human sperm in the other three groups are statistically compared using the non-parametric Wilcoxon paired-sample test. Distributions for VCL, Pesc and MMP are shown in figure 8.9 (a), (b), and (c) respectively as the black "Antimycin A" set of data. The velocity distributions of sperm in media containing glucose (BWW and HTF) with antimycin A are found to be statistically equal ($P > 0.05$). In addition, they were found to be faster than sperm in media lacking glucose (control group). For the Pesc distributions, HTF media appears to be a better buffer against the adverse effects of antimycin A than BWW with glucose. Even still, sperm in either media containing glucose with antimycin A is found to be statistically stronger than sperm in media lacking glucose without the inhibitor. Sperm in the HTF media with antimycin A are found to have a statistically greater median MMP value than the sperm in either of the other two groups. Sperm in the media lacking glucose (control group) have a greater median MMP value than the sperm in the BWW media containing glucose with antimycin A. Again, HTF is a better buffer against the effects of the inhibitor than BWW.

Rotenone: Human sperm in the media lacking glucose exposed to rotenone are found to be immotile (marked as an 'X' in figure 8.9 a-c) and therefore were not measured. The velocity, escape power and MMP ratio value (pre-trap) distributions of the human sperm in the other three groups are statistically compared using the non-

parametric Wilcoxon paired-sample test. Distributions for VCL, Pesc and MMP are shown in figure 8.9 (a), (b), and (c) respectively as the green "Rotenone" set of data. The velocity distributions of sperm in the two media containing glucose with rotenone are found to be statistically equal ($P > 0.05$). In addition, they were found to be faster than sperm in media lacking glucose (control group). For the Pesc distributions, HTF media appears to be a better buffer against the adverse effects of rotenone than BWW with glucose. Even still, sperm in either media containing glucose with rotenone is found to be statistically stronger than sperm in media lacking glucose without the inhibitor. The MMP of sperm in the HTF media with rotenone is found to be statistically the same as that of the sperm in the media lacking glucose (control group, $P > 0.05$). The MMP of sperm in both of these groups is statistically greater than that of sperm in the BWW media containing glucose with rotenone. Again, HTF appears to be a better buffer against the effects of the inhibitor than BWW.

Figure 8.9: Effects of glucose (blue), DOG (red), Antimycin A (black) and Rotenone (green) on human sperm (a) swimming speed (VCL), (b) swimming force (Pesc) and (c) mitochondrial membrane potential (MMP): Stars ('*') within each category indicate statistically equal distributions. The Pesc distributions in (b) are shown twice: the top image displays the full escape power range, whereas the bottom image magnifies the box plots to emphasize differences in median values. 'HTF' stands for Human Tubal Fluid media containing glucose; 'G+' stands for BWW+BSA media containing glucose; 'G-' stands for BWW+BSA media lacking glucose; 'ctr' stands for control group (BWW+BSA media lacking glucose, without inhibitor); 'D' stands for DOG; 'A' stands for antimycin A; 'R' stands for rotenone.

(a) Effects of Glucose and Inhibitors on Sperm Motility: Velocity

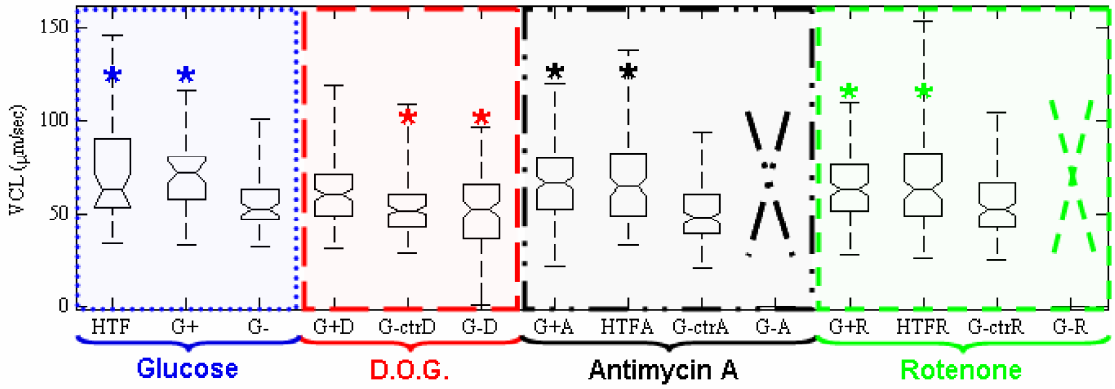

(b) Effects of Glucose and Inhibitors on Sperm Motility: Escape Power

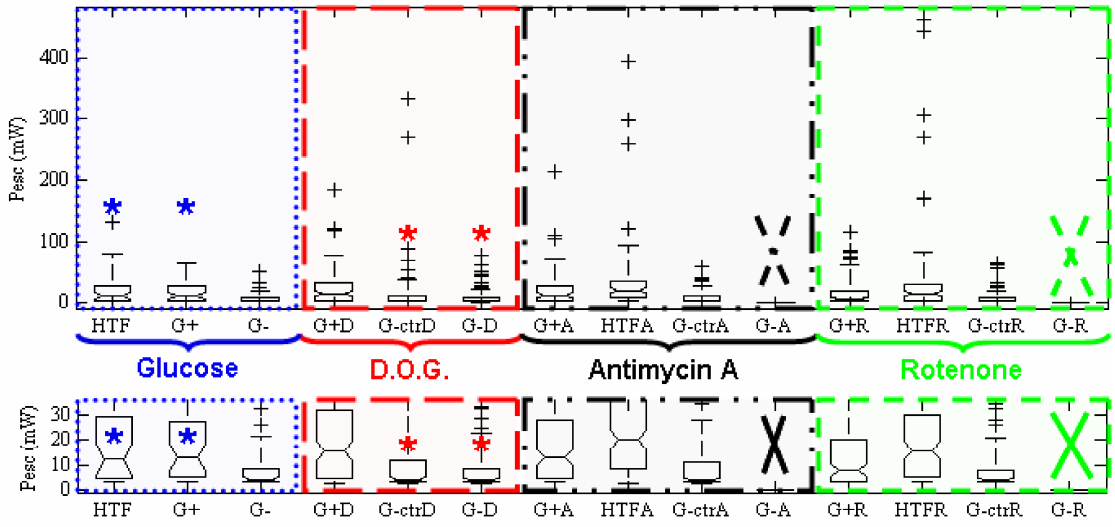

(c) Effects of Glucose and Inhibitors on Sperm Motility: Membrane Potential

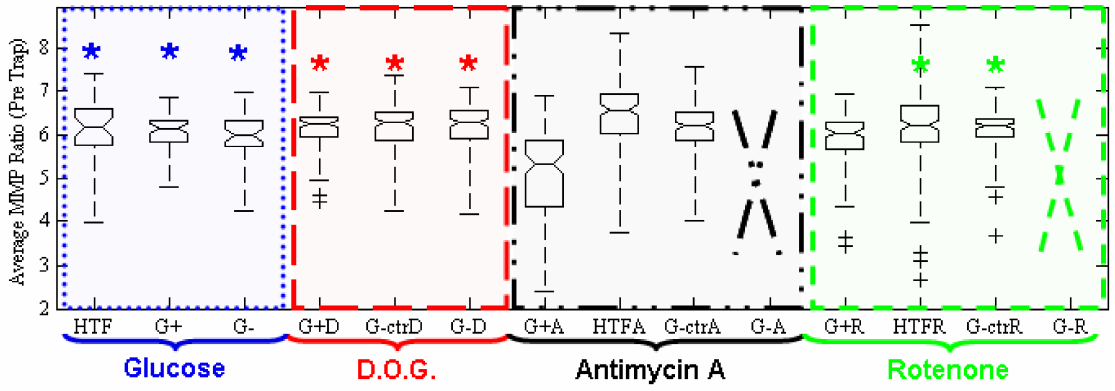

8.4 Discussion

In this chapter, a mitochondrial membrane potential probe was used in combination with a custom automated tracking and trapping system. I have demonstrated how this technique can be applied to the study of sperm motility and energetics. Moreover, I have created a protocol that can be used to compare various MMP probes. First, the effects of the probe on sperm swimming speed were established. Specifically, $DiOC_2(3)$ was shown to not affect sperm swimming speed (VCL). Second, the probe's ability to report an expected decrease in MMP was verified. The ratio measurement of the red to green fluorescent signal from $DiOC_2(3)$ showed a significant decrease in MMP caused by the addition of the proton ionophore, CCCP (see figure 8.3). This also demonstrates that the system's hardware and software, including the custom algorithms, are sensitive to changes in MMP. Third, the system was used to monitor MMP of individual sperm over a long period of time and assess the adverse effects of prolonged exposure to optical traps. As shown in figure 8.4, both VCL and MMP values post trapping are less than those prior to trapping. These results show that the ratio value can reflect the varying degrees of cell damage induced by the laser trap as well as partial cell recovery once the laser trap is turned off. Fourth, this system was used to simultaneously measure sperm swimming speed, escape laser power, and sperm MMP in real-time.

Since previous studies showed a relationship between VCL and Pesc (Nascimento *et al.* 2006; chapter 4), one might expect there would also be a relationship between sperm motility and oxidative phosphorylation. Thus, the custom

system was used to analyze the relationships between (a) VCL and MMP and (b) Pesc and MMP for dog, human and gorilla sperm. Interestingly, none of the species showed any relationship between either set of parameters. This suggests that sperm motility is independent of mitochondrial respiration as measured by MMP. Furthermore, this suggests that sperm rely on an alternative pathway for the energy needed to sustain motility.

Next, the effects of glucose on human sperm motility were examined. No statistical difference in motility (VCL or Pesc) or MMP was found for sperm incubated in either of the two media containing glucose even though the concentration of glucose for each was different. Only when the sperm were deprived of glucose did a significant decrease in VCL and Pesc occur. More importantly, the MMP distributions of the sperm in both of the media containing glucose (BWW and HTF) and the media lacking glucose were statistically equal ($P > 0.05$, see figure 8.9c). These results demonstrate that mitochondria in sperm suspended in media lacking glucose are operating at a level equal to that of sperm in media containing glucose. Thus, the results further support glycolysis as an important pathway for ATP generation in sperm.

Cells in the media lacking glucose, however, were not immotile. Furthermore, the addition of the glycolytic inhibitor, DOG, did not further reduce motility of human sperm in the media lacking glucose. Only when antimycin A or rotenone was added to sperm in media lacking glucose was there a complete lack of motility. Therefore, one can conclude that ATP is being generated by the mitochondria and does indeed

contribute to sperm motility. However, at the same drug concentration (either antimycin A or rotenone), sperm in media containing glucose had higher motility (VCL and Pesc) than the sperm in the media lacking glucose (control group, no drug). The MMP distributions for the sperm exposed to antimycin A and rotenone (figure 8.9c) are interesting. MMP of the sperm in BWW+BSA media containing glucose exposed to either drug is found to be significantly lower than that of the sperm in the media lacking glucose. Although mitochondrial function is impaired for sperm exposed to either drug in BWW+BSA media containing glucose, motility remains unaffected. (Note, comparison of sperm in BWW+BSA with glucose exposed to either drug against the BWW+BSA with glucose control sperm shows that the distributions for VCL and Pesc are statistically equal; $P > 0.05$.) Thus, the ATP contribution from the mitochondria for motility can be considered negligible when glycolysis is not impaired. Comparing sperm from the two media containing glucose (BWW and HTF), we see that the subtle differences in concentrations of substrates in HTF make it a better buffer against the effects of the drug in terms of Pesc and MMP. These results indicate mitochondrial-generated ATP contributes to swimming force more so than to swimming speed. However, without glucose, swimming force is significantly reduced, and the ATP molecules from the mitochondria do not appear to be able to compensate in order to sustain high motility.

These results explain why no correlation between MMP and sperm motility (in terms of VCL) was found when the sperm were exposed to CCCP (there was no decrease in VCL even though MMP was significantly reduced; section 8.3.2). If

oxidative phosphorylation were providing the energy needed for motility, the inhibition of mitochondrial ATP production after exposure to this ionophore would have reduced sperm motility. In addition, the results of the effects of electron transport chain and glycolytic inhibitors for human sperm are consistent with those reported for bull sperm (Krzyzosiak *et al.* 1999). It seems that oxidative phosphorylation does contribute ATP for sperm motility, but apparently not enough to sustain high motility. The glycolytic pathway is shown to be a significantly important source of energy for sperm motility. The fact that no relationship exists between motility (VCL and Pesc) and MMP as seen in figures 8.6 – 8.8, therefore, is not surprising, but rather is to be expected since glucose is present in the media. Future studies should look at different concentrations of the inhibitory drugs as well as assess the effects of other inhibitors (such as valinomycin).

In conclusion, the technique demonstrated in this chapter can be used to quantitatively assess sperm quality and viability by providing a detailed description (measurements of VCL, Pesc, and MMP) of individual sperm. Furthermore, this system can be used to gain better understanding of the role of oxidative phosphorylation in sperm cell motility. The results of the experiments reported here suggest that ATP from glycolysis is the primary source of energy for sperm motility. This begs the question, what, then, is the primary role of the mitochondria if not for energy production? Further studies should be done to address this question.

Acknowledgements

The material presented in Chapter 8 is, in part, a reprint of the material as it appears in "The use of laser tweezers to analyze sperm motility and mitochondrial membrane potential," by J. M. Nascimento, L. Z. Shi, C. Chandsawangbhuwana, J. Tam, B. Durrant, E. Botvinick, M.W. Berns, *J. Biomed. Opt.* In-press (October 2007) and in "Anaerobic Respiration (Glycolysis) is a Main Source of Energy (ATP) for Sperm Motility," by J. M. Nascimento, L. Z. Shi, J. Tam, C. Chandsawangbhuwana, B. Durrant, E. Botvinick, M.W. Berns, In submission (October 2007). The dissertation author was the first author of the two papers.

References

Alberts, B., Johnson, A., Lewis, J., Raff, M., Roberts, K., Walter, P. (2002). Energy Conversion: Mitochondria and Chloroplasts *in* The Molecular Biology of the Cell 4th Ed., Garland Science, NY, NY, pp 769.

Amann, R. P., Katz, D. F. (2004). Reflections on CASA after 25 years. *J Androl.* **25**(3), 317-325.

Anderson, M. J., Dixson, A. F. (2002). Motility and the midpiece in primates. *Nature* **416**, 496.

Biggers, J. D., Whitten, W. D., Whittingham, D. G. (1971). The culture of mouse embryos in vitro. in *Methods of mammalian embryology*, J. C. Daniel, Jr., Ed., pp 86-116, Freeman, San Francisco, CA.

Dantas, Z. N., Araujo, E. Jr., Tadir, Y., Berns, M. W., Schell, M. J., Stone, S. C. (1995). Effect of freezing on the relative escape force of sperm as measured by a laser optical trap. *Fertil. Steril.* **63**(1), 185-188.

Durrant, B. S., Harper, D., Amodeo, A., Anderson, A. (2000). Effects of freeze rate on cryosurvival of domestic dog epididymal sperm. *J. Andrology*, **21(Suppl)**(59).

Ford, W. C. L. (2006). Glycolysis and sperm motility: does a spoonful of sugar help the flagellum go round? *Human Reproduction Update*, **12** (3) 269-274.

Gallon, F., Marchetti, C., Jouy, N., Marchetti, P. (2006). The functionality of mitochondria differentiates human spermatozoa with high and low fertilizing capability. *Fertility and Sterility* **86**(5), 1526-1530.

Guzman-Grenfell, A. M., Bonilla-Hernandez, M. A., Gonzalez-Martinez, M. T. (2000). Glucose induces a NA+, K+-ATPase-dependent transient hyperpolarization in human sperm. I. Induction of changes in plasma membrane potential by the proton ionophore CCCP. *Biochimica et Biophysica Acta* **1464**, 188-198.

Harper, S. A., Durrant, B. S., Russ, K. D., Bolamba, D. (1998). Cryopreservation of domestic dog epididymal sperm: A model for the preservation of genetic diversity. *J. Andrology* **19 (Suppl)**(50).

Kasai, T., Ogawa, K., Mizuno, K., Nagai, S., Uchida, Y., Ohta, S., Fujie, M., Suzuki, K., Hirata, S., Hoshi, K. (2002). Relationship between sperm mitochondrial membrane potential, sperm motility, and fertility potential. *Asian J. Andrology* **4**(2), 97-103.

Kim, Y. H., Haidl, G., Schaefer, M., Egner, U., Mandal, A., Herr, J. C. (2007). Compartmentalization of a unique ADP/ATP carrier protein SFEC (Sperm Flagellar Energy Carrier, AAC4) with glycolytic enzymes in the fibrous sheath of the human sperm flagellar principal piece. *Developmental Biology*, **302**, 463-476.

Konig, K., Svaasand, L., Liu, Y., Sonek, G., Patrizio, P., Tadir, Y., Berns, M. W., Tromberg, B. J. (1996). Determination of motility forces of human spermatozoa using an 800 nm optical trap. *Cell. Mol. Biol. (Noisy-le-grand)* **42**(4), 501-509.

Krisfalusi, M., Miki, K., Magyar, P. L., O'Brien, D. A. (2006). Multiple Glycolytic Enzymes are Tightly Bound to the Fibrous Sheath of Mouse Spermatozoa. *Biology of Reproduction*, **75**, 270-278.

Krzyzosiak, J., Molan, P., Vishwanath, R. (1999). Measurements of bovine sperm velocities under true anaerobic and aerobic conditions. *Animal Reproduction Science* **55**, 163-173.

Liaw, L. H., Berns, M. W. (1981). Electron microscope autoradiography on serial sections of preselected single living cells. *J. Ultrastruct* **75**, 187–194.

Marchetti, C., Jouy, N., Leroy-Martin, B., Deffosez, A., Formstecher, P., Marchetti, P. (2004). Comparison of four fluorochromes for the detection of the inner mitochondrial membrane potential in human spermatozoa and their correlation with sperm motility. *Human Reproduction* **19**(10), 2267-2276.

Marchetti, C., Obert, G., Deffosez, A., Formstecher, P., Marchetti, P. (2002). Study of mitochondrial membrane potential, reactive oxygen species, DNA fragmentation and

cell viability by flow cytometry in human sperm. *Human Reproduction* **17**(5), 1257-1265.

Mei, A., Botvinick, E., Berns, M. W. (2005). Monitoring sperm mitochondrial respiration response in a laser trap using ratiometric fluorescence. *Proc. SPIE,* **5930**(2F), 1-11.

Miki, K., Qu, W., Goulding, E. H., Willis, W. D., Bunch, D. O., Strader, L. F., Perreault, S. D., Eddy, E. M., O'Brien, D. A. (2004). Glyceraldehyde 3-phosphate dehydrogenase-S, a sperm specific glycolytic enzyme, is required for sperm motility and male fertility. *PNAS*, **101** (47), 16501-16506.

Mortimer, D. (1994). *Practical laboratory andrology,* Oxford University Press, New York, NY.

Mukai, C., Okuno, M. (2004). Glycolysis Plays a Major Role for Adenosine Triphosphate Supplementation in Mouse Sperm Flagellar Movement. *Biology of Reproduction* **71**, 540-547.

Nascimento, J. M., Botvinick, E. L., Shi, L. Z., Durrant, B., Berns, M. W. (2006). Analysis of sperm motility using optical tweezers. *J. Biomed. Opt.* **11**(4), 044001.

Nascimento, J. M., Shi, L. Z., Meyers, S., Gagneux, P., Loskutoff, N. M., Botvinick, E. L., Berns, M. W. (2006). The use of optical tweezers to study sperm competition and motility in primates. *J. R. Soc. Interface* DOI 10.1098/rsif.2007.1118

Novo, D., Perlmutter, N. G., Hunt, R. H., Shapiro, H. M. (1999). Accurate flow cytometric membrane potential measurement in bacteria using diethyloxacarbocyanine and a ratiometric technique. *Cytometry* **35**, 55-63.

Novo, D., Perlmutter, N. G., Hunt, R. H., Shapiro, H. M. (2000). Multiparameter flow cytometric analysis of antibiotic effects on membrane potential, membrane permeability, and bacterial counts of *Staphylococcus aureus* and *Micrococcus luteus. Antimicrobial Agents and Chemotherapy* **44**(4), 827-834.

O'Brien, J. K., Crichton, E. G., Evans, K. M., Schenk, J. L., Stojanov, T., Evans, G., Maxwell, W. M. C., Loskutoff, N. M. (2002). Sex ratio modification using sperm sorting and assisted reproductive technology – a population management strategy. In *Proceedings of the Second International Symposium on Assisted Reproductive Technology for the Conservation and Genetic Management of Wildlife* (Omaha's Henry Doorly Zoo), pp. 224-231.

Shi, L. Z., Nascimento, J., Berns, M. W., Botvinick, E. (2006a) Computer-based tracking of single sperm," *J. Biomed. Opt.* **11**(5), 054009 (2006).

Shi, L. Z., Nascimento, J. M., Chandsawangbhuwana, C., Berns, M. W., Botvinick, E. (2006b). Real-time automated tracking and trapping system (RATTS). *Microscopy Research and Technology* **69**(11), 894-902.

Shi, L. Z., Botvinick, E. L., Nascimento, J., Chandsawangbhuwana, C., Berns, M. W. (2007). A real-time single sperm tracking, laser trapping, and ratiometric fluorescent imaging system. *Biomedical Microdevices* In submission.

Tadir, Y., Wright, W. H., Vafa, O., Ord, T., Asch, R. H., Berns, M. W. (1990). Force generated by human sperm correlated to velocity and determined using a laser generated optical trap. *Fertil. Steril.* **53**(5), 944-947.

Turner, R. M. (2003). Tales From the Tail: What Do We Really Know About Sperm Motility? *J. Andrology*, **24** (6), 790-803.

Williams, A.C., Ford, C. L. (2001). The Role of Glucose in Supporting Motility and Capacitation in Human Spermatozoa. *J. Andrology* **22** (4), 680-695.

IX. Conclusions and Outlook

9.1 Conclusions

The purpose of this dissertation was to (1) develop an objective and quantitative method to analyze sperm motility and (2) use this method to study sperm quality, effects of sperm competition and sperm energetics. Chapter 3 first described the optical setup used to create the laser tweezers. Then, the effects of optical trapping (trap duration and laser trapping power) on sperm motility were measured. It was shown that a 10s trap duration at 420mW or less should not significantly affect sperm motility. These parameters were used in subsequent track and trap experiments. In chapter 4, the modification to the optical setup used to control laser power and measure sperm swimming force was described. The subjective nature of the SOP scoring method was demonstrated. It was shown that three fertility experts that work in the same facility achieved only 41.3% agreement in SOP scoring and 7.6% complete disagreement. It was also shown that sperm swimming force is a valuable and quantitative variable to be used for sperm characterization. This measurement, in conjunction with other established motility parameters, helps create a comprehensive evaluation of overall sperm quality.

Chapter 5 describes the custom developed algorithm, Real-time Automated Tracking and Trapping System (RATTS). RATTS is then used to measure sperm swimming speed and swimming force. The effects of cryopreservation on sperm motility are determined for several species. Sperm motility (swimming speed and force) for three out of the five species analyzed was not affected by cryopreservation.

However, sperm from the remaining two species were affected by cryopreservation. Moreover, the quantitative analysis was able to detect changes in West Caucasian tur sperm motility that were not detected using the SOP scoring analysis. This further demonstrates the importance of using an objective system to assess sperm motility. The results from that chapter should be used to optimize the freezing protocol and/or freezing media used for sperm cryopreservation.

In chapter 6, the abilities of the custom system were demonstrated. The system was shown to (1) achieve high throughput (hundreds of data points in a few hours) and (2) be quite versatile (adaptable to sperm from various species without excess modification to the tracking algorithm). This achievement, combined with the fact that sperm swimming force has been shown to be a useful parameter for assessing sperm quality (chapter 4), is considerably valuable for both basic and applied infertility research. The relationships between sperm swimming force and swimming speed for eleven mammalian species were found to be, in general, unique. These data sets provide baseline measurements for each species that can be used for analysis of sperm from other males. Chapter 7 analyzed the data of four of the primate species from chapter 6 in more depth. A direct correlation between sperm motility and mating type was demonstrated. Specifically, swimming force and swimming speed were found to increase as the level of sperm competition increases.

In chapter 8, modifications to the optical design as well as to the hardware and software used to automatically track, trap, and calculate the fluorescence ratio of sperm in real-time was described. The fluorescent probe was found not to affect

sperm motility. Also, both the probe and the system were able to accurately report a decrease in mitochondrial membrane potential (MMP) when sperm were exposed to the uncoupling agent, CCCP. No relationship between either swimming speed and MMP or swimming force and MMP was found for domestic dog, human or gorilla species. This suggests that sperm motility is independent of mitochondrial respiration as measured by MMP and that sperm rely on an alternative pathway for their energy. Therefore, the roles of two potential sources of ATP, oxidative phosphorylation which occurs in the mitochondria located in the sperm midpiece and glycolysis which occurs along the principal piece (sperm tail), were studied. The results demonstrated that sperm suspended in media lacking glucose were significantly slower and weaker than sperm in media containing glucose even though their mitochondria were operating at equivalent levels. Oxidative phosphorylation was shown to contribute ATP for sperm motility, but not at a high enough rate to sustain high motility. The glycolytic pathway was shown to be a significantly important source of energy for sperm motility.

9.2 Future Directions

In sperm trapping experiments using laser tweezers, the user must select which sperm are to be analyzed. This begs the question: does the subpopulation of sperm analyzed in "track and trap" experiments fully represent the entire (non-trapped) population? A study compared the velocity distribution of the entire sperm population with that of the sampled population from the laser "track and trap" experiments performed on human and chimpanzee sperm (see chapter 7). Video footage from the

"track and trap" experiments done in chapter 7 is used to measure sperm swimming speed (VCL, μm/sec) of the sperm not exposed to the laser trap. The swimming speed distributions of human and chimpanzee sperm that were trapped are compared to those of the entire non-trapped population of sperm using the non-parametric Wilcoxon rank sum test. Figure 9.1 shows the velocity histograms of (a) the entire non-trapped human sperm population and (b) the subpopulation of the laser-trapped human sperm. The entire population and trapped subpopulation of human sperm are found to be statistically equal ($P > 0.95$). Figure 9.2 shows the velocity histograms of (a) the entire non-trapped chimpanzee sperm population and (b) the subpopulation of the laser trapped chimpanzee sperm. The entire population and trapped subpopulation of chimpanzee sperm are found to be statistically different ($P < 0.001$).

(a)

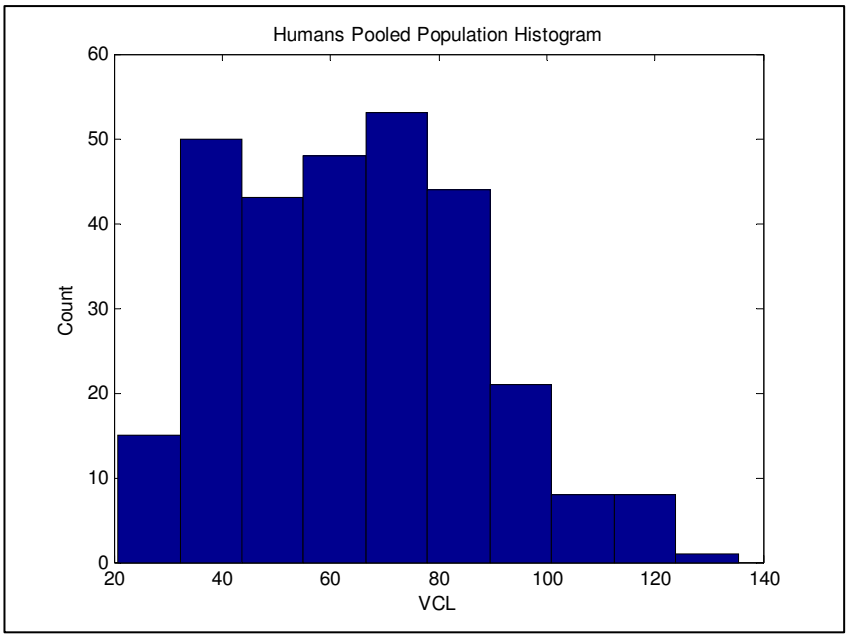

(b)

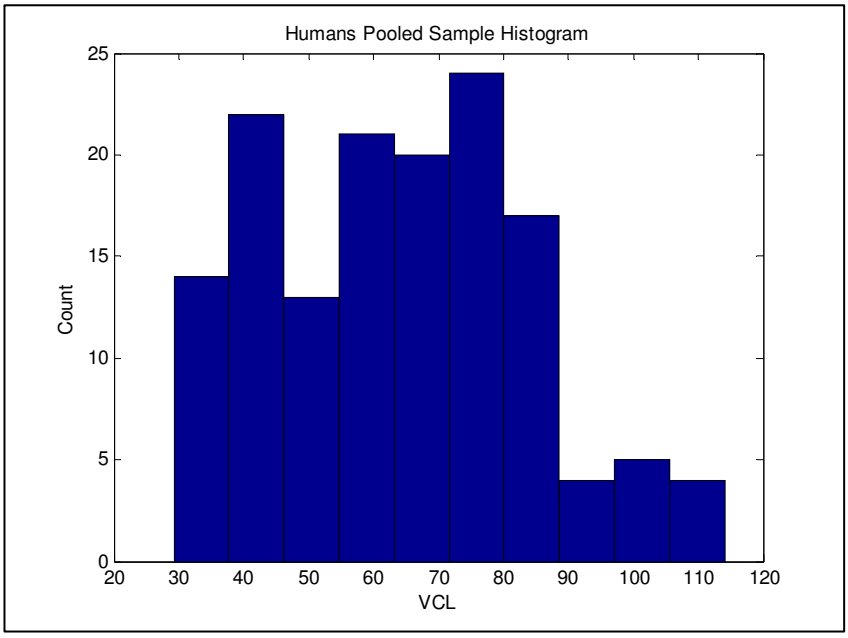

Figure 9.1: Human Sperm Velocity Histograms: (a) Entire population of human sperm (non-trapped). (b) Subpopulation of trapped human sperm.

(a)

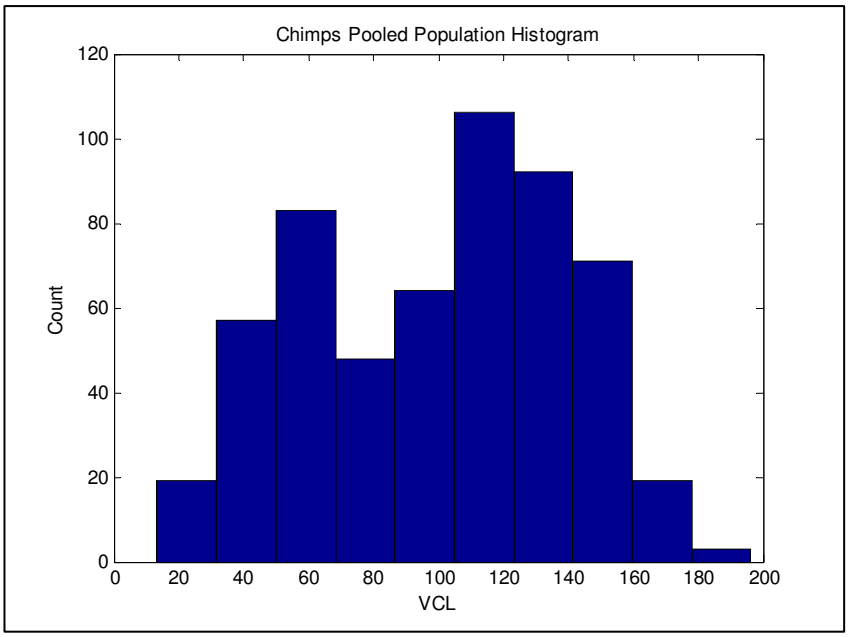

(b)

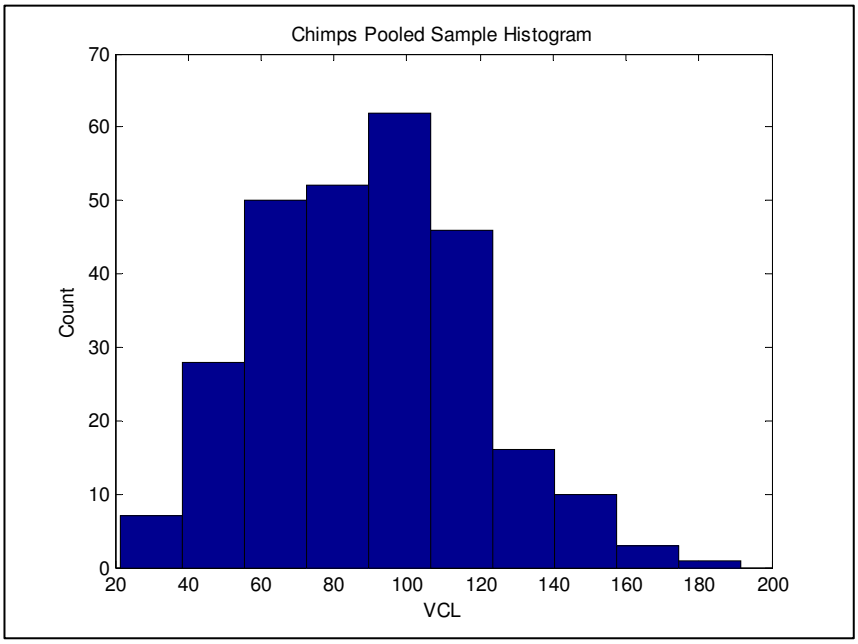

Figure 9.2: Chimpanzee Sperm Velocity Histograms: (a) Entire population of chimpanzee sperm (non-trapped). (b) Subpopulation of trapped chimpanzee sperm.

Sperm swimming with a velocity within an arbitrarily designated range are labeled as "fast" sperm to estimate the proportion of fast sperm trapped compared to the proportion of fast sperm in the entire population. Table 9.1 lists the speed range for each species. For human sperm, the "fast" swimming speed range is designated to be 80μm/s to 140μm/s. About 21% of the sperm trapped are "fast," reflecting the 25% "fast" sperm in the entire population. The subpopulation sampled in "track and trap" experiments is thus highly representative of the entire population. For chimpanzee sperm, the faster swimming group range from 120μm/s to 200μm/s. Approximately 14% of the sperm trapped are "fast," compared to the 36% "fast" sperm in the entire population. Although the subpopulation in the chimpanzee "track and trap" experiments does sample sperm from the full velocity range in the entire population, it does not do so at high enough frequency to have equal velocity distributions.

Table 9.1: Comparison of trapped subpopulation against the entire population based on velocity range. Sperm for each species are divided into three groups based on swimming speed. The percentage of sperm in each speed group is listed for both the trapped subpopulation of sperm and the entire population.

Chimpanzee			
	Velocity Range (μm/s)	**Trapped Sample**	**Entire Population**
Slow	0-60	16%	23%
Medium	60-120	70%	41%
Fast	120-200	14%	36%
Human			
	Velocity Range (μm/s)	**Trapped Sample**	**Entire Population**
Slow	0-40	15%	15%
Medium	40-80	64%	60%
Fast	80-120	21%	25%

These results suggest that the track and trap algorithm should be modified to trap faster moving sperm more efficiently. Additionally, the algorithm should be modified to completely eliminate the user interaction. The algorithm should track all the sperm in the field of view automatically, without waiting for the user to select a sperm of interest, and decide which sperm should be tracked and trapped based on a given sperm's velocity.

Furthermore, in efforts to make the system more commercially feasible, a method for trapping more than one sperm at a time should be developed. For example, this could be done using a high-resolution spatial light modulator (SLM). SLMs have been used to generate and control multiple optical traps (Eriksen *et al.* 2002; Schonbrun *et al.* 2005). The number of traps generated can be adjusted. In addition, the location and intensity of each trap can be manipulated in real-time (Eriksen *et al.* 2002). By including this element in the optical setup, more than one sperm can be trapped at a given time. Subsequently, the swimming forces of each trapped sperm can be measured independently. Thus, RATTS could be modified to first track multiple sperm at a time, as discussed above, and to then trap each of these sperm to measure swimming force. These modifications could significantly increase throughput and avoid user-biases as seen for chimpanzee sperm in table 9.1. The limitation, however, is the size of the field of view. Since multiple sperm would be tracked and trapped, the stage cannot be moved to continuously track a sperm if it swims out of the field of view. Nonetheless, such a design should be given serious consideration.

Acknowledgements

The material presented in Chapter 9 is, in part, a reprint of the material as it appears in "Analysis of Human and Chimpanzee Sperm Swimming Speed in Laser Trapping Experiments," by J. S. Tam, J. M. Nascimento, L. Z. Shi, and M. W. Berns, *Frontiers in Optics*, Connie J. Chang-Hasnain and Gregory J. Quarles, chairs, September 2007, San Jose, CA. The dissertation author was the second author of this paper and mentor of the first author.

References

Eriksen, R. L., Daria, V. R., Gluckstad, J. (2002). Fully dynamic multiple-beam optical tweezers. *Optical Express* **10**(14), 597-602.

Schonbrun, E., Piestun, R., Jordan, P., Cooper, J., Wulff, K.D., Courtial, J., Padgett, M. (2005). 3D interferometric optical tweezers using a single spatial light modulator. *Optics Express* **13**(10), 3777-3786.

Appendix: Effects of mating pattern on sperm evolution - Mice

A. 1 Introduction

In chapter 7, the theory of sperm competition was introduced and how it has affected sperm morphology, sexual behavior, and the structure of accessory sexual organs, particularly in primate species, was discussed. The genus *Peromyscus* contains several species of mice that have a variety of mating patterns. For example, *P. polionotus* is known to be monogamous (Foltz 1981), exhibiting strong pair bonding and parental cooperation in child-rearing. Likewise, *P. californicus* is known to be monogamous (Ribble 1991). Evidence indicates that *P. leucopus* and *P. maniculatus* are polygamous (Xia and Millar 1991). In this section, the RATTS system, as described in previous chapters and in Shi *et al.* 2006, is used to assess the effects of sperm competition on motility (swimming speed, VCL, and swimming force, in terms of escape laser power, Pesc) for the different *Peromyscus* mice species.

A.2 Materials and Methods

A.2.1 Specimen

The following species of mice from the genus *Peromyscus* are sacrificed: *leucopus, polionotus, californicus, maniculatus bairdii* and *maniculatus sonoriensis*. As stated in the introduction, *P. leucopus* and *P. maniculatus* are noted to by polygamous, whereas *P. californicus* and *P. polionotus* are found to be monogamous. Sperm from the epididymis from each mouse are extracted and diluted in BWW + BSA. Sperm samples of 30,000 sperm per mL of media dilutions were loaded into

rose chambers and mounted into a microscope stage holder and kept at 37^{o}C using an air curtain incubator (NEVTEK, ASI 400 Air Stream Incubator, Burnsville, VA) interfaced with a thermocouple feed-back system. A total of 165 sperm from *P. leucopus*, 197 from *P. maniculatus bairdii,* 205 from *P. maniculatus sonoriensis,* 185 from *P. polionotus,* and 125 from *P. californicus* are analyzed.

A.2.2 Hardware and Software

The optical design used to create the laser tweezers, hardware and sperm tracking software, experimental procedure and analysis of sperm have been described in greater detail in chapter 7 and in Shi *et al.* 2006. Briefly, sperm swimming speed (VCL, μm/sec) and swimming force (in terms of escape laser power, Pesc, mW) are measured automatically for sperm from each species.

A.3 Results

Figure A.1 shows the box plots for distributions of (a) sperm swimming speed (curvilinear velocity, VCL, μm/sec) and (b) sperm escape power (Pesc, mW) for the different mice species. Each box plot graphically displays the following parameters for a given distribution: (a) median (center line of box), (b) lower and upper quartile values (bottom and top line of box, respectively), (c) the range of the data (dashed lines extending from the top and bottom of box), and (d) the data points lying outside three times the interquartile range (labeled as '+' marks). Notches in the box represent an estimate of the uncertainty about the median value. If notches on the box plots of two groups do not overlap, it can be concluded with 95% confidence that the two medians differ.

Swimming speed and escape power distributions for each species are statistically compared using the Wilcoxon rank sum test for equal medians (Zar 1984) (VCL and Pesc distributions are found to be non-Gaussian using Lilliefors test (Zar 1984), thus requiring the use of the non-parametric Wilcoxon test). The asterisks (*) in figure A.1 indicate which distributions are found to be statistically equal. The VCL distributions of *P. maniculatus sonoriensis, P. californicus, and P. leucopus* are found to be statistically equal ($P > 0.05$). All other VCL distributions are found to be statistically different ($P < 0.05$). The Pesc distribution of *P. maniculatus sonoriensis* is found to be statistically equal only to that of *P. californicus* ($P > 0.05$). The Pesc distributions of *P. maniculatus bairdii*, *P. leucopus*, *P. polionotus* and *P. californicus* are all found to be statistically equal ($P > 0.05$).

(a)

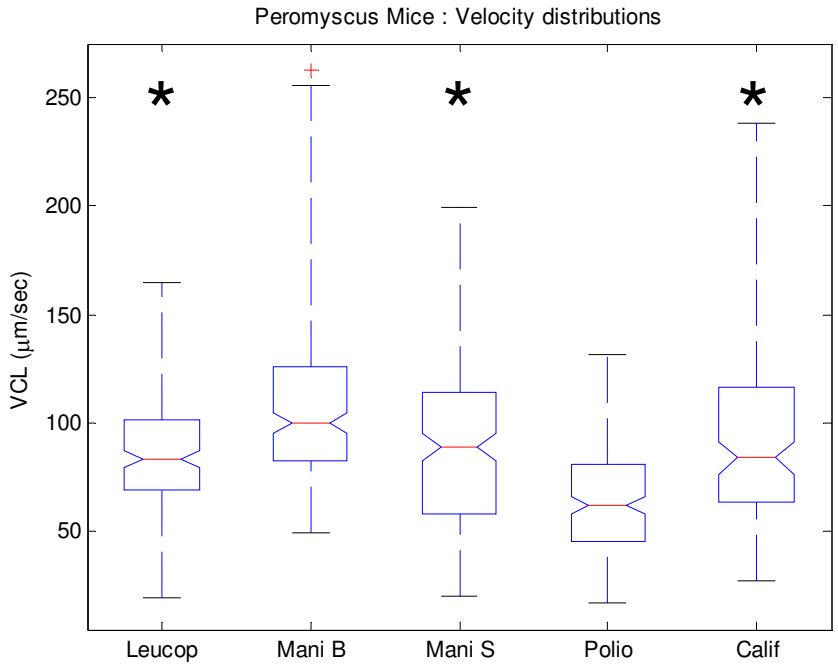

Figure A.1: (a) VCL and (b) Pesc distributions for all five subspecies of *Peromyscus*. '*' based on color indicates which distributions are found to be statistically equal. "Leucop" stands for *P. leucopus*, "Mani B" stands for *P. maniculatus bairdii*, "Mani S" stands for *P. maniculatus sonoriensis*, "Polio" stands for *P. polionotus*, and "Calif" stands for *P. californicus*.

(b)

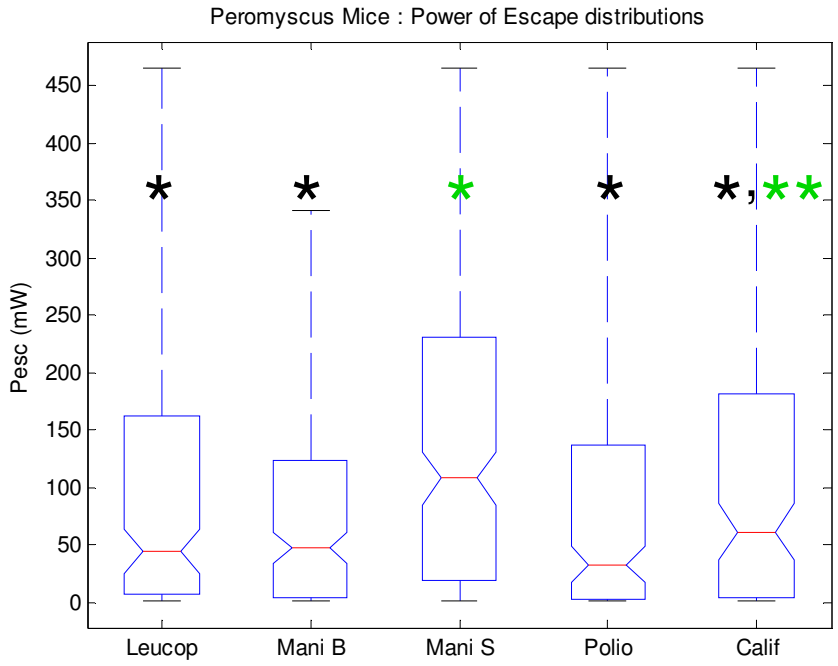

Figure A.1 (continued): (b) Pesc distributions for all five subspecies of *Peromyscus*. '*' based on color indicates which distributions are found to be statistically equal.

Figure A.2 (a through e) plot Pesc against VCL for *P. leucopus, P. maniculatus bairdii*, *P. maniculatus sonoriensis*, *P. polionotus,* and *P. californicus* respectively. Regressions fit to the data sets were found to have low R^2 values (data not shown). Thus, for each mouse species, unlike for the other mammals analyzed in chapter 6, no relationship between VCL and Pesc exists.

(a)

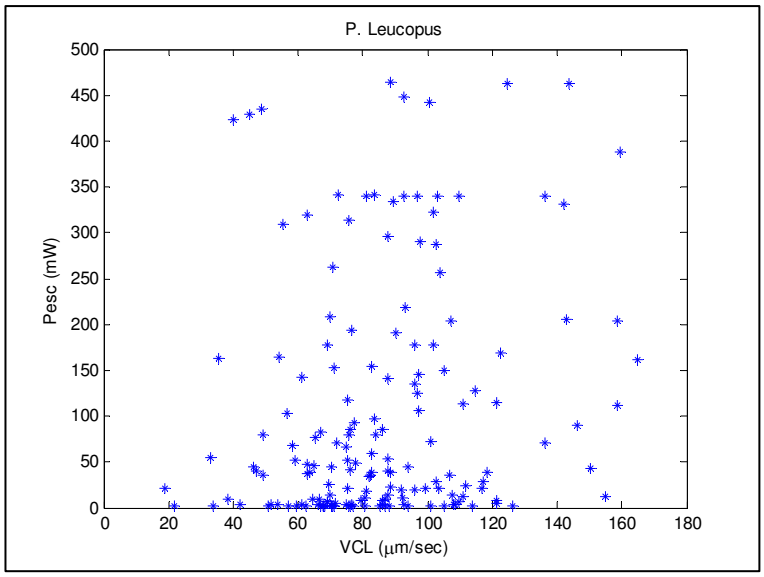

Figure A.2: Pesc (mW) vs. VCL (μm/sec) for (a) *P. leucopus*, (b) *P. maniculatus bairdii*, (c) *P. maniculatus sonoriensis*, (d) *P. polionotus*, and (e) *P. californicus*.

(b)

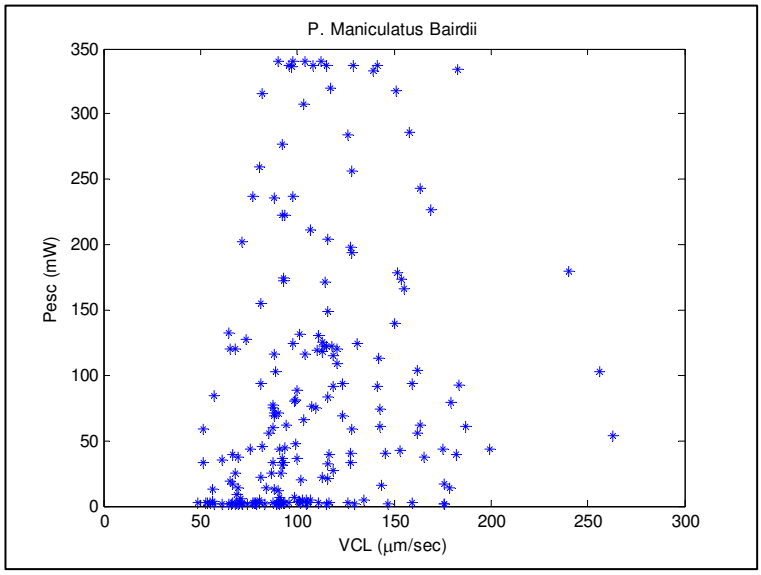

Figure A.2 (continued): (b) Pesc (mW) vs. VCL (mm/sec) for *P. maniculatus bairdii*

(c)

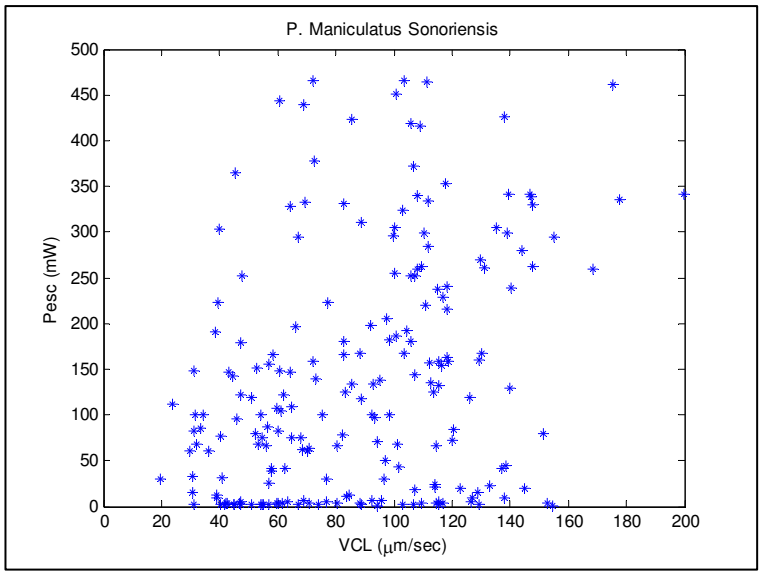

Figure A.2 (continued): (c) Pesc (mW) vs. VCL (mm/sec) for *P. maniculatus sonoriensis*

(d)

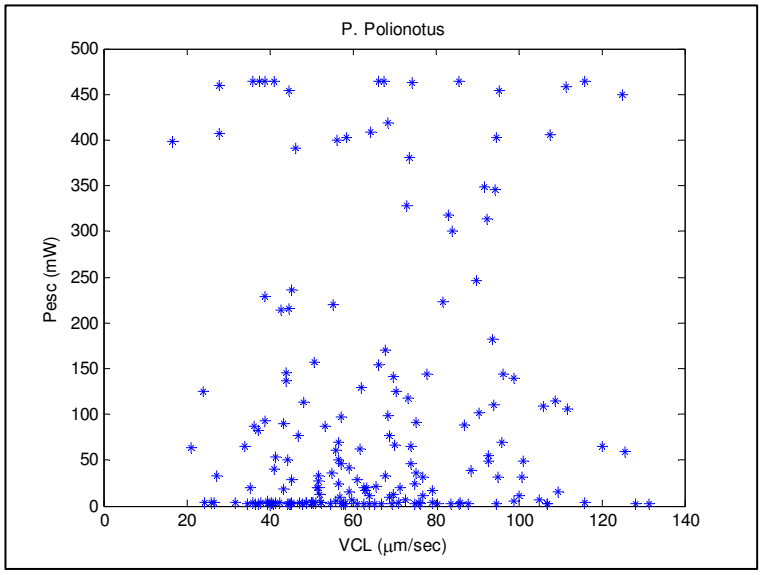

Figure A.2 (continued): (d) Pesc (mW) vs. VCL (mm/sec) for *P. polionotus*

(e)

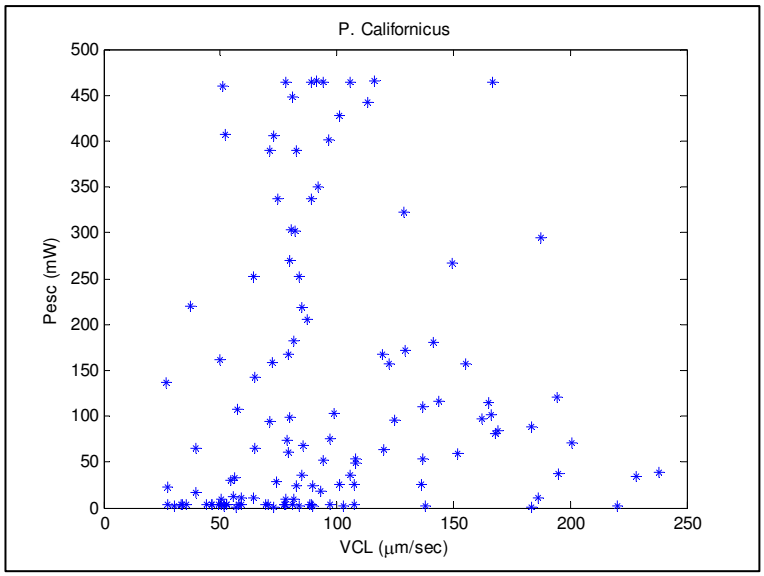

Figure A.2 (continued): (e) Pesc (mW) vs. VCL (mm/sec) for *P. californicus*

A.4 Discussion

With the exception of *P. californicus*, sperm swimming speed correlates to level of sperm competition (median swimming speed is greater for species where level of sperm competition is high). However, escape laser power does not correlate with level of sperm competition. This result is inconsistent with the results found in chapter 7. In addition, no distinct relationship exists between Pesc and VCL for any of the mice species. This is not consistent with what was found for eleven other mammal species analyzed in chapter 6. A possible explanation of these inconsistencies may be the mice sperm head geometry. Geometry is crucial calculating the forces generated using optical tweezers. The model used for the other mammalian species (chapters 4 – 7) which says there is a linear relationship between force and Pesc, assumes the sperm

have a spherical and/or elliptical head geometry. A mouse sperm head, however, has a "hooked" tip (a scanning electronmicrograph image of a sperm head can be found in van der Spoel *et al.* 2002). Therefore, the model breaks down when applied to mice sperm and the relationship between escape power and swimming force most likely becomes non-linear. Rigorous mathematical modeling should be done to calculate the forces generated on a mouse sperm head before a conclusive decision can be made about the relationships between swimming force and (a) mating pattern and (b) swimming speed.

References

Foltz, D. W. (1981). Genetic evidence for long-term monogamy in a small rodent, *Peromyscus polionotus*. *Am. Nat.* **117**, 665–675

Ribble, D. O. (1991). The monogamous mating system of *Peromyscus californicus* as revealed by DNA fingerprinting. *Behav. Ecol. Sociobiol.* **29**, 161-166.

Shi, L. Z., Nascimento, J. M., Chandsawangbhuwana, C., Berns, M. W., Botvinick, E. (2006b). Real-time automated tracking and trapping system (RATTS). *Microscopy Research and Technology* **69**(11), 894-902.

van der Spoel, A. C., Jeyakumar, M., Butters, T. D., Charlton, H. M., Moore, H. D., Dwek, R. A., Platt, F. M. (2002). Reversible infertility in male mice after oral administration of alkylated amino sugars: A nonhormonal approach to male contraception. *PNAS* **99**(26), 17173-17178.

Xia, X., Millar, J. S. (1991). Genetic evidence of promiscuity in *Peromyscus leucopus*. *Behav. Ecol. Sociobiol.* **28**, 171-178.

Zar, J. H. (1984). in *Biostatistical Analysis,* 2nd end. pp. 150-161 and pp. 292-305. Prentice Hall, Englewood Cliffs.